SOME STUDIES ON THE STATICAL ANALYSIS OF CIRCULARLY CURVED BOX GIRDER BRIDGES(Dissertation_全文)

AUTHOR(S):

Kambe, Shun-ichi

SOME STUDIES ON THE STATICAL ANALYSIS OF CIRCULARLY CURVED BOX GIRDER BRIDGES

by

Shun-ichi KAMBE

Department of Civil Engineering

Tottori University

August, 1974

SOME STUDIES ON THE STATICAL ANALYSIS OF CIRCULARLY CURVED BOX GIRDER BRIDGES

by

Shun-ichi KAMBE

Department of Civil Engineering

Tottori University

August, 1974

ACKNOWLEDGEMENTS

The author should like to express his special thanks to Professor Ichiro Konishi of Kyoto University for his encouragement and advice on various points throughout this investigation. The author also wishes to express his sincere gratitude for the helpful consel in this investigation received from Assistant Professor Naruhito Shiraishi of Kyoto University.

The author also wishes to thank Mr. T. Kondō, one of his classmates at the Graduate School of Kyoto University, for providing some specifications of the bridges constructed by Hanshin Express Highway Corporation.

The numerical works in this investigation were greatly assisted by the continued efforts of Mr. H. Tanaka, former assistant of Tottori University. The computers used for the numerical works were FACOM-230-60 at the Data Processing Center of Kyoto University and TOSBAC-3400 Model 21 at Tottori University. A special acknowledgement is due to Mr. A. Hayashi, technical official of Tottori University, who assisted in prparing the figures in the manuscript.

The author wishes to express his sincere gratitude to his wife, Miyuki, and Mr. R. Terhune who helped with the proofreading of the manuscript.

TABLE OF CONTENTS

I. INTRODUCTION

In recent years, many highway systems have been established even in our country to cope with the situation of tremendously increasing urban traffic flows. In view of the lack of space when constructing an urban express highway in the congested area of a large city, the use of the girder bridges on curved alignment has become increasingly popular.

Curved girder bridges under transverse loadings develope much higher torsional moments throughout their lengths owing to the curvature effects of their longitudinal axes. Therefore, torsional moments play a still more important role in the design of the bridges. For practical design purposes, it is highly desirable to develope the simplified analytical method with reasonable accuracy, thereby making it possible to evaluate more precisely the stresses produced by torsional moments. From the aforementioned view point, the author has developed two types of the Modified Torsional Bending Theories for analysing the curved box girder bridges, in which the influence of the secondary shear deformation due to restrained torsion is taken into consideration.

The major objectives of this thesis is to represent the developement of these theories and to provide some results obtained from the numerical examples calculated by using these theories.

1.1 Contents of Thesis

The thesis contains five chapters. It begins with a brief introductory chapter in which the objective of the present study is stated after a short review on the contemporary trends of statical analysis of box girder bridges. In the review, the author classified the various available papers reported in the last few decades under three major analytical methods, i.e., Thin-Walled Beam Method of Analysis, Generalized Coordinates Method of Analysis, and Direct Stiffness Method of Analysis, and gave the outline of these analytical methods.

In the second chapter, the physical arguments on the state of pure torsion to which a circularly curved girder bridge is subjected are presented, and at the same time some basic formulae regarding this subject are explained. This is because they are needed for the developement of the two types of Modified Torsional Bending Theories treated in the following chapter, in which account is taken of the secondary shear deformation due to restrained torsion.

The third chapter consists of three parts. The first two parts are mainly dedicated to the derivation of the fundamental equations in two types of the Modified Torsional Bending Theories developed by the author. In the last part, some physical arguments on the developement of the theories are given. In addition, it is shown that there exists an inequality between two types of the "warping-shear correction parameters" (dimensionless cross-sectional characteristics)

newly introduced in the theories. This will provide us with the information as to which one of the theories gives a moderate or higher estimate of the statical and kinematical quantities related to restrained torsion.

Chapter IV deals with the numerical examples obtained by using these theories: It is interesting to investigate to what extent the aforementioned cross-sectional characteristics affect the statical and kinematical quantities, such as the stress couples related to restrained torsion, the intensity of warping displacement, and the angle of rotation of cross section, of the curved box girder bridges. For numerical illustration purposes, the curved box girder bridges continuous over two spans, which have the same developed span lengths and the same radii of curvatures along their longitudinal axes, were chosen. Thereupon, with the objective of providing an insight into the characteristics of the influence-lines for those quantities at some sections of the bridges referred to, parametric studies using the various values of the selected structural characteristics, were performed. Referring to the results thus obtained, the effect of the warping-shear correction parameter (explained later) on the distributions of the shear flows and normal stresses was also investigated for the specified cross sections of two types of the curved composite box girder bridges.

1.2 Broad View of the Problem [40]

1.2.1 General Remarks

Box girder bridges are frequently used in the highway structures, since they have the following favorable structural advantages and features:

(1) They provide desirable load distribution characteristics across the width of the bridges, produced by the large torsional rigidities inherent in their cross-sectional shapes.

(2) They are probably lighter than other type of bridges, therefore, they may possess the advantage of weight reduction.

(3) They have the pleasing appearances from an aesthetic standpoint because of their streamlined shape and slenderness.

Accordingly, the increased use of box girder bridges has stimulated considerable interest for research in this area. As can be seen from an extensive list of the references given by P. F. McManus et al [41], a large amount of literature has been published all over the world in the last few decades, even though it is restricted to the statical analysis of curved box girder bridges.

Since this is the case, a comprehensive review of all the existing theoretical studies on this subject is obviously beyond the scope of this thesis. In the following, therefore, a simple survey will be made to classify the various available analytical methods for curved box girder bridges under

three major analytical methods, i.e., Thin-Walled Beam Method of Analysis, Generalized Coordinates Method of Analysis, and Direct Stiffness Method of Analysis.

1.2.2 Methods of Analysis

A. Thin-Walled Beam Method of Analysis

This method of analysis is based on the two kinds of hypotheses named after Euler-Bernoulli and Wagner, respectively, by which the cross-sectional deformation of a girder bridge can be described in terms of the three linear and one angular displacement components of the reference axis of the girder chosen in an appropriate manner. The former hypothesis[1)] is one of the most common hypotheses in structural analysis and is sometimes called the "law of plane section" : plane sections normal to the bar's geometric axis before deformation remain plane and normal to this axis after deformation. The latter one deals with the longitudinal distorsion of cross section, called "warping", by assuming that its basic transverse distribution would be the same as occurs in pure torsion (Saint-Venant's torsion). According to these hypotheses, it can be assumed that the cross section is deformed in such a manner that it translates and rotates according to the law of plane section and distorts longitudinally according to Saint-Venant's torsion theory. In other words, the theory thus

---

1) In analysing the bars of small curvature, this hypothesis was first introduced 1858 by E. Winkler [39].

constructed assumes that the cross sections distort in the longitudinal direction only in one mode irrespective of their shapes, that is, they may be single-celled or multiple-celled or separate twin-celled cross sections, and that the in-plane distorsional deformation of the cross sections can be disregarded.

Finally, if the equilibrium equations are expressed in terms of the displacement components of the reference axis, in general they reduce to a set of simultaneous linear ordinary differential equations of fourth order for the four unknown displacements.

The analytical method outlined above is often called the "Torsional Bending Theory". The theories developed for analysing the thin-walled straight box girder bridges are closely associated with the names of Th. von Kármán and N. B. Christensen [1] and F. W. Bornscheuer [2]. The significant contributions to develope the theory to the case of a box girder bridge with a circular axis have been made by such Japanese investigators as I. Konishi and S. Komatsu [3, 4, 5], S. Kuranishi [6], and Y. Fukazawa [7].

The so-called conventional torsional bending theories mentioned above can be modified in such a way as to deal with the secondary shear deformation due to restrained torsion and the transverse distorsion of a cross section. This can be done by introducing, respectively, an unknown quantity as the intensity of warping instead of the rate of twist of the reference axis (Modified Torsional Bending Theory) [8, 9, 10, 11, 13, 14, 15]

and a distorsion angle in a global sense [16, 17, 18]. However, the modification of the latter case was performed only for the case of bridge with mono-symmetrical single-celled cross section. R. Dabrowski[2] [19] from Poland has developed his theory only for the case of a curved box girder bridge with mono-symmetrical single-celled or separate twin-celled cross section, and has summarized much of his work in his book [20]. The author of this thesis has developed the modified torsional bending theories [21, 22] in a different way from R. Dabrowski so as to cover the curved box girder bridges with arbitrary shape of cross sections.

B. Generalized Coordinate Method of Analysis

This method of analysis originated with V. Z. Vlasov [23]. Several decades later, G. Lacher [24] formulated it in a matrix form for the convenience of computer's use and proposed a method of analysing the effects of flexible or rigid interior diaphragms on the structural behaviour. Then, by applying V. Z. Vlasov's theory to a special case of the straight box girder bridges with mono-symmetrical, single-celled, rectangular or trapezoidal cross section, the effects of the intermediate diaphragms were studied by S. R. Abdel-Samad et al [25], T. Okumura and F. Sakai [26], S. Ochiai[27], and S. Ochiai and

---

2) He derived the fundamental equations in his theory in analogous fashion to that of E. Winkler. So far as the author knows, much more rigorous formulation of the theory in terms of cylindrical coordinates was made for the first time by I. Konishi and S. Komatsu [3].

S. Kitahara [28]. It is a comparatively simple matter to extend V. Z. Vlasov's theory to the case of a curved box girder bridge, and this is to be referred to in a work by Z. P. Bazant [29].

The thin-walled bridge structure is idealized for the analysis as an assemblage of the plate elements interconnected with hinges to one another along their longitudinal edges (Fig. 1.1). The points at which the plate elements meet together will be called hereafter the nodes or node point. Then, major assumptions for analysis are as follows:

(1) The longitudinal displacement of cross section varies linearly between node points.

(2) The plate elements are inextensible in the transverse direction.

Under these assumptions, V. Z. Vlasov developed an ingenious way which allows the cross-sectional deformation to be represented by finite sums of pair of functions. Each pair consists of the preselected function of the circumferential arc length coordinate s and the unknown function of the axial coordinate x (Fig. 1.2). Thus, the axial and tangential displacement components, $u(x, s)$ and $v(x, s)$, are expressed in the form of finite series as follows:

$$u(x, s) = \sum_{j=1}^{m} U_j(x)\phi_j(s)$$

$$v(x, s) = \sum_{k=1}^{n} V_k(x)\psi_k(s)$$

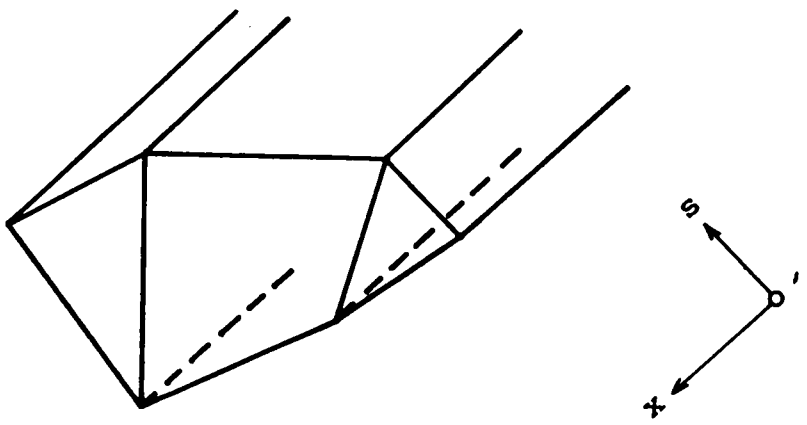

Fig. 1.1 Multi-Celled Structure

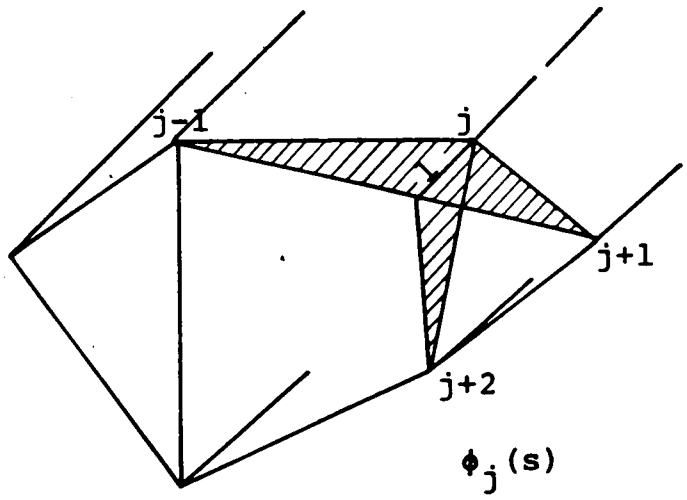

(a) Longitudinal Displacement of Node j .

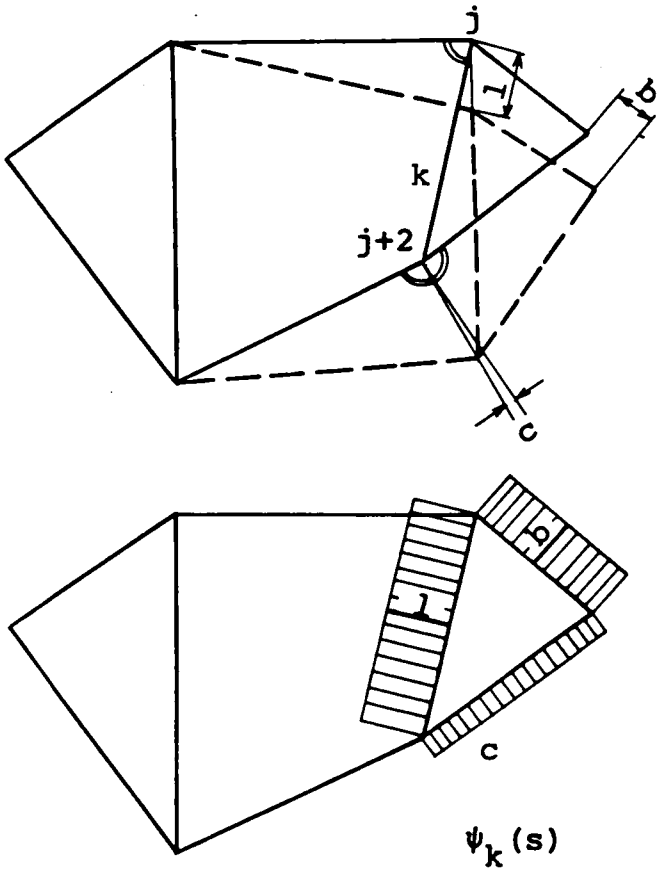

(b) Transverse Displacement of Member k

Fig 1.2 Longitudinal and Transverse Displacement Patterns

in which $\phi_j(s)$ and $\psi_k(s)$ are the j-th longitudinal and k-th transverse generalized coordinates, respectively. Here, the number m is equal to the total number of nodes owing to the assumption (1). Similarly, the number n is equal to $2m - e$, in which e is the total number of the plate segments forming the cross section, because the assumption (2) reduces the number of transverse degrees of freedom by one for every plate segment. In effect, the number of degrees of freedom of the cross-sectional deformation is regarded as $m + n$.

It should be noted that the out-of-plane and in-plane distorsional deformation of cross section, i.e., the deviation from the deformation obeying the law of plane section, can be determined by $m - 3$ independent functions of the longitudinal displacements and $n - 3$ independent functions of the transverse displacements, respectively. This makes it possible to describe satisfactorily the variety of distorsional deformation involved in the multiply connected cross sections.

Then, equilibrium equations are derived by using the principle of virtual displacement [23] or the principle of stationary potential energy [29]. They reduce to a system of $m + n$ simultaneous linear ordinary differential equations of the second order with respect to the generalized longitudinal displacements $U_j(x)$ $(j = 1, 2, \ldots, m)$ and transverse displacements $V_k(x)$ $(k = 1, 2, \ldots, n)$.

C. Direct Stiffness Method of Analysis

This method of analysis can be regarded as an extension of the folded plate theories [30, 31, 32], which were originally developed with the hope of analysing the roof structures to the case of a box girder bridge. Significant contributions to develope the theories to the analysis of multi-cell box girder bridges (multiple folded plate structures) with straight axes may be closely associated with the names of K. H. Chu and S. G. Pinjarkar [33], K. S. Loo and A. C. Scordelis [34]. A matrix analysis technique of the folded plate theory, called the "Direct Stiffness Method", was developed for the first time by A. DeFrie-Skene and A. C. Scordelis [35] in order to take full advantage of the capabilities of digital couputers. More recently (1971), the method has been developed by C. Meyer and A. C. Scordelis [36], and K. H. Chu and S. G. Pinjarkar [37] to analyse the curved box girder bridges.

The unknown quantities used in the direct stiffness method are the three linear displacement components in the longitudinal, horizontal, and vertical directions, respectively, and one angular displacement (rotation about a longitudinal axis) at each node (joint) of the plate elements composing the cross section. The number of nodal degrees of freedom is equal to four. Therefore, the total degrees of freedom is equal to four times the total numbers of nodes included in the cross section.

The necessary fundamentals will be explained first: The element stiffness matrix which relates the unknown joint displacements and the joint internal forces is a fundamental idea in this analytical method. In forming the element stiffness matrix, there exist two major ways called the "ordinary method" and "elasticity method". The former is based on the displacements assumed in a certain fashion so as to vary in the transverse direction of a plate element as functions of some unknown nodal displacements. On the other hand, the latter is based on the displacements obtained from the direct application of the elasticity theory (theory of plate and shell) to a plate or shell element. These ways of forming a element stiffness matrix make it possible to analyse fairly exactly the phenomenon of stresses diffusion due to shear deformation, called the "shear lag", as well as the states of the warping stresses and flexural ones due to, respectively, the out-of-plane and in-plane distorsional deformations of cross sections.

Secondly, only the main steps in the procedure of analysis can be briefly summarized as follows [38]:

(1) Determine the element stiffness matrix for each plate element in the local coordinate system [Fig. 1.3(b)].

(2) Transform the element stiffness to a global-coordinate system [Fig. 1.3(c)] and assemble these into the structure stiffness matrix K.

(3) Solve the equilibrium equations $R = K r$, where R represents the applied equivalent joint loads, for the

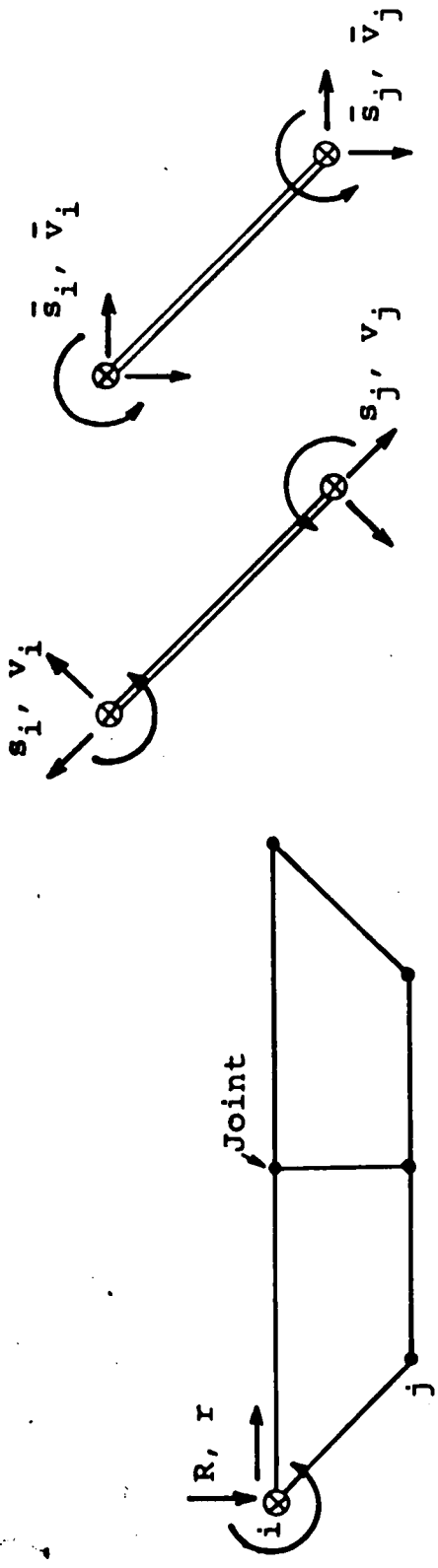

(a) Joint-global (b) Plate-local (c) Plate-global

Fig. 1.3 Joint and Plate Edge Forces and Displacements in Global and Local Coordinate Systems

unknown joint displacements r [Fig. 1.3(a)].

(4) Determine the plate element internal forces and displacements by using expressions relating these quantities to the joint displacement r.

The equations of equilibrium are solved by expanding all of the quantities in the equations into Fourier series in the longitudinal direction. The final results are then obtained by summing up the various harmonic contributions.

1.2.3 Concluding Remarks

The latter two analytical methods explained in the preceding paragraph may be more accurate than the former one in the sense that they can analyse the stresses in more detail due to the distorsional deformations of cross sections in the transverse one as well as in the longitudinal direction. This is because the degrees of freedom sufficient to describe these distorsional deformations are introduced in these analytical methods. The last one, in particular, makes it possible to analyse the shear lag phenomenon. However, it should be noted that this accuracy is achieved at the cost of substantial computing time on a large computer and of complexity in the procedures of analysis, which probably conceals the main design parameters. Moreover, in these methods of analysis the problem is often solved by expanding the unknown or required quantities into Fourier series in the longitudinal direction. It is, therefore, unavoidable that the solution is limited to the case of a bridge with simply supported ends.

On the other hand, the thin-walled beam method of analysis may describe the structural behaviour of curved box girder bridges in a fairly rational manner by using a few parameters, as long as the cross sections are sufficiently stiff. It seems that in most cases of steel or composite box girder bridges encountered in practice this is so because their cross sections are stiffened with sufficient numbers of intermediate diaphgrams or cross frames in order to make their portions secure during transportation and construction. In the author's opinion, these diaphgrams or cross frames are probably in excess for the strength of the bridges after completion.

As is well known, it is necessary for the design of a bridge to repeat the trial proportioning of its structural elements until the design criteria are satisfied. Therefore, the simplified analytical methods are highly desirable as a tool during a design process in which the designer is required to assess the effect of varying certain parameters as quickly as possible.

Moreover, it should be noted that torsional moments developed in a curved girder bridge loaded by both its own weight and the live loads may reach a comparatively large amount because of curvature effects of its longitudinal axis, as compared with those developed in a straight girder bridge of the same span length under the same loading condition. In the curved girder bridges, therefore, the shearing stresses produced by torsional moments together with those produced by

shearing forces will play a still more important role in the determination of the strength of web plates required to prevent buckling and in the design of shear connectors.

From the aforementioned view point, the author has studied the Thin-Walled Beam Theory for the curved box girder bridges and extended two types of the Modified Torsional Bending Theories in which account is taken of the secondary shear deformation due to restrained torsion.

II. SOME PRELIMINARIES[1)]

2.1 General

There exists a close analogy between Euler-Bernoulli's hypothesis and Wagner's hypothesis in the sense that the former assumes the mode of cross-sectional deformation in flexure accompanied with shear to be similar to that in pure bending and the latter assumes, in like manner, the mode of cross-sectional deformation in restrained torsion to be similar to that in pure torsion. On the basis of these hypotheses, the Torsional Bending Theory is constructed. It is, therefore, desirable for the developement of the theories followed in Chapter III to elucidate the physical interpretation of the state of pure torsion to which a circularly curved box girder bridge is subjected, and to derive some basic formulae concerning this theme.

Accordingly, this is the prime objective of the following sections in this chapter.

2.2 Coordinate Systems and Displacements

Let us now begin our study by establishing the following coordinate systems shown in Fig. 2.1:

(1) The origin O of the left-handed cylindrical coordinate system $(O\text{-}\rho\theta\zeta)$ is located at the center of curvature

---

1) The material in this chapter is drawn mainly from the References [3] and [7].

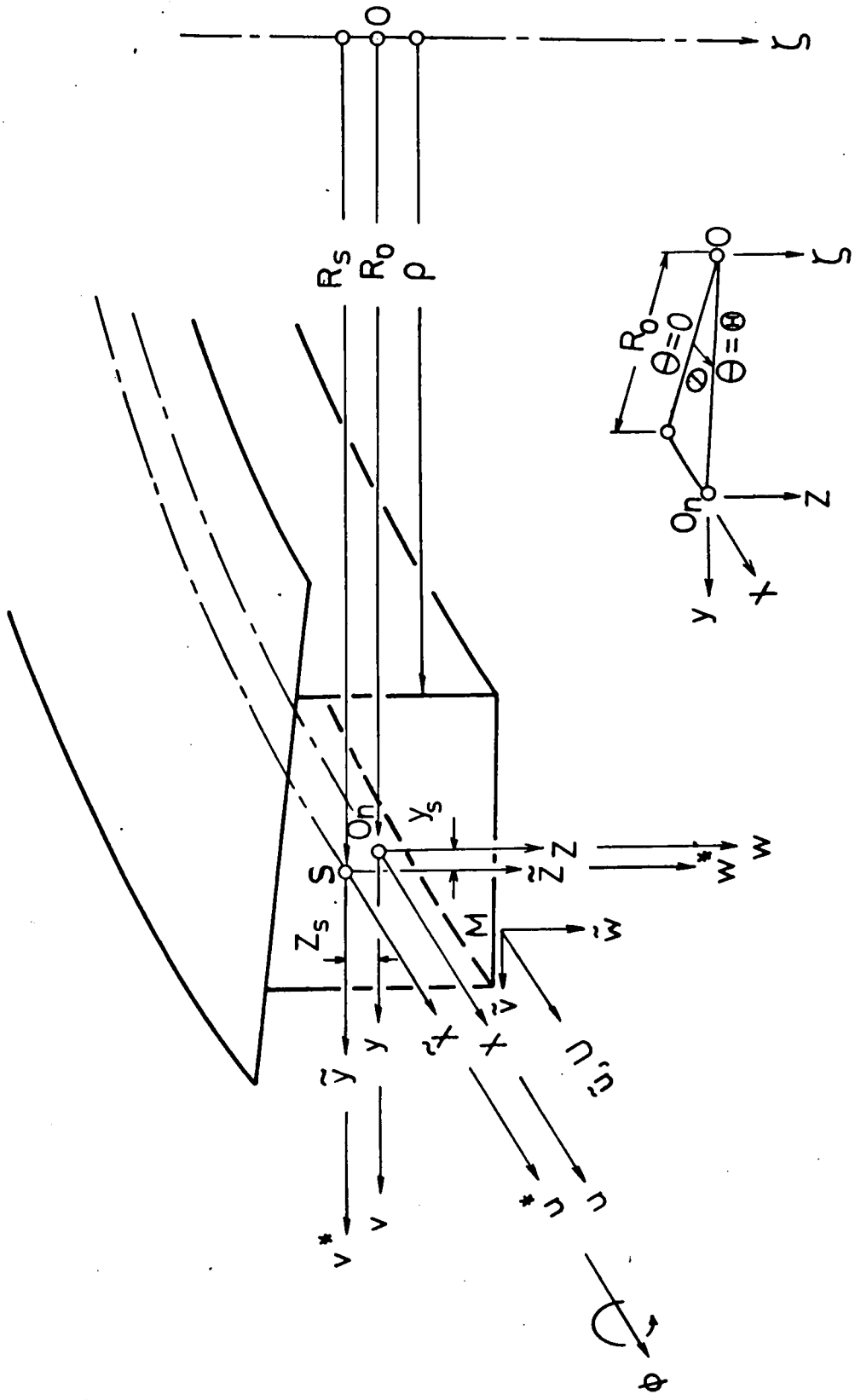

Fig. 2.1 Coordinate Systems and Displacement Components

of the generatrix passing through the cross-sectional center of figure O_n (defined later) of a circularly curved girder bridge. Here, ρ is a radial coordinate, θ is an angular coordinate measured from the right end of the girder bridge, and ζ is directed vertically downwards.

(2) For any cross section of the girder bridge defined by the angle θ, we take three kinds of the right-handed rectangular coordinate systems, $(C\text{-}\bar{x}\bar{y}\bar{z})$, $(O_n\text{-}xyz)$, and $(S\text{-}\tilde{x}\tilde{y}\tilde{z})$ with the origins at an arbitrarily chosen point C, the center of figure O_n, and the shear center S (defined later) in the cross section, respectively. The axes are chosen so that $\bar{y}$ $(y, \tilde{y})$ and $\bar{z}$ $(z, \tilde{z})$ may be directed in the radial outward and vertical downward directions, respectively, while $\bar{x}$ $(x, \tilde{x})$ may be directed normal to the cross section, in the direction corresponding to an increase of the angle θ.

(3) A circumferential coordinate system (s, n) is also taken in the cross section along the middle line of the wall of each plate element, in which s is measured positive along this line in the counterclockwise direction and n is directed normal to this line. In the interior webs of multi-celled cross section, however, the coordinate s is measured positive in the downward direction.

The displacement of an arbitrary point M on the profil line (the center of figure O_n, the shear center S) of the cross section is resolved into three components, $\tilde{u}$ (u, u^*), $\tilde{v}$ (v, v^*), and $\tilde{w}$ (w, w^*) in the directions of the x, y, and

z axes, respectively. The warping displacement of the aforementioned point M is denoted by the symbol U. The angle of rotation of the cross section about a longitudinal axis of the girder bridge is denoted by the symbol ϕ and is taken as positive when the rotation is in the direction indicated in Fig. 2.1.

2.3 Outline of Pure Torsion

Pure torsion of a circularly curved girder bridge is defined by the state of the girder bridge caused by the combined action of the torques T_0 and vertical forces V_0 with equal magnitudes and opposite signs, applied at both free ends, as shown in Fig. 2.2. The vertical forces in this case, as opposed to the case of a straight girder bridge, are needed to stabilize the curved girder bridge.

In what follows, the statical, the kinematical, and the geometrical quantities with respect to a girder axis passing through the cross-sectional shear center (called hereafter the shear center axis) will be indicated with an asterisk. For the sake of convenience, the shear center axis will be taken hereafter as a reference axis. The radius of curvature of this axis is denoted by R_s.

Then, the magnitudes of the aforementioned vertical forces are found to be T_0/R_s by taking moments separately about the radial axes OA and OB in Fig. 2.2, that is

$$V_0 = T_0/R_s \qquad \text{(a)}$$

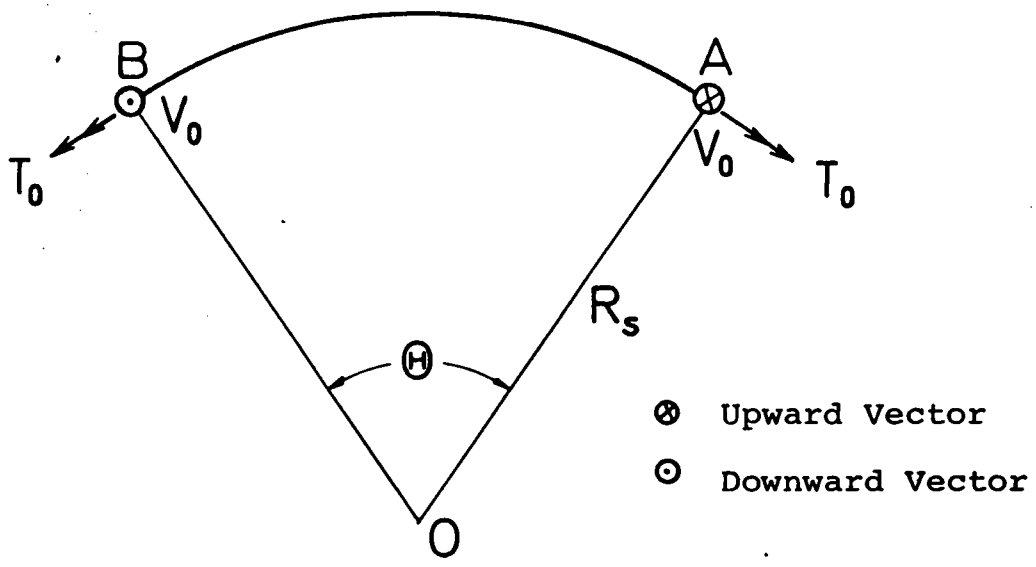

Fig. 2.2 Curved Girder Bridge in Pure Torsion

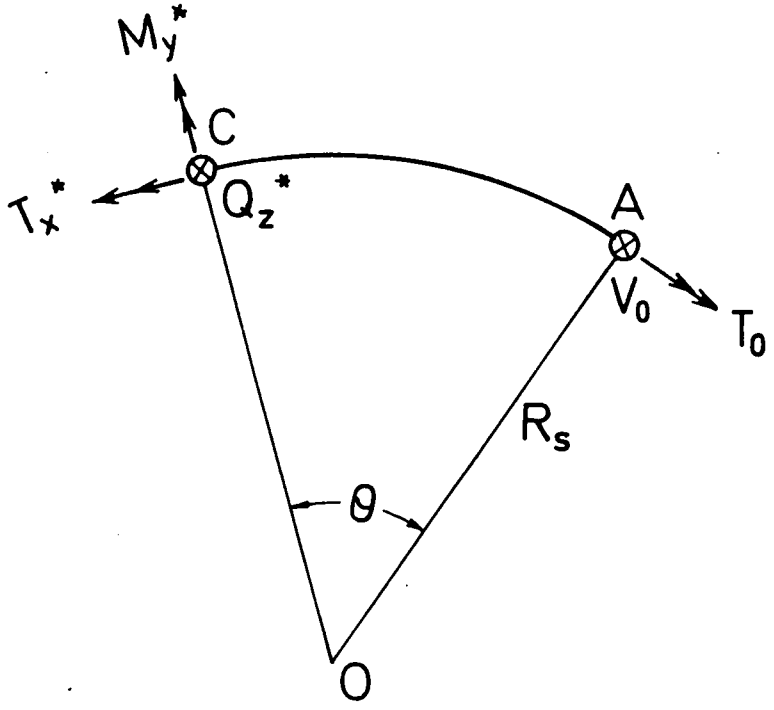

Fig. 2.3 Curved Girder Element

Under these conditions, the stress resultant and couples acting at any point on the girder's axis defined by the angle θ can now be found from a simple statics for the girder segment AC in Fig. 2.3 as follows:

$$T_x^* = T_0\cos\theta + V_0R_s(1 - \cos\theta)$$

$$M_y^* = T_0\sin\theta - V_0R_s\sin\theta \qquad (b)$$

$$Q_z^* = - V_0$$

in which T_x^* and M_y^* are the torsional moment and bending moment about the $\tilde{x}$ and $\tilde{y}$ axes, respectively, and Q_z^* is the shearing force acting in the $\tilde{z}$ direction, positive as shown in the figure. By substituting Eq. (a) into the first two of Eq. (b), it is found that uniform torsional moment and shearing force acting in the vertical direction are developed along the girder axis and no bending moments are produced, namely

$$T_x^* = T_0, \quad Q_z^* = - V_0, \quad M_y^* = 0 \qquad (c)$$

2.4 Saint Venant's Torsion Function and Warping Function

The results obtained in the preceding section suggest that any longitudinal fiber of the girder bridge is in the state of uniform twisting and of no stretching. It seems, therefore, reasonable to proceed in the further analysis by assuming that the following relationships hold all over the range of the angle θ

$$\varepsilon_x^* = \psi_y^* = \psi_z^* = 0$$
$$\psi_x^* = \text{const.} \qquad (2.1)$$

where

ε_x^* = rate of stretch of the shear center axis,

ψ_x^* = rate of twist of the shear center axis,

ψ_y^* = change in curvature in the xz-plane of the shear center axis,

ψ_z^* = change in curvature in the xy-plane of the shear center axis.

Furthermore, the warping displacement U_s may be assumed after the analogy to the case of a straight girder bridge to take the form

$$U_s = - \omega^*(s) \cdot \psi_x^*(\theta) \qquad (2.2)$$

where ω^* is called the "warping function" with respect to the shear center.

In the developement to follow, however, the shearing strain corresponding to the shearing force mentioned in the preceding section will be disregarded as an approximation employed in the engineering beam theory. Following this approximation and the assumptions on the deformational mode of a cross section mentioned in the preceding chapter, the components of the displacement field in a cross section can be expressed in the form:

$$\tilde{u} = u^* - \tilde{y}\phi_z^* + \tilde{z}\phi_y^* - \omega^*\psi_x^*$$

$$\tilde{v} = v^* - \tilde{z}\phi_x^* \qquad (2.3)$$

$$\tilde{w} = w^* + \tilde{y}\phi_x^*$$

where ϕ_x^*, ϕ_y^*, and ϕ_z^* are the angular displacement components in the $\tilde{x}$, $\tilde{y}$, and $\tilde{z}$ directions, respectively, of the shear center axis after deformation. Then, the aforementioned kinematical quantities with respect to the shear center axis can be expressed in terms of the displacement components, through geometrical considerations or by using analytical geometry, as follows:

$$\phi_x^* = \phi, \qquad \phi_y^* = -\frac{1}{R_s}\frac{dw^*}{d\theta}$$

$$\phi_z^* = \frac{1}{R_s}\left(\frac{dv^*}{d\theta} - u^*\right) \qquad (2.4)$$

and

$$\varepsilon_x^* = \frac{1}{R_s}\left(\frac{du^*}{d\theta} + v^*\right)$$

$$\psi_x^* = \frac{1}{R_s}\left(\frac{d\phi}{d\theta} - \frac{1}{R_s}\frac{dw^*}{d\theta}\right) \qquad (2.5)$$

$$\psi_y^* = -\frac{1}{R_s}\left(\phi + \frac{1}{R_s}\frac{d^2w^*}{d\theta^2}\right)$$

$$\psi_z^* = \frac{1}{R_s^2}\left(\frac{d^2v^*}{d\theta^2} - \frac{du^*}{d\theta}\right)$$

Substituting the displacement components in Eqs. (2.3) into strain-displacement relations and taking the relationships given by Eqs. (2.1), (2.2), (2.4), and (2.5) into consideration

yields the following strain components [3, 7]:

$$\varepsilon_\theta = \varepsilon_\rho = \varepsilon_\zeta = \gamma_{\rho\zeta} = 0$$

$$\gamma_{\rho\theta} = -\left\{\frac{R_s}{\rho}\,\tilde{z} + \rho\,\frac{\partial}{\partial\rho}\left(\frac{\omega^*}{\rho}\right)\right\}\psi_x^* \tag{2.6}$$

$$\gamma_{\theta\zeta} = \left\{\frac{R_s}{\rho}\,\tilde{y} - \frac{\partial\omega^*}{\partial\zeta}\right\}\psi_x^*$$

Referring to Fig. 2.4 and applying the proper strain transformation formulae to the strain components in Eqs. (2.6), we find the strain components referred to the circumferential coordinate system (s, n) as follows:

$$\gamma_s \equiv \left\{\frac{R_s}{\rho}\,r_t^* - \rho\,\frac{\partial}{\partial s}\left(\frac{\omega^*}{\rho}\right)\right\}\psi_x^*$$

$$\gamma_n \equiv \left\{\frac{R_s}{\rho}\,r_n^* - \rho\,\frac{\partial}{\partial n}\left(\frac{\omega^*}{\rho}\right)\right\}\psi_x^* \tag{2.7}$$

where r_t^* and r_n^* are the perpendiculars from the shear center S to the tangent line and normal line at the point M considered herein, respectively. In the case of a thin-walled cross section, the strain component γ_n can be, in general, regarded as a negligibly small quantity.

Now, the equilibrium equation in a longitudinal direction for a differential plate element is expressed in terms of the stress components as follows [44]:

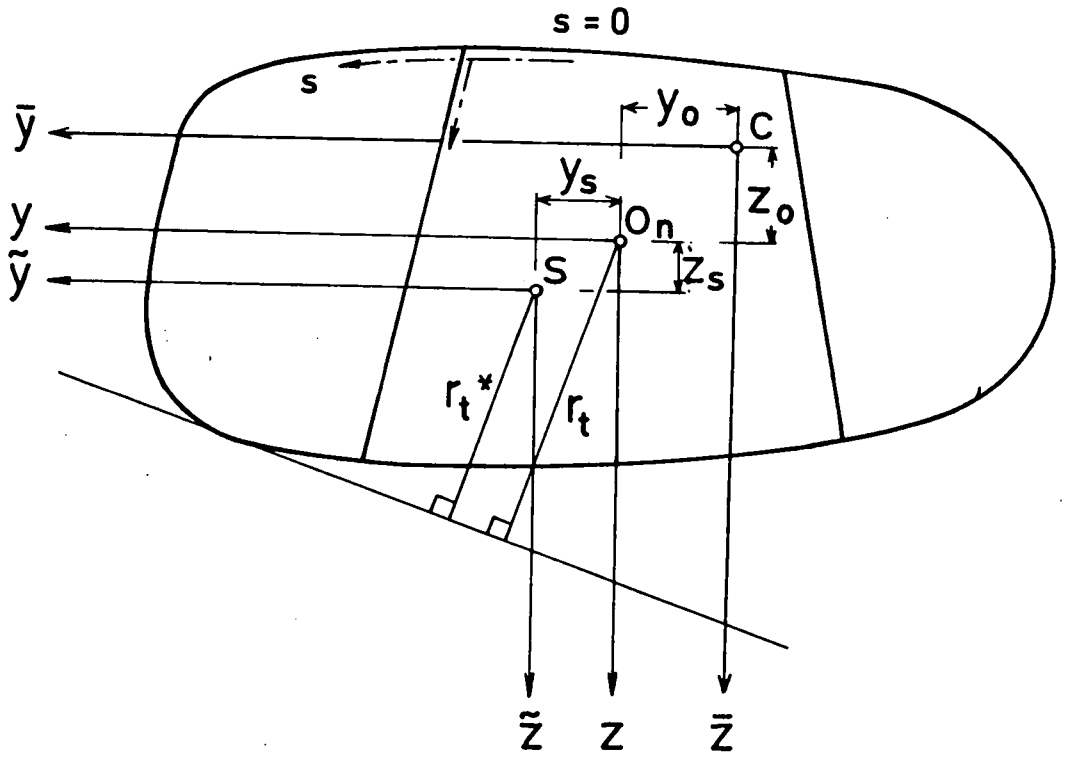

Fig. 2.4 Geometry of a Multicell Cross Section

$$\frac{\partial}{\partial\theta}(\sigma_\theta t) + \frac{1}{\rho}\frac{\partial}{\partial s}(\rho^2 q_s) = 0 \qquad (2.8)$$

in which the quantity q_s is called the "shear flow" and is defined by

$$q_s = \frac{1}{n_g} G_s \gamma_s t \qquad (2.9)$$

where

G_s, G_c = shear moduli of elasticity of steel and concrete, respectively,

$$n_g = \begin{cases} 1 & \text{for steel plate elements and shear connectors,} \\ G_s/G_c & \text{for concrete slabs in composite action with steel web plates,} \end{cases}$$

t = thickness of plate elements.

Remembering that $\varepsilon_\theta = 0$ from Eqs. (2.6), that is, $\sigma_\theta = 0$, and $\psi_x^* = \text{const.}$ from Eqs. (2.1), we can solve Eq. (2.8) for q_s to obtain

$$\rho^2 q_s = \tilde{\text{const.}} \equiv R_s^2 G_s \psi_x^* \tilde{q}_s \qquad (2.10)$$

where the quantity $\tilde{q}_s$ is called the "Saint-Venant's torsion function" and takes a constant value on the wall of each plate element. Furthermore, on account of the condition of balancing at any junction of the palte elements for the flow type of quantity $\tilde{q}_s$, the quantity can be expressed in terms of the new quantities $\tilde{q}^0_{s,k}$ which are constant in the k-th cell, as follows (Fig. 2.5):

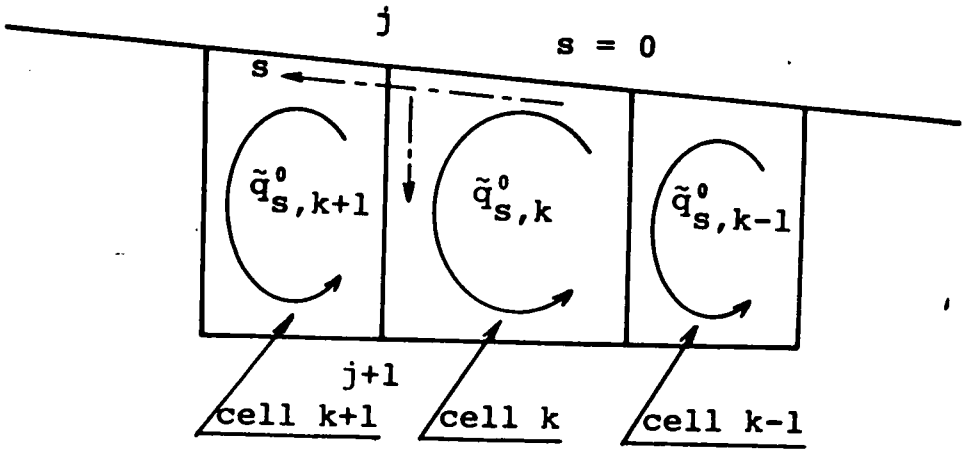

Fig. 2.5 Saint-Venant's Torsion Function

$$\tilde{q}_s = \begin{cases} \tilde{q}^0_{s,k} - \tilde{q}^0_{s,k-1} & \text{on the wall of the plate element common to cells } k-1 \text{ and } k, \\ \tilde{q}^0_{s,k} & \text{on the wall of the plate element belonging to } k\text{-th cell only,} \\ \tilde{q}^0_{s,k} - \tilde{q}^0_{s,k+1} & \text{on the wall of the plate element common to cells } k \text{ and } k+1. \end{cases} \quad \ldots\ldots\ldots\ldots\ldots \quad (2.11)$$

Combining Eqs. (2.7), (2.9), and (2.10) and cancelling out the common factor $G_s\psi_x^*$ gives the following differential equation for determining the warping function ω^*:

$$\frac{R_s^2}{\rho^2}\tilde{q}_s = \frac{t}{n_g}\left\{\frac{R_s}{\rho} r_t^* - \rho \frac{\partial}{\partial s}\left(\frac{\omega^*}{\rho}\right)\right\} \quad (2.12)$$

from which ω^* is solved in the form

$$\omega^*(s) = R_s\rho\int_0^s \frac{1}{\rho^2} r_t^* \, ds - R_s^2\rho\tilde{q}_s\int_0^s \frac{1}{\rho^3}\frac{n_g}{t} ds + \frac{\rho}{R_s}\omega_0 \quad (2.13)$$

The integration constant ω_0 is to be determined from the condition of balancing the warping displacement over the entire cross section, the condition is

$$R_s\int_F \frac{1}{\rho}\omega^* \frac{t}{n_e} ds = 0 \quad (2.14)$$

where the subscript F on the integral indicates that the integration is carried over the entire cross-sectional area and

E_s, E_c = Young's moduli of elasticity of steel and concrete, respectively,

$$n_e = \begin{cases} 1 & \text{for steel plate elements and shear connectors,} \\ E_s/E_c & \text{for concrete slabs in composite action with steel web plates.} \end{cases}$$

Let us now return to the evaluation of the quantities $\tilde{q}^0_{s,k}$ defined in Eq. (2.11). The quantities are to be determined from the compatibility condition—the condition that the continuity on the warping displacement should be restored at the hypothetical slit introduced temporarily in each cell. The condition is

$$\oint_k \frac{\partial}{\partial s}\left(\frac{\omega^*}{\rho}\right) ds = 0 \qquad (2.15)$$

where the subscript k on the circuital integral indicates that the integration is to be carried around k-th cell. Then, substituting into Eq. (2.15) the expression for the integrand obtained from Eq. (2.12) and noting the relationships given by Eq. (2.11) yields the following equation for determining the quantities $\tilde{q}^0_{s,k}$:

$$
\begin{aligned}
&- \tilde{q}^0_{s,k-1}\int_{k-1,k} \frac{1}{\rho^3}\frac{n_g}{t}\,ds + \tilde{q}^0_{s,k}\oint_k \frac{1}{\rho^3}\frac{n_g}{t}\,ds \\
&- \tilde{q}^0_{s,k+1}\int_{k,k+1} \frac{1}{\rho^3}\frac{n_g}{t}\,ds = \frac{1}{R_s}\oint_k \frac{1}{\rho^2} r_t^*\,ds
\end{aligned}
\qquad (2.16)
$$

where the subscript, say k-1,k on the integral indicates that the integration is to be carried over the path along the wall of the plate element common to cells k - 1 and k, and so on. One such equation is to be written for each cell.

It is known that the right side of the above equation is a constant which depends on the cross-sectional geometry only, irrespective of any choice of the center of twist [7]. Furthermore, it is evident that the coefficients in the left side of the above equation are also the constants depending upon the cross-sectional geometry and elasticity property only, so that the same may be said of the quantities $\tilde{q}^0_{s,k}$ as can be seen from Eq. (2.16).

2.5 Torsion Constant and Central Moment of Inertia

The torsional moment about the $\tilde{x}$-axis developed on any cross section, denoted by T_s^*, is related to the shear flow[2] q_s from Eq. (2.10) as follows:

---

2) The formula for q_s given by Eq. (2.10) is available only for the closed parts of the cross section. For hybrid cross sections composed of closed cells plus open "fin" elements, such as that shown in Fig. 2.5, the contributions of the shear flows developed in the latter parts to the total value of the torsional moment are extremely small, so that they may be disregarded practically.

$$T_s^* = \int_F q_s r_t^* \, ds = G_s \psi_x^* R_s^2 \int_F \frac{1}{\rho^2} \tilde{q}_s r_t^* \, ds$$

$$\equiv G_s J_T^* \, \psi_x^* \tag{2.17}$$

where the quantity J_T^* is called the "torsion constant" of the cross section and defined as

$$J_T^* = R_s^2 \int_F \frac{1}{\rho^2} \tilde{q}_s r_t^* \, ds \quad ^{3)} \tag{2.18}$$

It is necessary, however, in the developement of the theories followed in Chapter III to rewrite the constant J_T^* in another form and to derive a relationship between this constant and the "central moment of inertia" of the cross section (defined later). This can be done in the following way: To begin with, let $\sum_j$ and $\sum_j'$ be the summation signs which indicate that the summations are taken all over the

---

3) For the aforementioned hybrid cross section, there exists an additional term arising from the shear flows developed in the "fin" elements. The term, denoted by ΔJ_T^*, is approximately given by

$$\Delta J_T^* = \sum_{j=1}^{m} \frac{1}{3} R_s^3 \int_{s_j} \frac{1}{\rho^3} \frac{t^3}{n_g} \, ds$$

where the subscript s_j on the integral indicates that the integration is to be carried all over the length of the j-th "fin" element and m stands for the total number of the "fin" elements.

The quantity ΔJ_T^* is negligibly small as compared with the quantity J_T^*, as can be seen from the argument presented in the footnote 2). Therefore, the formula for J_T^* given by Eq. (2.18) shows a fairly exact result for the general case of a hybrid closed cross section with "fin" elements.

walls j, $j+1$ and the junctions j of the plate elements, respectively. Moreover, let Δ_j be an operator which indicates that the algebraic summation of the inflows and outflows of any "flow" type of quantity is to be carried out at the j-th junction of the plate elements.

Then, by substituting the expression for r_t^* obtained from Eq. (2.12) into Eq. (2.18), we can rewrite the constant J_T^* as follows:

$$J_T^* = R_s^2 \int_F \frac{1}{\rho^2} \tilde{q}_s r_t^* \, ds$$

$$= R_s^3 \int_F \frac{1}{\rho^3} \tilde{q}_s^2 \frac{n_g}{t} \, ds + R_s \int_F \tilde{q}_s \frac{\partial}{\partial s}\left(\frac{\omega^*}{\rho}\right) ds \qquad \text{(d)}$$

Recalling that the quantities $\tilde{q}_s$ are constant on the respective walls of the plate elements, the second integral on the right side of the above equation can be evaluated as follows:

$$R_s \int_F \tilde{q}_s \frac{\partial}{\partial s}\left(\frac{\omega^*}{\rho}\right) ds = R_s \sum_j \int_{j,j+1} \tilde{q}_s \frac{\partial}{\partial s}\left(\frac{\omega^*}{\rho}\right) ds$$

$$= R_s \sum_j \left[\tilde{q}_s \left(\frac{\omega^*}{\rho}\right)\right]_j^{j+1} \qquad \text{(e)}$$

The right side of the above equation is found to vanish, after rearrangement of the order of summation of the bracketed terms, because the "flow" type of quantities $\tilde{q}_s$ should satisfy the aforementioned condition of equilibrium at every junction

of the plate elements. This can be verified as follows:

$$R_s \sum_j [\tilde{q}_s(\frac{\omega^*}{\rho})]_j^{j+1} = R_s \sum_j \{\frac{\omega^*}{\rho}(\Delta_j \tilde{q}_s)\} = 0 \qquad (f)$$

Finally, combining Eqs. (d), (e), and (f) yields another expression for J_T^* in the form:

$$J_T^* = R_s^3 \int_F \frac{1}{\rho^3} \tilde{q}_s^2 \frac{n_g}{t} ds \qquad (2.19)$$

Now, the "central moment of inertia" with respect to the shear center is defined by

$$J_c^* = R_s \int_F \frac{1}{\rho} r_t^{*2} \frac{t}{n_g} ds \qquad (2.20)$$

In the following, it will be shown that there exists an inequality between the two constants, J_c^* and J_T^*. Then, by substituting the expression for r_t^* obtained from Eq. (2.12) into Eq. (2.20), we can rewrite the constant J_c^* as follows:

$$J_c^* = R_s^3 \int_F \frac{1}{\rho^3} \tilde{q}_s^2 \frac{n_g}{t} ds + 2R_s \int_F \tilde{q}_s \frac{\partial}{\partial s}(\frac{\omega^*}{\rho}) ds + R_s^2 \int_F (\frac{\rho}{R_s})^3 \{\frac{\partial}{\partial s}(\frac{\omega^*}{\rho})\}^2 \frac{t}{n_g} ds \qquad (g)$$

It is evident that the first integral in the above equation is nothing else but the torsion constant J_T^* according to

Eq. (2.19) and that the second integral vanishes on account of Eqs. (e) and (f). Thus, equation (g) becomes

$$J_C^* = J_T^* + R_s^2 \int_F \left(\frac{\rho}{R_s}\right)^3 \left\{\frac{\partial}{\partial s}\left(\frac{\omega^*}{\rho}\right)\right\}^2 \frac{t}{n_g}\, ds \tag{2.21}$$

Since the integral in the above equation is not less than zero, the following inequality holds

$$J_C^* \geq J_T^* \tag{2.22}$$

2.6 Principal Generalized Coordinates

Let R_o and R_c be the radii of curvature of the girder axes passing through the cross-sectional center of figure O_n and arbitrary point C, respectively. Then, the basic functions 1, y(s), z(s), and $\omega^*(s)$ chosen so as to satisfy the following orthogonality conditions with a weight function $(1/\rho)(t/n_e)$

$$G_y \equiv R_o \int_F \frac{1}{\rho}\, z\, \frac{t}{n_e}\, ds = 0$$

$$G_z \equiv R_o \int_F \frac{1}{\rho}\, y\, \frac{t}{n_e}\, ds = 0 \tag{2.23}$$

$$J_{yz} \equiv R_o \int_F \frac{1}{\rho}\, yz\, \frac{t}{n_e}\, ds = 0$$

and

$$G_\omega^* \equiv R_s \int_F \frac{1}{\rho}\, \omega^*\, \frac{t}{n_e}\, ds = 0$$

$$C_y^* \equiv R_s \int_F \frac{1}{\rho}\, \omega^* \tilde{z}\, \frac{t}{n_e}\, ds = 0 \qquad (2.24)$$

$$C_z^* \equiv R_s \int_F \frac{1}{\rho}\, \omega^* \tilde{y}\, \frac{t}{n_e}\, ds = 0$$

are called the "principal generalized coordinates" of the cross section of a curved girder bridge. These coordinates are important in the sense that the governing differential equations followed in Chapter III will fall into simpler forms when they are used[4].

The first two of Eq. (2.23) determine the location of the rectangular coordinate origin called the "center of figure" of the cross section, and the last one determines the direction of the coordinate axes. Let y_o and z_o be the coordinates of this point referred to an arbitrarily chosen coordinate system $(C\text{-}\bar{x}\bar{y}\bar{z})$, as shown in Fig. 2.4. Then, the equations to determine them are obtained by substituting the relationships $y = \bar{y} - y_o$ and $z = \bar{z} - z_o$ into the first two of Eq. (2.23)

---

4) The cross sections of a curved girder bridge is not symmetrical, in general, with respect to its vertical axis; therefore, the last one of Eq. (2.23) is not necessarily fulfilled under the coordinate system $(O_n\text{-}xyz)$ established earlier. In deriving the fundamental equations, however, complexity arising from this circumstance is inconsiderably small, as can be seen later.

as follows:

$$0 = G_y = \frac{R_o}{R_s}(G_{\bar{y}} - z_o F_c)$$

$$0 = G_z = \frac{R_o}{R_s}(G_{\bar{z}} - y_o F_c) \tag{2.25}$$

where

$$G_{\bar{y}} = R_c\int_F \frac{1}{\rho}\,\bar{z}\,\frac{t}{n_e}\,ds \qquad G_{\bar{z}} = R_c\int_F \frac{1}{\rho}\,\bar{y}\,\frac{t}{n_e}\,ds$$

$$F_c = R_c\int_F \frac{1}{\rho}\,\frac{t}{n_e}\,ds \tag{2.26}$$

Then, solving Eq. (2.25) for y_o and z_o gives:

$$y_o = \frac{G_{\bar{z}}}{F_c} \qquad z_o = \frac{G_{\bar{y}}}{F_c} \tag{2.27}$$

Next, the "shear center" of the cross section is defined as the origin of the radius vector for the sectorial coordinate ω^* which satisfies the last two of Eq. (2.24). The remaining one determines the terminus of the initial radius vector, i.e., the sectorial coordinate origin. Let y_s and z_s be the coordinates of the shear center referred to the coordinate system $(O_n\text{-}xyz)$. Then, referring to Fig. 2.4, it follows that

$$r_t^* = r_t - \frac{dz}{ds}\,y_s + \frac{dy}{ds}\,z_s \tag{2.28}$$

By using Eqs. (2.23), (2.24), and (2.28), equation (2.13) can be rewritten to obtain the relationship between the warping function with respect to the shear center, ω^*, and that with respect to the center of figure, ω, in the form:

$$\omega^* = \frac{R_s}{R_o}\left\{\frac{R_s}{R_o}\,\omega - y_s z + z_s y\right\} \tag{2.29}$$

Then, substituting Eq. (2.29) into the last two of Eq. (2.24) and noting the orthogonality conditions given by the first two of Eq. (2.23) and first one of Eq. (2.24) and the relationships, $\tilde{y} = y - y_s$, $\tilde{z} = z - z_s$, and $R_s = R_o + y_s$, yields a set of equations for determining y_s and z_s as follows:

$$\begin{aligned} -\left\{J_y - \frac{C_y}{R_o}\right\} y_s + J_{yz} z_s + C_y &= 0 \\ -\left\{J_{yz} - \frac{C_z}{R_o}\right\} y_s + J_z z_s + C_z &= 0 \end{aligned} \tag{2.30}$$

where J_y and J_z are the moments of inertia of the cross-sectional area with respect to the y and z axes, respectively, and J_{yz} is the product of inertia, which are defined by

$$\begin{aligned} J_y &= R_o \int_F \frac{1}{\rho}\, z^2 \frac{t}{n_e}\, ds \qquad J_z = R_o \int_F \frac{1}{\rho}\, y^2 \frac{t}{n_e}\, ds \\ J_{yz} &= R_o \int_F \frac{1}{\rho}\, yz\, \frac{t}{n_e}\, ds \end{aligned} \tag{2.31}$$

and C_y and C_z are the sectorial products of inertia with respect to the y and z axes, respectively, defined by

$$C_y = R_o \int_F \frac{1}{\rho} \omega z \frac{t}{n_e} ds$$

$$C_z = R_o \int_F \frac{1}{\rho} \omega y \frac{t}{n_e} ds \qquad (2.32)$$

Finally, solving Eq. (2.30) for y_s and z_s gives:

$$y_s = \frac{J_z C_y - J_{yz} C_z}{\left\{J_y - \frac{C_y}{R_o}\right\} J_z - \left\{J_{yz} - \frac{C_z}{R_o}\right\} J_{yz}}$$

$$z_s = \frac{J_{yz} C_y - J_y C_z}{\left\{J_y - \frac{C_y}{R_o}\right\} J_z - \left\{J_{yz} - \frac{C_z}{R_o}\right\} J_{yz}} \qquad (2.33)$$

What is mentioned above can be briefly summarized as follows: For every cross-sectional shape of a curved girder bridge, there exist two special points on the cross section, called the "center of figure" and the "shear center", respectively. These are characterized by the conditions that $G_y = G_z = 0$ and $C_y^* = C_z^* = 0$, respectively. The locations of these points are dependent upon only the cross-sectional dimensions and

elasticity properties (n_e and n_g) of the material composing the cross section and are independent of the boundary and loading conditions.

These points have the following physical meanings: If the center of figure is chosen for the coordinates's origin, there occurs no coupling between the normal force acting in the direction of the longitudinal coordinate axis and the bending moments about the in-plane coordinate axes. In other words, the normal stresses due to these bending moments give rise to no changes in length of the longitudinal coordinate axis [see Eqs. (3.8)]. Similarly, if the shear center is chosen for the coordinates's origin, there occurs no coupling between the bending moments about the in-plane coordinate axes and torsional moment about the longitudinal coordinate axis. In other words, the shear flows due to these bending moments produce no torsional moment about the longitudinal coordinate axis, as can be seen from Eq. (3.29), along with Eqs. (3.18), (3.20), and (3.56). Hence, the resultant of the shear flows due to these bending moments passes through the shear center.

However, it should be noted that the results mentioned above hold only so far as the assumptions employed in engineering beam theory are satisfied. The assumptions are stated as follows:

(1) The displacement field in a cross section is represented by the superposition of two types of deformations obeying Euler-Bernoulli's hypothesis and Wagner's one.

(2) The shear flows due to normal force and bending

moments are determined by integrating the equilibrium equation in the longitudinal direction for a differential plate element.

(3) The integration constants in the resulting expressions for the shear flows are determined from the ficticious conditions of compatibility as indicated in Eq. (3.15).

III. MODIFIED TORSIONAL BENDING THEORIES TAKING THE INFLUENCE OF SECONDARY SHEAR DEFORMATION INTO CONSIDERATION

3.1 Introduction

As is well known, the conventional torsional bending theories [1, 2, 3, 4, 5, 6] are based on the assumption that the warping in the case of nonuniform torsion of a thin-walled girder bridge can be evaluated from the Saint-Venant theory corresponding to the local value of the rate of change of twist at the cross section considered (Wagner's hypothesis). This assumption may be allowable if the variation of twist along the axis of the girder is small, in other words, the twist is almost uniform along the axis; conversely, it is doubtful to apply this assumption to the cross sections highly restrained against warping.

The axial rate of change of the warping induces a secondary normal stress called the "warping normal stress". Then, the shear stress in equilibrium with this induced normal stress may provide the approximate so-called secondary shear stress as a correction to the first order approximation of the shear stress in restrained torsion, calculated from the Saint-Venant solution in the sense mentioned above.

It seems that, in the conventional theories, the influence of the deformation corresponding to the secondary shear stress is regarded as negligibly small. In the case of a girder with closed cross sections, however, the question that disregard of the secondary shear deformation will lead to an unsatisfactory

result, especially at the cross sections highly restrained against torsion, was brought out by Th. von Kármán and W. Z. Chien [42] and R. Heilig [10]. This is because the secondary shear deformations appear, in general, to be about the same amount as, or, according to circumstances, to be considerably greater than the primary ones evaluated from the Saint-Venant solution in the sense mentioned above. Furthermore, it should be noted that more rigid cross sections of the bridges, stiffened with sufficient numbers of diaphgrams or cross-frames, cause more accurate analysis of the shearing stresses to become more important.

Due to these reasons, some attempts to improve the weakness of the conventional theories mentioned above were made by such investigators as E. Reissner [8], S. U. Benscoter [9], R. Heilig [10], W. Graße [11], E. Schlechte [12], and K. Roik and G. Sedlacek [13]. These works, with the exception of [8], were done only in the case of a box girder bridge with a straight axis. E. Reissner's work, however, was carried out on a straight cylindrical rod with one end built in.

All of the fundamental differential equations governing torsional bending phenomenon, derived by these investigators, are of the same form and very similar to the conventional one. The coefficients in the equations serve as a measure for evaluating the effects of the secondary shear deformations on the distributions of stresses and will be called hereafter the "warping shear correction parameters". The parameters can be classified into two groupes, with the exceptions of those in

[8] and [12]: one is the parameter derived by S. U. Benscoter and the other is that derived by R. Heilig and others. Finally, by assuming that transverse shearing strain and warping one are closely connected with transverse shearing forces and warping torque or secondary torsional moment through "shear correction factors", the theory of R. Heilig's type was generalized by D. Schade [14]. In the theory, five kinds of factors in addition to that derived by R. Heilig are newly introduced. In the paper, however, no methods are presented for finding the solutions for the stress resultants and displacements developed in the girder under various loading and boundary conditions.

In the modified torsional bending theories mentioned above, however, attention is focused only on the axial displacement component of the secondary shear deformation. Recently, for the case of a single-celled straight girder bridge, N. Saeki [43] has developed another type of torsional bending theory by taking only the circumferential displacement component of the secondary shear deformation into consideration and noting the directions of the secondary shear flows in the cross sections.

It should be noted that, as stated before, torsional moments developed in the curved girder bridges play an important role in the analysis of stresses as compared with those in the straight girder bridges. In fact, they will become increasingly important with higher curvatures of the girder axes. Therefore, it would seem desirable to extend the modified torsional bending theories to the case of a curved box girder

bridge. The extension of the modified theory presented by S. U. Benscoter has been carried out by R. Dabrowski [19], in which he required that the shear flows obtained from the condition of equilibrium should satisfy the condition of compatibility as well. However, the method of formulation performed by R. Dabrowski may be available only in the case of a curved box girder bridge with a mono-symmetrical single-celled or separate twin-celled cross section. The author [22], together with his co-researcher, found that the theory of S. U. Benscoter's type could be extended to the case of a curved girder bridge with closed cross sections of arbitrary shape if Galerkin's method was applied to the condition of equilibrium expressed in terms of the kinematical quantities, such as the rate of stretch, changes in curvature, and rate of twist, of the reference axis of the girder. Similarly, the author [21], together with his co-researchers, succeeded to extend the theory presented by R. Heilig so as to be applicable to the curved box girder bridges.

3.2 Assumptions

Throughout the theories treated in this chapter, the following assumptions will be made:

(1) Cross-sectional dimensions and shape of curved box girder bridge are constant throughout its length.

(2) Any characteristic dimension of the cross section (its height or width) is small compared with the developed span length so that elastic properties can be assumed to be

concentrated along the reference axis of the girder.

(3) Deformation of an arbitrary cross section consists of that obeying Euler-Bernoulli's hypothsis and Wagner's one.

(4) Cross sections do not distort transversely.

(5) Shear lag phenomenon can be disregarded.

The other assumptions required for the developement of the theories will be made in the following sections, if necessary.

Part 1. Modified Torsional Bending Theory of First Type [21]

3.3 Developement of the Theory

3.3.1 Normal Strain and Stress

There appears to be no satisfactory theory appropriate for practical use to take the influence of the secondary shear deformation due to restrained torsion into account precisely; therefore, in the theory considered herein, the deformation will be considered only in the direction normal to the cross-sectional plane as follows: It is assumed that the transverse distribution of the warping is the same as that in pure torsion, but on the other hand, its intensity can be represented by a certain unknown function $\chi(\theta)$ instead of the rate of twist $\psi_x(\theta)$ of the reference axis of the girder, unlike the conventional theories.

Denoting by 'U' the warping at any point on the middle line

of the cross section, it then follows that

$$U = - \omega^*(s)\chi^*(\theta) \tag{3.1}$$

Moreover, one more assumption will be made that the displacement field in the cross section can be represented by superimposing the two types of deformations--the deformation which obeys the law of plane section, i.e., Euler-Bernoulli's hypothesis, and the out-of-plane deformation which obeys the law of sectorial area as indicated in Eq. (3.1). Following these assumptions, we find the components of the displacement field in the cross section in the form:

$$\begin{aligned} \tilde{u} &= u^* - \tilde{y}\phi_z^* + \tilde{z}\phi_y^* - \omega^*\chi^* \\ \tilde{v} &= v^* - \tilde{z}\phi_x^* \\ \tilde{w} &= w^* + \tilde{y}\phi_x^* \end{aligned} \tag{3.2}$$

where the quantities ϕ_x^*, ϕ_y^*, and ϕ_z^* are the rotation components of the shear center axis, which are the same as those defined in Eqs. (2.4).

Then, introducing Eq. (3.1) into the proper strain-displacement relation, the total normal strain ε_θ of any fiber of the girder can be expressed in terms of the kinematical quantities of the shear center axis, such as the rate of change of stretch ε_x^*, and the changes in curvature ψ_y^* and ψ_z^* in the $\tilde{x}\tilde{z}$ and $\tilde{x}\tilde{y}$ planes, respectively, as follows:

$$\varepsilon_\theta = \frac{R_s}{\rho}(\varepsilon_x^* - \tilde{y}\psi_z^* + \tilde{z}\psi_y^* - \omega^* \frac{1}{R_s}\frac{d\chi^*}{d\theta}) \qquad \text{(a)}$$

or, by virtue of the relationships, $\tilde{y} = y - y_s$ and $\tilde{z} = z - z_s$

$$\varepsilon_\theta = \frac{R_s}{\rho}(\varepsilon_x^* + y_s\psi_z^* - z_s\psi_y^*) - \frac{R_s}{\rho}(y\psi_z^* - z\psi_y^* + \omega^* \frac{1}{R_s}\frac{d\chi^*}{d\theta}) \qquad \text{(b)}$$

where the quantities ε_x^*, ψ_y^*, and ψ_z^* are to be referred to Eqs. (2.5). The quantity within the first parenthesis on the right side of the above equation is related to the rate of change of stretch of the centroidal axis, signified by ε_x, the relation [7] is

$$\frac{R_o}{R_s}\varepsilon_x = \varepsilon_x^* + y_s\psi_z^* - z_s\psi_y^* \qquad (3.3)$$

where the quantity ε_x is expressed as

$$\varepsilon_x = \frac{1}{R_o}(\frac{du}{d\theta} + v) \qquad (3.4)$$

Thus, Eq. (b) can be written in the more concise form:

$$\varepsilon_\theta = \frac{R_o}{\rho}\varepsilon_x - \frac{R_s}{\rho}(y\psi_z^* - z\psi_y^* + \omega^* \frac{1}{R_s}\frac{d\chi^*}{d\theta}) \qquad (3.5)$$

Since the other two normal stress components except for

the axial one may be disregarded, as is usually done in the engineering beam theory, the total normal stress σ_θ acting on the cross-sectional plane is given by

$$\sigma_\theta = \frac{1}{n_e} E_s \varepsilon_\theta \tag{3.6}$$

When this stress distribution is integrated over the entire cross-sectional area, it yields four independent stress resultants: a normal force N_x, two bending moments M_y and M_z acting about the y and z axes, respectively, and a warping moment or bimoment M_ω^* with respect to the shear center axis (Fig. 3.1). They are defined by

$$\begin{aligned} N_x &= \int_F \sigma_\theta t \, ds & M_y &= \int_F \sigma_\theta z t \, ds \\ M_z &= -\int_F \sigma_\theta y t \, ds & M_\omega^* &= \int_F \sigma_\theta \omega^* t \, ds \end{aligned} \tag{3.7}$$

Now, the problem consists in finding the expression of the normal stress represented in terms of these stress resultants. To this end, we introduce into Eqs. (3.7) the expression for σ_θ obtained from the combination of Eqs. (3.5) and (3.6) and perform the indicated integrations by taking the first two of Eqs. (2.23) and Eqs. (2.24) into account. This gives the following set of equations after some algebraic manupulations:

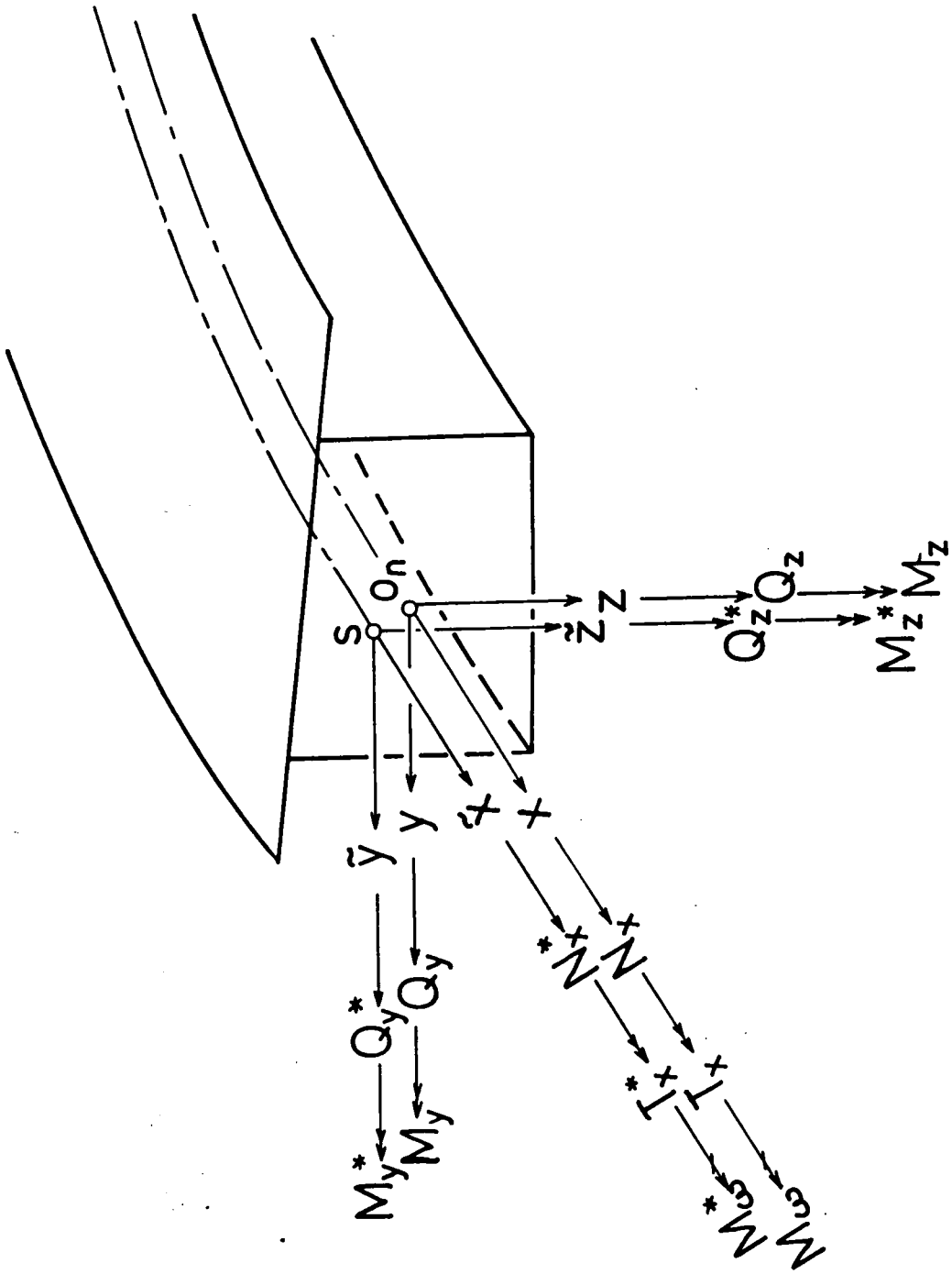

Fig. 3.1 Stress Resultants and Couples

$$\epsilon_x = \frac{N_x}{E_s F_o}$$

$$\psi_y^* = \frac{R_o}{R_s} \frac{J_z M_y + J_{yz} M_z}{E_s (J_y J_z - J_{yz}^2)}$$

$$\psi_z^* = \frac{R_o}{R_s} \frac{J_{yz} M_y + J_y M_z}{E_s (J_y J_z - J_{yz}^2)} \qquad (3.8)$$

$$\frac{1}{R_s} \frac{d\chi^*}{d\theta} = - \frac{M_\omega^*}{E_s C_\omega^*}$$

where J_y, J_z, and J_{yz} are the cross-sectional constants defined in Eq. (2.31), and the quantities C_ω^*, called the "warping constant" with respect to the shear center, and F_o are defined by

$$C_\omega^* = R_s \int_F \frac{1}{\rho} \omega^{*2} \frac{t}{n_e} ds \qquad (3.9)$$

$$F_o = R_o \int_F \frac{1}{\rho} \frac{t}{n_e} ds \qquad (3.10)$$

Finally, combining Eqs. (3.5), (3.6), and (3.8) gives:

$$\sigma_\theta = \frac{1}{n_e} \frac{R_o}{\rho} \left\{ \frac{N_x}{F_o} - \frac{J_{yz} M_y + J_y M_z}{J_y J_z - J_{yz}^2} y + \frac{J_z M_y + J_{yz} M_z}{J_y J_z - J_{yz}^2} z + \frac{R_s}{R_o} \frac{M_\omega^*}{C_\omega^*} \omega^* \right\}$$

..... (3.11)

The first three terms on the right side of Eq. (3.11) indicate the normal stress components σ_b due to stretching and bendings, determined according to the law of plane sections. The fourth term, on the other hand, indicates the normal stress component σ_ω due to the restraint against warping, determined according to the law of sectorial areas.

3.3.2 Shear Flows

Let us denote by q_σ the shear flow determined from the condition of equilibrium of a differential plate element in the longitudinal direction. The desired equilibrium equation is given by

$$\frac{\partial}{\partial\theta}(\sigma_\theta t) + \frac{1}{\rho}\frac{\partial}{\partial s}(\rho^2 q_\sigma) + \rho\tilde{p}_x = 0 \qquad (3.12)$$

where $\tilde{p}_x$ is the x component of the external forces per unit area of the middle surface of the plate elements making up the cross sections. Solving Eq. (3.12) for q_σ, we find

$$q_\sigma = \frac{R_o^2}{\rho^2}\tilde{q}_\sigma - \frac{1}{\rho^2}\int_0^s \rho\frac{\partial}{\partial\theta}(\sigma_\theta t)ds - \frac{R_o^2}{\rho^2}\int_0^s \frac{\rho^2}{R_o^2}\tilde{p}_x\, ds \qquad (3.13)$$

where the quantity $\tilde{q}_\sigma$ is an integration constant, which can be interpreted physically as the quantity related to the statically indeterminate part of the shear flow q_σ. In the case of the loading conditions encountered in practice, however,

the last term on the right side of Eq. (3.12) scarcely contributes to the value of the shear flow q_σ. Therefore, it will be disregarded hereafter. In view of Eq. (3.11), the shear flow q_σ obtained in this way, therefore, can be regarded as the sum of two components: q_b, the shear flow due to streching and bending, and q_ω, the secondary shear flow due to nonuniform torsion.

Returning now to the evaluation of the quantity $\tilde{q}_\sigma$, as in the preceeding case, we will express the quantity in terms of the new quantities $\tilde{q}^0_{\sigma,k}$ which are constant in the k-th cell, as follows (Fig. 3.2):

$$\tilde{q}_\sigma = \begin{cases} \tilde{q}^0_{\sigma,k} - \tilde{q}^0_{\sigma,k-1} & \text{on the wall of the plate element common to cells } k-1 \text{ and } k, \\ \tilde{q}^0_{\sigma,k} & \text{on the wall of the plate element belonging to k-th cell only,} \\ \tilde{q}^0_{\sigma,k} - \tilde{q}^0_{\sigma,k+1} & \text{on the wall of the plate element common to cells } k \text{ and } k+1. \end{cases} \quad \ldots\ldots\ldots\ldots\ldots\ldots \quad (3.14)$$

As in the preceeding case, the unknown quantities $\tilde{q}^0_{\sigma,k}$ can be determined from the compatibility conditions — the condition in which the continuity on the axial displacement component u_σ of the shearing strain caused by the combined action of streching, bending, and nonuniform torsion, should be restored at the hypothetical slit introduced temporarily in each cell. The condition is given by

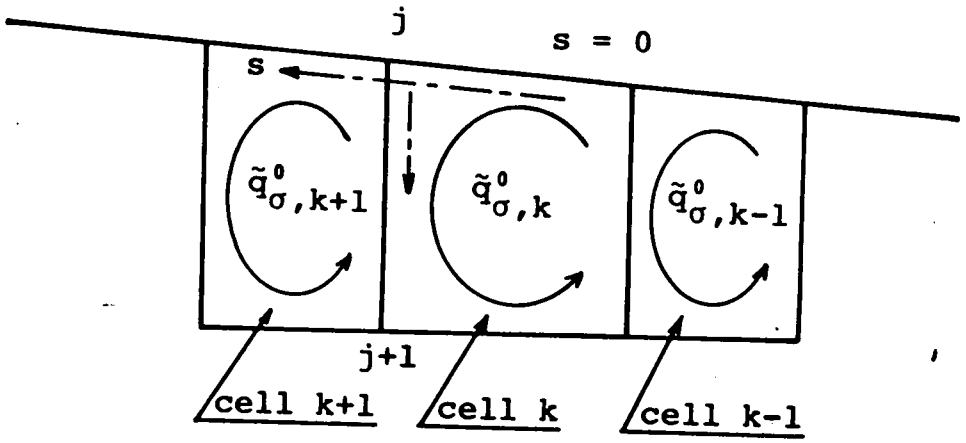

Fig. 3.2 Shear Flows in Equilibrium with Normal Stresses

$$0 = \oint_k \frac{\partial}{\partial s}\left(\frac{1}{\rho}\, u_\sigma\right) ds = \frac{1}{G_s} \oint_k \frac{1}{\rho}\, q_\sigma \frac{n_g}{t}\, ds \quad ^{1)} \qquad (3.15)$$

Substituting Eq. (3.13), together with Eq. (3.14), into Eq. (3.15), we obtain the following equation for determining the unknown quantities $\tilde{q}^0_{\sigma,k}$:

$$- \tilde{q}^0_{\sigma,k-1} \int_{k-1,k} \frac{1}{\rho^3} \frac{n_g}{t}\, ds + \tilde{q}^0_{\sigma,k} \oint_k \frac{1}{\rho^3} \frac{n_g}{t}\, ds$$

$$- \tilde{q}^0_{\sigma,k+1} \int_{k,k+1} \frac{1}{\rho^3} \frac{n_g}{t}\, ds = \frac{1}{R_o^2} \oint_k \frac{1}{\rho^3} \left\{ \int_0^s \rho \frac{\partial}{\partial \theta}(\sigma_\theta t)\, ds \right\} \frac{n_g}{t}\, ds$$

..... (3.16)

As before, one such equation is to be written for each cell.

Once the resulting set of equations is solved for the unknown quantities $\tilde{q}^0_{\sigma,k}$ in terms of the definite integrals on the right side of the equations, calculated using Eq. (3.11), the shear flow q_σ is found from Eqs. (3.11), (3.13), and (3.14). After rearrangement of the resulting expression for

---

1) According to the law of plane sections, there arises, in fact, no shearing strain corresponding to the shear flow q_b. One can, therefore, give a reason for the compatibility condition by supposing that it is based on the assumption that the contribution from tangential displacement component to the ficticious shearing strain corresponding to the shear flow q_σ may be disregarded.

I. Konishi and S. Komatsu [3], on the other hand, employed the principle of least work to find the equations of consistent deformations (the compatibility conditions) from which the statically indeterminate parts of the shear flows q_σ are determined, and obtained, of course, a result exactly agreeing with Eq. (3.15).

q_σ, it can be written finally in the form:

$$q_\sigma = q_b + q_\omega \tag{3.17}$$

where

$$q_b = K_n \frac{R_o^2}{\rho^2}(\tilde{q}_n - S_n) + K_y \frac{R_o^2}{\rho^2}(\tilde{q}_y - S_y) + K_z \frac{R_o^2}{\rho^2}(\tilde{q}_z - S_z) \tag{3.18}$$

$$q_\omega = K_\omega^* \frac{R_s^2}{\rho^2}(\tilde{q}_\omega - S_\omega^*) \tag{3.19}$$

Here, the quantities K_n, K_y, K_z, and K_ω^* are given by the formulae

$$K_n = \frac{1}{F_o} \frac{1}{R_o} \frac{dN_x}{d\theta}$$

$$K_y = -\frac{1}{J_y J_z - J_{yz}^2}\left\{J_{yz} \frac{1}{R_o} \frac{dM_y}{d\theta} + J_y \frac{1}{R_o} \frac{dM_z}{d\theta}\right\}$$

$$K_z = \frac{1}{J_y J_z - J_{yz}^2}\left\{J_z \frac{1}{R_o} \frac{dM_y}{d\theta} + J_{yz} \frac{1}{R_o} \frac{dM_z}{d\theta}\right\} \quad \ldots\ldots\ldots\ldots \tag{3.20}$$

and

$$K_\omega^* = \frac{1}{C_\omega^*} \frac{1}{R_s} \frac{dM_\omega^*}{d\theta} \tag{3.21}$$

The quantities S_n, S_y, S_z, and S_ω^* are the functions of the coordinate s defined as follows:

$$S_n(s) = \int_0^s \frac{t}{n_e}\, ds \qquad S_y(s) = \int_0^s y\, \frac{t}{n_e}\, ds$$

$$S_z(s) = \int_0^s z\, \frac{t}{n_e}\, ds \tag{3.22}$$

and

$$S_\omega^*(s) = \int_0^s \omega^*\, \frac{t}{n_e}\, ds \tag{3.23}$$

Furthermore, the quantities $\tilde{q}_n$, $\tilde{q}_y$, $\tilde{q}_z$, and $\tilde{q}_\omega$ can be represented in the forms similar to that defined in Eq. (3.14) by making use of the quantities $\tilde{q}^0_{n,k}$, $\tilde{q}^0_{y,k}$, $\tilde{q}^0_{z,k}$, and $\tilde{q}^0_{\omega,k}$ determined in the following way, respectively. The quantities $\tilde{q}^0_{n,k}$, $\tilde{q}^0_{y,k}$, $\tilde{q}^0_{z,k}$, and $(R_s/R_o)^2\tilde{q}^0_{\omega,k}$ are determined by solving the sets of equations obtained by replacing the integral within braces in Eq. (3.16) by S_n, S_y, S_z, and S_ω^*, multiplied by R_o^2, respectively. This is clear from the theory of linear algebraic equations.

As explained in Section 3.1, the shear flow q_t due to twisting is assumed to consist of a primary part q_s and a secondary one q_ω. Then, the primary shear flow q_s can be represented by eliminating ψ_x^* from Eqs. (2.10) and (2.17) as follows:

$$q_s = \frac{T_s^*}{J_T^*}\, \frac{R_s^2}{\rho^2}\, \tilde{q}_s \tag{3.24}$$

Combining Eqs. (3.19); (3.21), and (3.39), we find the expression for q_ω in the form:

$$q_\omega = \frac{T_\omega^*}{C_\omega^*} \frac{R_s^2}{\rho^2}(\tilde{q}_\omega - S_\omega^*) \tag{3.25}$$

Therefore, it follows from Eqs. (3.24) and (3.25) that

$$\begin{aligned} q_t &= q_s + q_\omega \\ &= \frac{T_s^*}{J_T^*} \frac{R_s^2}{\rho^2} \tilde{q}_s + \frac{T_\omega^*}{C_\omega^*} \frac{R_s^2}{\rho^2}(\tilde{q}_\omega - S_\omega^*) \end{aligned} \tag{3.26}$$

where T_ω^* is the secondary torsional moment about the shear center axis, which is defined by

$$T_\omega^* = \int_F q_\omega r_t^* \, ds \tag{3.27}$$

In the following, we will prove that the shear flows q_b due to stretching and bendings, determined from Eq. (3.18), create no torsional moment about the shear center axis. To this end, we will derive first the following relationship from Eq. (2.12)

$$r_t^* = \frac{1}{R_s} \rho^2 \frac{\partial}{\partial s}\left(\frac{\omega^*}{\rho}\right) + R_s \frac{1}{\rho} \tilde{q}_s \frac{n_g}{t} \tag{3.28}$$

---

2) After the analogy of a way of deriving the expression for $\dot{q}_\sigma$, the effect of distributed external warping moment m_ω^* (defined later) on the value of q_ω is disregarded

It is convenient for the derivation of the desired result to denote the components of the shear flow q_b given by the first, the second, and the third terms on the right side of Eq. (3.18) by q_n, q_y, and q_z, respectively. Then, the contribution from the shear flow q_n to the torsional moment can be evaluated using Eqs. (3.18) and (3.28) as follows:

$$\int_F q_n r_t^* \, ds = K_n \frac{R_o^2}{R_s} \sum_j \int_{j,j+1} (\tilde{q}_n - S_n) \frac{\partial}{\partial s}\left(\frac{\omega^*}{\rho}\right) ds$$

$$+ K_n R_o^2 R_s \sum_j \int_{j,j+1} \tilde{q}_s (\tilde{q}_n - S_n) \frac{1}{\rho^3} \frac{n_g}{t} \, ds$$

..... (c)

The second integral on the right side of Eq. (c) vanishes on account of the orthogonality relation given by the first one of Eqs. (3.30). The first integral on the right side of Eq. (c) can be evaluated as follows. Performing an integration by parts on the integral and transforming the result, with the definitions for q_n and S_n in mind, yields

$$K_n \frac{R_o^2}{R_s} \sum_j \int_{j,j+1} (\tilde{q}_n - S_n) \frac{\partial}{\partial s}\left(\frac{\omega^*}{\rho}\right) ds$$

$$= K_n \frac{R_o^2}{R_s} \sum_j \left[\frac{\omega^*}{\rho}(\tilde{q}_n - S_n)\right]_j^{j+1}$$

$$- K_n \frac{R_o^2}{R_s} \sum_j \int_{j,j+1} \frac{\omega^*}{\rho} \frac{\partial}{\partial s}(\tilde{q}_n - S_n) ds$$

$$= \frac{1}{R_s} \sum_j{}' \left\{ \frac{\omega^*}{\rho} \Delta_j (\rho^2 q_n) \right\} + K_n \frac{R_o^2}{R_s} \int_F \frac{1}{\rho} \omega^* \frac{t}{n_e} \, ds$$

..... (d)

It should be noted that the quantities q_n are the flow type of quantities determined in such a way that the algebraic sum of the "inflow" and "outflow" of these quantities must be equal to zero at any junctions of the plate elements. According to this fact and the first one of Eqs. (2.24), it is evident that the right side of Eq. (d) vanishes. Therefore, equation (c) becomes finally

$$\int_F q_n r_t^* \, ds = 0 \qquad \text{..... (e)}$$

Proceeding in a similar manner, with Eqs. (2.24) and (3.31) in mind, we also find that

$$\int_F q_y r_t^* \, ds = 0 \qquad \int_F q_z r_t^* \, ds = 0$$

..... (f)

Therefore, combining Eqs. (3.18), (e), and (f), we obtain the desired result as follows:

$$\int_F q_b r_t^* \, ds = 0 \qquad \text{..... (3.29)}$$

3.3.3 Orthogonality Relations

The object of this subsection is to show that there exist the orthogonality relations with a weight function $(1/\rho)(n_g/t)$ between the Saint-Venant's torsion function $\tilde{q}_s$ and a set of the shear flows q_n, q_y, q_z, and q_ω. The orthogonality relations are

$$\int_F \tilde{q}_s q_n \frac{1}{\rho}\frac{n_g}{t}\,ds = 0 \qquad \int_F \tilde{q}_s q_y \frac{1}{\rho}\frac{n_g}{t}\,ds = 0$$

$$\int_F \tilde{q}_s q_z \frac{1}{\rho}\frac{n_g}{t}\,ds = 0 \qquad \text{..... (3.30)}$$

and

$$\int_F \tilde{q}_s q_\omega \frac{1}{\rho}\frac{n_g}{t}\,ds = 0 \qquad \text{..... (3.31)}$$

These orthogonality relations can be verified in the following way. To begin with, we will take the orthogonality relation (3.31), as an example. As explained before, the compatibility condition for the shear flow q_ω developed in the k-th cell of the cross section can be expressed in terms of the quantities $\tilde{q}^0_{\omega,k}$ as follows:

$$\begin{aligned} &-\tilde{q}^0_{\omega,k-1}\int_{k-1,k}\frac{1}{\rho^3}\frac{n_g}{t}\,ds + \tilde{q}^0_{\omega,k}\oint_k \frac{1}{\rho^3}\frac{n_g}{t}\,ds \\ &-\tilde{q}^0_{\omega,k+1}\int_{k,k+1}\frac{1}{\rho^3}\frac{n_g}{t}\,ds = \oint_k \frac{1}{\rho^3} S_\omega^* \frac{n_g}{t}\,ds \end{aligned} \qquad (3.32)$$

Multiplying through both sides of Eq. (3.32) by $\tilde{q}^0_{s,k}$ and summing up a similar expression thus obtained for each cell with respect to all the cells, and then rearranging skillfully the terms on the left side of the resulting equation, leads to

$$\int_F \tilde{q}_s \tilde{q}_\omega \frac{1}{\rho^3} \frac{n_g}{t} ds = \sum_j \tilde{q}^0_{s,j} \oint_j \frac{1}{\rho^3} S_\omega^* \frac{n_g}{t} ds \qquad (3.33)$$

At the same time, the right side of Eq. (3.33) can be again transformed into the following alternative form if attention is paid to the positive directions of the flow type of quantities S_ω^*, namely,

$$\sum_j \tilde{q}^0_{s,j} \oint_j \frac{1}{\rho^3} S_\omega^* \frac{n_g}{t} ds = \int_F \tilde{q}_s S_\omega^* \frac{1}{\rho^3} \frac{n_g}{t} ds \qquad (3.34)$$

Combining Eqs. (3.33) and (3.34), we obtain

$$\int_F \tilde{q}_s (\tilde{q}_\omega - S_\omega^*) \frac{1}{\rho^3} \frac{n_g}{t} ds = 0 \qquad (3.35)$$

It is evident from Eq. (3.19) that Eq. (3.35) is equivalent to the orthogonality relation (3.31). Similarly, the remaining orthogonality relations (3.30) can be easily verified, if the same general procedure as in the preceeding case is followed.

In Appendix I, for the case of a two-celled structure, as shown in Fig. 3.3(a), we will describe Eqs. (3.33) and

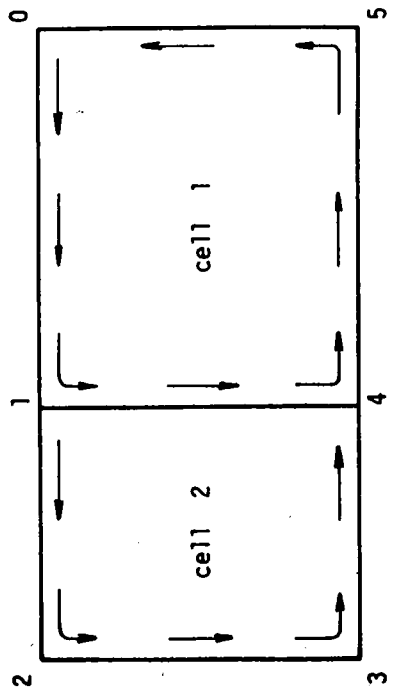

(a)

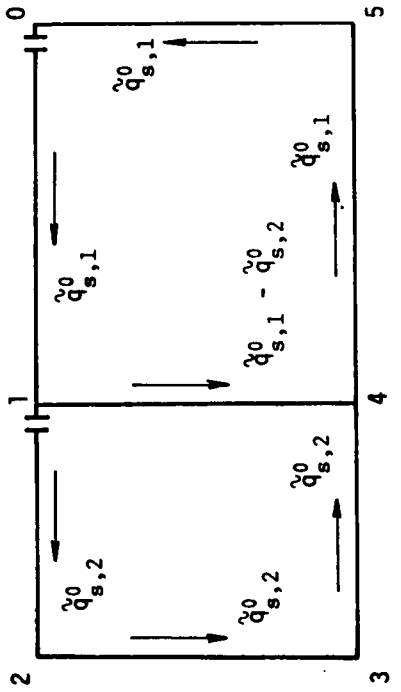

(b)

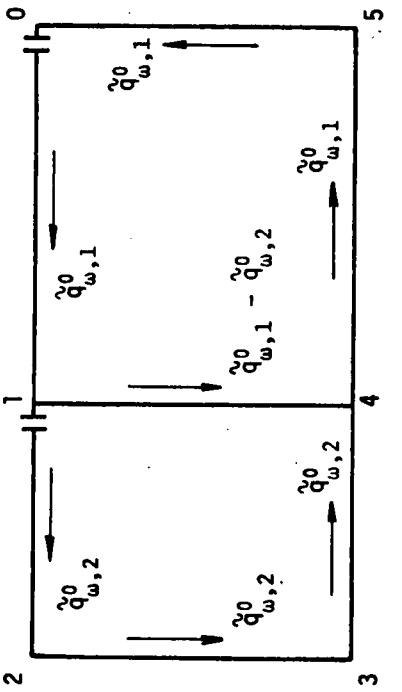

(c)

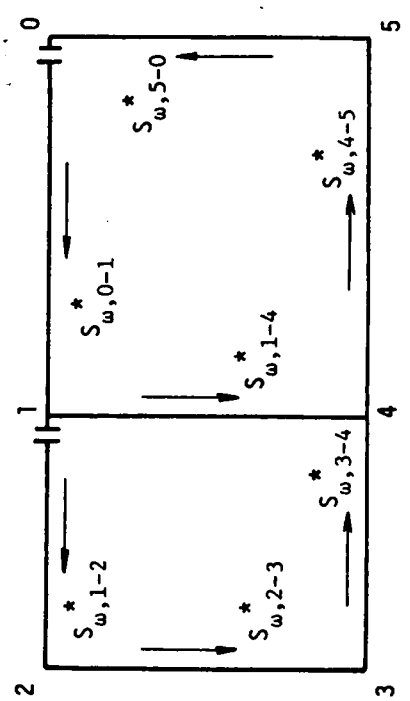

(d)

Fig. 3.3 Positive Directions of the Paths of Circumferential Integration and of the Qunatities of Flow Type for a Two-Celled Structure

(3.34) in full detail to afford a better understanding of the process of deriving these equations.

3.3.4 Relation between Warping Moment and Secondary Torsional Moment

The Galerkin's averaging technique will be employed to derive the equation relating warping moment to secondary torsional moment. Multiplying through Eq. (3.12) by ω^* and integrating the result over the entire cross-sectional area yields

$$0 = \int_F \{\frac{\partial}{\partial\theta}(\sigma_\theta t) + \frac{1}{\rho}\frac{\partial}{\partial s}(\rho^2 q_\sigma) + \rho\tilde{p}_x\}\omega^* \, ds$$

$$= \int_F \frac{\partial}{\partial\theta}(\sigma_\theta t)\omega^* \, ds + \int_F \frac{1}{\rho}\frac{\partial}{\partial s}(\rho^2 q_\sigma)\omega^* \, ds + R_s m_\omega^*$$

..... (3.36)

where the quantity m_ω^* is the external warping moment per unit length of the shear center axis, which is defined by the equation

$$m_\omega^* = \int_F \frac{\rho}{R_s}\tilde{p}_x\omega^* \, ds \qquad (3.37)$$

Introducing Eq. (3.11) into the first integral on the right side of Eq. (3.36) and performing the integration with Eqs. (2.24) and (3.9) in mind gives

$$\int_F \frac{\partial}{\partial\theta}(\sigma_\theta t)\omega^* \, ds = \frac{dM_\omega^*}{d\theta} \qquad (q)$$

An evaluation of the second integral on the right side of Eq. (3.36), however, requires performing an integration by parts on the integral, which gives

$$\int_F \frac{1}{\rho} \frac{\partial}{\partial s}(\rho^2 q_\sigma)\omega^* \, ds$$

$$= \sum_j \left[(\rho^2 q_\sigma)\frac{\omega^*}{\rho} \right]_j^{j+1} - \sum_j \int_{j,j+1} \rho^2 q_\sigma \frac{\partial}{\partial s}\left(\frac{\omega^*}{\rho}\right) ds \qquad \text{(h)}$$

By rearranging the bracketed terms in Eq. (h) and recalling that the shear flows q_σ are determined in such a way that at any junction of the plate elements the total of the "inflow" balances with that of the "outflow", we find that the first summation on the right side of Eq. (h) vanishes. This can be verified as follows:

$$\sum_j \left[(\rho^2 q_\sigma)\frac{\omega^*}{\rho} \right]_j^{j+1} = \sum_j' \left\{ \frac{\omega^*}{\rho} \Delta_j (\rho^2 q_\sigma) \right\} = 0 \qquad \text{(i)}$$

To evaluate the remaining integral on the right side of Eq. (h), it is necessary to derive the expression for $\frac{\partial}{\partial s}\left(\frac{\omega^*}{\rho}\right)$ from Eq. (2.12) as follows:

$$\frac{\partial}{\partial s}\left(\frac{\omega^*}{\rho}\right) = R_s \frac{1}{\rho^2} r_t^* - R_s^2 \tilde{q}_s \frac{1}{\rho^3} \frac{n_g}{t} \qquad (3.38)$$

Then, introducing Eq. (3.38) into the integral on the right side of Eq. (h) gives

$$\sum_j \int_{j,j+1} \rho^2 q_\sigma \frac{\partial}{\partial s}\left(\frac{\omega^*}{\rho}\right) ds$$

$$= \int_F \rho^2 q_\sigma \frac{\partial}{\partial s}\left(\frac{\omega^*}{\rho}\right) ds$$

$$= R_s \int_F q_\sigma r_t^* \, ds - R_s^2 \int_F \tilde{q}_s q_\sigma \frac{1}{\rho} \frac{n_g}{t} \, ds$$

$$= R_s \int_F q_\omega r_t^* \, ds + R_s \int_F q_b r_t^* \, ds - R_s \int_F \tilde{q}_s q_\sigma \frac{1}{\rho} \frac{n_g}{t} \, ds$$

..... (j)

According to Eq. (3.27), the first integral on the right side of Eq. (j) is nothing else but the secondary torsional moment T_ω^* about the shear center axis. The second and third integrals, on the other hand, vanish on account of Eq. (3.29) and Eqs. (3.17), (3.30), and (3.31), respectively. Thus, combining Eqs. (h), (i), and (j) yields

$$\int_F \frac{\omega^*}{\rho} \frac{\partial}{\partial s}(\rho^2 q_\sigma) ds = - R_s T_\omega^* \qquad (k)$$

Finally, by substituting Eqs. (g) and (k) into Eq. (3.36), we obtain the desired equation in the following form:

$$\frac{dM_\omega^*}{d\theta} - R_s T_\omega^* + R_s m_\omega^* = 0 \qquad (3.39)$$

3.3.5 Constitutive Equation for Warping Torque

There still remains a serious problem in establishing the constitutive equation for warping torque (secondary torsional moment). The problem encountered can be approached by making use of the principle of complementary virtual work.

Let us denote the total internal and external complementary virtual work by δU_i^* and δW_e^*, respectively. Then, the mathematical statement of the principle of complementary virtual work with the conditions of constraint is given in the form:

$$\delta J^* \equiv \delta U_i^* + \delta W_e^* + \delta \int_0^{\Theta} \left\{ \sum_{j=1}^{7} \lambda_j \Gamma_j \right\} d\theta = 0 \qquad (3.40)$$

where

Θ = opening angle of curved girder bridge,

λ_j's = Lagrange multipliers,

Γ_j's = conditions of equilibrium for stress resultants and couples.

A. Total Internal Complementary Virtual Work

Provided that the effects of the shear flows q_b due to stretching and bendings are negligible, the total internal complementary virtual work is given by the equation

$$\delta U_i^* = \int_0^{\Theta} \int_F (\varepsilon_\theta \delta\sigma_\theta + \gamma_t \frac{1}{t} \delta q_t) \rho t \, ds d\theta$$

$$= \int_0^{\Theta}\int_F \frac{n_e}{E_s}\sigma_\theta\delta\sigma_\theta\rho t\, ds d\theta + \int_0^{\Theta}\int_F \frac{n_g}{G_s}\frac{1}{t}q_t\delta q_t\rho\, ds d\theta$$

..... (3.41)

where the quantity γ_t is the shearing strain corresponding to the shear flow q_t. When the values of σ_θ from Eq. (3.11) and of its variation are introduced into the first integral on the right side of Eq. (3.41) and the integration is carried out over the entire cross-sectional area by taking the first two of Eq. (2.23) and Eq. (2.24) into account, the integral can be written as

$$\int_0^{\Theta}\int_F \frac{n_e}{E_s}\sigma_\theta\delta\sigma_\theta\rho t\, ds d\theta$$

$$= R_o\int_0^{\Theta}\frac{N_x}{E_sF_o}\delta N_x d\theta + R_o\int_0^{\Theta}\frac{J_zM_y + J_{yz}M_z}{E_s(J_yJ_z - J_{yz}^2)}\delta M_y d\theta$$

$$+ R_o\int_0^{\Theta}\frac{J_{yz}M_y + J_yM_z}{E_s(J_yJ_z - J_{yz}^2)}\delta M_z d\theta + R_s\int_0^{\Theta}\frac{M_\omega^*}{E_sC_\omega^*}\delta M_\omega^* d\theta$$

..... (1)

Substituting the values of q_t from Eq. (3.26) and of its variation into the second integral on the right side of Eq. (3.41) and noting the orthogonality condition (3.35), we find

$$\int_0^{\Theta}\int_F \frac{n_g}{G_s}\frac{1}{t}q_t\delta q_t\rho\, ds d\theta$$

$$= R_s \int_0^\Theta \frac{T_s^*}{G_s J_T^*} \delta T_s^* d\theta \frac{R_s^3}{J_T^*} \int_F \frac{1}{\rho^3} \tilde{q}_s^2 \frac{n_g}{t} ds$$

$$+ R_s \int_0^\Theta \frac{T_\omega^*}{G_s C_\omega^*} \delta T_\omega^* d\theta \frac{R_s^3}{C_\omega^*} \int_F (\tilde{q}_\omega - S_\omega^*)^2 \frac{1}{\rho^3} \frac{n_g}{t} ds$$

..... (m)

Here, we introduce the notation

$$\frac{1}{\nu^*} = R_s^3 \frac{J_T^*}{C_\omega^{*2}} \int_F (\tilde{q}_\omega - S_\omega^*)^2 \frac{1}{\rho^3} \frac{n_g}{t} ds \qquad (3.42)$$

where the quantity ν^* is a dimensionless cross-sectional constant. Then, by virtue of Eqs. (2.19) and (3.42), we can rewrite Eq. (m) as follows:

$$\int_0^\Theta \int_F \frac{n_g}{G_s} \frac{1}{t} q_t \delta q_t \rho \, ds d\theta$$

$$= R_s \int_0^\Theta \frac{T_s^*}{G_s J_T^*} \delta T_s^* d\theta + R_s \int_0^\Theta \frac{1}{\nu^*} \frac{T_\omega^*}{G_s J_T^*} \delta T_\omega^* d\theta$$

..... (n)

Finally, substituting Eqs. (m) and (n) into Eq. (3.41) gives

$$\delta U_i^* = R_o \int_0^\Theta \frac{N_x}{E_s F_o} \delta N_x d\theta + R_o \int_0^\Theta \frac{J_z M_y + J_{yz} M_z}{E_s (J_y J_z - J_{yz}^2)} \delta M_y d\theta$$

$$+ R_o \int_0^{\Theta} \frac{J_{yz}M_y + J_yM_z}{E_s(J_yJ_z - J_{yz}^2)} \delta M_z d\theta + R_s \int_0^{\Theta} \frac{M_\omega^*}{E_s C_\omega^*} \delta M_\omega^* d\theta$$

$$+ R_s \int_0^{\Theta} \frac{T_s^*}{G_s J_T^*} \delta T_s^* d\theta + R_s \int_0^{\Theta} \frac{1}{\nu^*} \frac{T_\omega^*}{G_s J_T^*} \delta T_\omega^* d\theta$$

..... (3.43)

B. Total External Complementary Virtual Work

By definition, we obtain the formula for the total external complementary virtual work in the form:

$$\delta W_e^* = - \int_{F_e} (\tilde{u}\delta\sigma_\theta + \tilde{v}\delta\tau_{\rho\theta} + \tilde{w}\delta\tau_{\theta\zeta})t \, ds$$

$$- \int_0^{\Theta} \int_F (\tilde{u}\delta\tilde{p}_x + \tilde{v}\delta\tilde{p}_y + \tilde{w}\delta\tilde{p}_z)\rho ds d\theta \qquad (3.44)$$

where the subscript F_e on the integral indicates that the integration is to be carried out over the entire cross-sectional areas at the both ends of the curved girder bridge, and

$\delta\tilde{p}_x$, $\delta\tilde{p}_y$, $\delta\tilde{p}_z$ = variations of the x, y, and z components of the distributed external loads acting on the middle surface of the plate elements.

Here, we will write down the formulae for the stress

resultants Q_y^* and Q_z^* and stress couple T_x^*, produced by the shearing stress components $\tau_{\rho\theta}$ and $\tau_{\theta\zeta}$ (Fig. 3.1). They are defined by the equations

$$Q_y^* = \int_F \tau_{\rho\theta} t \, ds \qquad Q_z^* = \int_F \tau_{\theta\zeta} t \, ds$$

$$T_x^* = \int_F (\tau_{\theta\zeta}\tilde{y} - \tau_{\rho\theta}\tilde{z}) t \, ds \tag{3.45}$$

Then, substituting Eq. (3.2) into the first integral in Eq. (3.44) and using the notations defined in Eqs. (3.7) and (3.45) yields

$$\int_{F_e} (\tilde{u}\delta\sigma_\theta + \tilde{v}\delta\tau_{\rho\theta} + \tilde{w}\delta\tau_{\theta\zeta}) t \, ds$$

$$= [u^*\delta N_x^*]_0^\Theta + [v^*\delta Q_y^*]_0^\Theta + [w^*\delta Q_z^*]_0^\Theta \tag{o}$$

$$+ [\phi_x^*\delta T_x^*]_0^\Theta + [\phi_y^*\delta M_y^*]_0^\Theta + [\phi_z^*\delta M_z^*]_0^\Theta - [\chi^*\delta M_\omega^*]_0^\Theta$$

Substituting Eqs. (3.2) into the second integral in Eq. (3.44) and performing the integration over the entire cross-sectional area gives

$$\int_0^\Theta \int_F (\tilde{u}\delta\tilde{p}_x + \tilde{v}\delta\tilde{p}_y + \tilde{w}\delta\tilde{p}_z) \rho ds d\theta$$

$$= \int_0^\Theta (u^*\delta p_x^* + v^*\delta p_y^* + w^*\delta p_z^*) R_s d\theta \tag{p}$$

$$+ \int_0^{\Theta} (\phi_x^* \delta m_x^* + \phi_y^* \delta m_y^* + \phi_z^* \delta m_z^*) R_s d\theta$$

$$- \int_0^{\Theta} \chi^* \delta m_\omega^* \, R_s d\theta$$

where

δp_x^*, δp_y^*, δp_z^* = variations of the x, y, and z components of the external loads per unit length of the shear center axis, respectively,

δm_x^*, δm_y^*, δm_z^* = variations of the x, y, and z components of the external torques per unit length of the shear center axis, respectively,

δm_ω^* = variation of the external warping moment per unit length of the shear center axis.

They are defined by the equations:

$$\delta p_x^* = \int_F \frac{\rho}{R_s} \delta \tilde{p}_x \, ds \qquad \delta p_y^* = \int_F \frac{\rho}{R_s} \delta \tilde{p}_y \, ds$$

$$\delta p_z^* = \int_F \frac{\rho}{R_s} \delta \tilde{p}_z \, ds$$

..... (3.46)

and

$$\delta m_x^* = \int_F \frac{\rho}{R_s}(\delta\tilde{p}_z\tilde{y} - \delta\tilde{p}_y\tilde{z})\, ds$$

$$\delta m_y^* = \int_F \frac{\rho}{R_s}\,\delta\tilde{p}_x\tilde{z}\, ds \qquad \delta m_z^* = \int_F \frac{\rho}{R_s}\,\delta\tilde{p}_x\tilde{y}\, ds$$

..... (3.47)

and

$$\delta m_\omega^* = \int_F \frac{\rho}{R_s}\,\delta\tilde{p}_x\omega^*\, ds \qquad (3.48)$$

We obtain finally the expression for δW_e^* by introducing Eqs. (o) and (p) into Eq. (3.44) as follows:

$$\begin{aligned}\delta W_e^* = {} & [u^*\delta N_x^*]_0^\Theta + [v^*\delta Q_y^*]_0^\Theta + [w^*\delta Q_z]_0^\Theta \\ & + [\phi_x^*\delta T_x^*]_0^\Theta + [\phi_y^*\delta M_y^*]_0^\Theta + [\phi_z^*\delta M_z^*]_0^\Theta - [\chi^*\delta M_\omega^*]_0^\Theta \\ & - \int_0^\Theta (u^*\delta p_x^* + v^*\delta p_y^* + w^*\delta p_z^*) R_s d\theta \\ & - \int_0^\Theta (\phi_x^*\delta m_x^* + \phi_y^*\delta m_y^* + \phi_z^*\delta m_z^*) R_s d\theta \\ & + \int_0^\Theta \chi^*\delta m_\omega^*\, R_s d\theta\end{aligned}$$

..... (3.49)

C. Auxiliary Conditions

The structural analysis with the aid of the principle of complementary virtual work introduces, in general, the stress resultants and couples as the argument functions [see Eqs. (3.43) and (3.49)]. However, not all the functions are independent because the stress resultants and couples are related with one another through the conditions of equilibrium. As is well known, the Lagrangian multiplier method makes it possible to treat these statical quantities as the independent argument functions if the conditions of equilibrium are taken as the auxiliary conditions.

Referring now to Fig. 3.4, we find the conditions of equilibrium for the stress resultants and couples from the geometrical considerations as follows:

(1) From the requirement of equilibrium of forces in the directions of the $\tilde{x}$, $\tilde{y}$, and $\tilde{z}$ axes, respectively, it follows that

$$\begin{aligned} \Gamma_1 &\equiv \frac{dN_x^*}{d\theta} + Q_y^* + R_s p_x^* = 0 \\ \Gamma_2 &\equiv \frac{dQ_y^*}{d\theta} - N_x^* + R_s p_y^* = 0 \\ \Gamma_3 &\equiv \frac{dQ_z^*}{d\theta} + R_s p_z^* = 0 \end{aligned} \tag{3.50}$$

(2) From the requirement of equilibrium of moments about

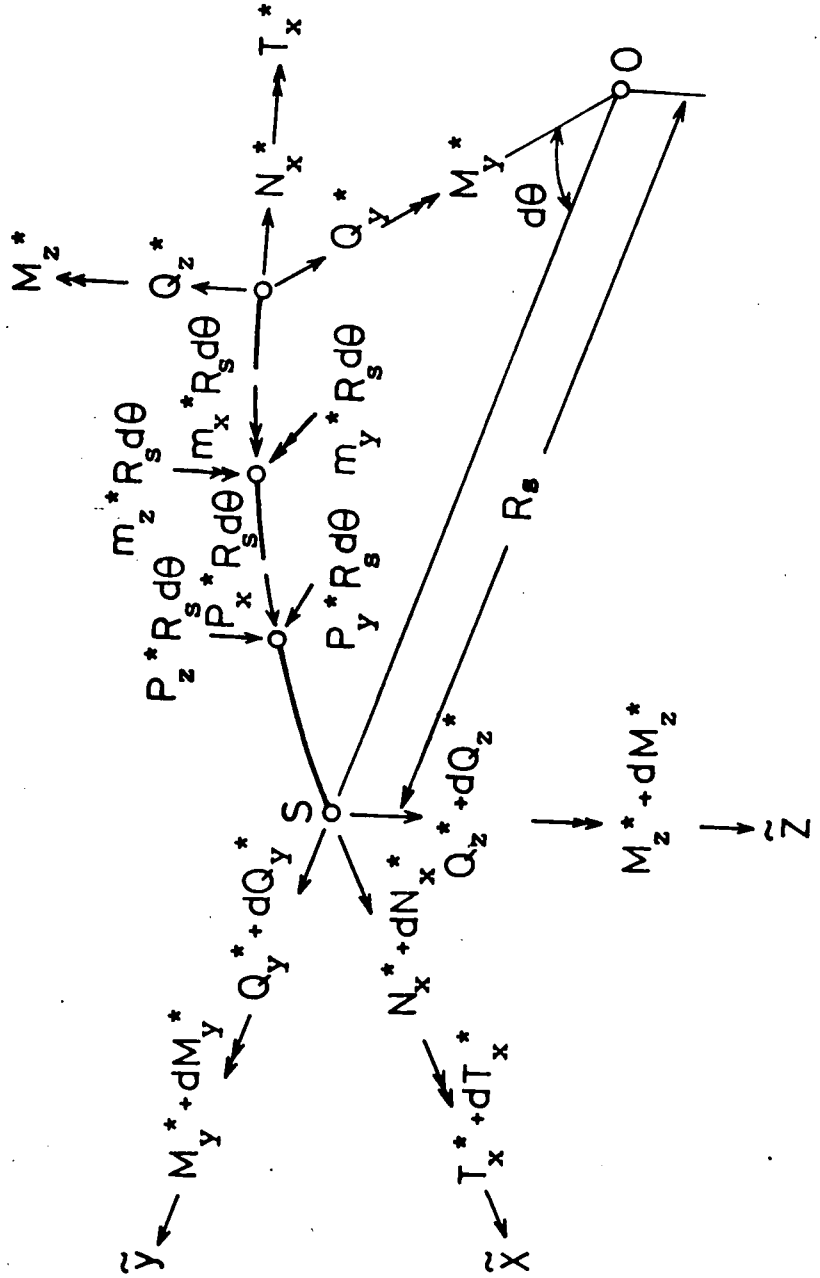

Fig. 3.4 Typical Differential Element of Curved Girder

the $\tilde{x}$, $\tilde{y}$, and $\tilde{z}$ axes, respectively, it follows that

$$\Gamma_4 \equiv \frac{dT_x^*}{d\theta} + M_y^* + R_s m_x^* = 0$$

$$\Gamma_5 \equiv \frac{dM_y^*}{d\theta} - T_x^* - R_s Q_z^* + R_s m_y^* = 0 \qquad (3.51)$$

$$\Gamma_6 \equiv \frac{dM_z^*}{d\theta} + R_s Q_y^* + R_s m_z^* = 0$$

(3) One more auxiliary condition is given by Eq. (3.39), namely,

$$\Gamma_7 \equiv \frac{dM_\omega^*}{d\theta} - R_s T_\omega^* + R_s m_\omega^* = 0 \qquad (3.52)$$

Then, integrating Γ_j ($j = 1, 2, \ldots, 7$) multiplied by λ_j ($j = 1, 2, \ldots, 7$) with respect to θ from 0 to Θ and taking the first variations of the resulting integrals yields

$$\delta \int_0^\Theta \lambda_1 \Gamma_1 \, d\theta$$

$$= [\lambda_1 \delta N_x^*]_0^\Theta + \int_0^\Theta \left\{ - \frac{d\lambda_1}{d\theta} \delta N_x^* + \lambda_1 \delta Q_y^* + \lambda_1 R_s \delta p_x^* \right\} d\theta$$

$$\delta \int_0^\Theta \lambda_2 \Gamma_2 \, d\theta$$

$$= [\lambda_2 \delta Q_y^*]_0^\Theta + \int_0^\Theta \left\{ - \frac{d\lambda_2}{d\theta} \delta Q_y^* - \lambda_2 \delta N_x^* + \lambda_2 R_s \delta p_y^* \right\} d\theta$$

$$\delta \int_0^{\Theta} \lambda_3 \Gamma_3 \, d\theta$$

$$= [\lambda_3 \delta Q_z^*]_0^{\Theta} + \int_0^{\Theta} \left\{ - \frac{d\lambda_3}{d\theta} \delta Q_z^* + \lambda_3 R_s \delta p_z^* \right\} d\theta$$

..... (3.53)

and

$$\delta \int_0^{\Theta} \lambda_4 \Gamma_4 \, d\theta$$

$$= [\lambda_4 \delta T_x^*]_0^{\Theta} + \int_0^{\Theta} \left\{ - \frac{d\lambda_4}{d\theta} \delta T_x^* + \lambda_4 \delta M_y^* + \lambda_4 R_s \delta m_x^* \right\} d\theta$$

$$\delta \int_0^{\Theta} \lambda_5 \Gamma_5 \, d\theta$$

$$= [\lambda_5 \delta M_y^*]_0^{\Theta} + \int_0^{\Theta} \left\{ - \frac{d\lambda_5}{d\theta} \delta M_y^* - \lambda_5 \delta T_x^* - \lambda_5 R_s \delta Q_z^* \right.$$

$$\left. + \lambda_5 R_s \delta m_y^* \right\} d\theta$$

$$\delta \int_0^{\Theta} \lambda_6 \Gamma_6 \, d\theta$$

$$= [\lambda_6 \delta M_z^*]_0^{\Theta} + \int_0^{\Theta} \left\{ - \frac{d\lambda_6}{d\theta} \delta M_z^* + \lambda_6 R_s \delta Q_y^* + \lambda_6 R_s \delta m_z^* \right\} d\theta$$

..... (3.54)

and

$$\delta \int_0^{\Theta} \lambda_7 \Gamma_7 \, d\theta$$

$$= [\lambda_7 \delta M_\omega^*]_0^{\Theta} + \int_0^{\Theta} \left\{ - \frac{d\lambda_7}{d\theta} \delta M_\omega^* - \lambda_7 R_s \delta T_\omega^* + \lambda_7 R_s \delta m_\omega^* \right\} d\theta$$

..... (3.55)

It is clear from the calculus of variation that the last term on the right side of Eq. (3.40) is equal to the summation of Eqs. (3.53), (3.54), and (3.55).

D. Final Result

Substituting Eqs. (3.43), (3.49), (3.53), (3.54), and (3.55) into Eq. (3.40) and then rearranging the resulting equation with the following relationships in mind, namely,

$$\begin{aligned} N_x^* &= N_x & T_x^* &= T_s^* + T_\omega^* \\ Q_y^* &= Q_y & M_y^* &= M_y - z_s N_x \\ Q_z^* &= Q_z & M_z^* &= M_z + y_s N_x \end{aligned} \qquad (3.56)$$

we obtain, finally, the expression for δJ^* in the following form:

$$0 = \delta J^* = [(\lambda_1 - z_s\lambda_5 + y_s\lambda_6 - u^* + z_s\phi_y^* - y_s\phi_z^*)\delta N_x]_0^{\Theta}$$

$$+ [(\lambda_2 - v^*)\delta Q_y^*]_0^{\Theta} + [(\lambda_3 - w^*)\delta Q_z^*]_0^{\Theta}$$

$$+ [(\lambda_5 - \phi_x^*)\delta T_s^*]_0^{\Theta} + [(\lambda_4 - \phi_x^*)\delta T_\omega^*]_0^{\Theta}$$

$$+ \left[(\lambda_5 - \phi_y^*)\delta M_y\right]_0^\Theta + \left[(\lambda_6 - \phi_z^*)\delta M_z\right]_0^\Theta$$

$$+ \left[(\lambda_7 + \chi^*)\delta M_\omega^*\right]_0^\Theta$$

$$+ \int_0^\Theta \left\{R_s \frac{N_x}{E_s F_o} - \frac{d\lambda_1}{d\theta} + z_s \frac{d\lambda_5}{d\theta} - y_s \frac{d\lambda_6}{d\theta} - \lambda_2 - z_s\lambda_4\right\}\delta N_x \, d\theta$$

$$+ \int_0^\Theta \left\{- \frac{d\lambda_2}{d\theta} + \lambda_1 + R_s\lambda_6\right\}\delta Q_y^* \, d\theta$$

$$+ \int_0^\Theta \left\{- \frac{d\lambda_3}{d\theta} - R_s\lambda_5\right\}\delta Q_z^* \, d\theta$$

$$+ \int_0^\Theta \left\{R_o \frac{J_z M_y + J_{yz} M_z}{E_s(J_y J_z - J_{yz}^2)} - \frac{d\lambda_5}{d\theta} + \lambda_4\right\}\delta M_y \, d\theta$$

$$+ \int_0^\Theta \left\{R_o \frac{J_{yz} M_y + J_y M_z}{E_s(J_y J_z - J_{yz}^2)} - \frac{d\lambda_6}{d\theta}\right\}\delta M_z \, d\theta$$

$$+ \int_0^\Theta \left\{R_s \frac{T_s^*}{G_s J_T^*} - \frac{d\lambda_4}{d\theta} - \lambda_5\right\}\delta T_s^* \, d\theta$$

$$+ \int_0^\Theta \left\{\frac{1}{\nu^*} R_s \frac{T_\omega^*}{G_s J_T^*} - \frac{d\lambda_4}{d\theta} - \lambda_5 - R_s\lambda_7\right\}\delta T_\omega^* \, d\theta$$

$$+ \int_0^\Theta \left\{R_s \frac{M_\omega^*}{E_s C_\omega^*} - \frac{d\lambda_7}{d\theta}\right\}\delta M_\omega^* \, d\theta$$

$$+ R_s\int_0^{\Theta}(\lambda_1 - u^*)\delta p_x^*\, d\theta + R_s\int_0^{\Theta}(\lambda_2 - v^*)\delta p_y^*\, d\theta$$

$$+ R_s\int_0^{\Theta}(\lambda_3 - w^*)\delta p_z^*\, d\theta + R_s\int_0^{\Theta}(\lambda_4 - \phi_x^*)\delta m_x^*\, d\theta$$

$$+ R_s\int_0^{\Theta}(\lambda_5 - \phi_y^*)\delta m_y^*\, d\theta + R_s\int_0^{\Theta}(\lambda_6 - \phi_z^*)\delta m_z^*\, d\theta$$

$$+ R_s\int_0^{\Theta}(\lambda_7 + \chi^*)\delta m_\omega^*\, d\theta$$

..... (3.57)

Since δJ^* vanishes for arbitrary variations δN_x, δQ_y^*, ... , δM_z, δM_ω^*, δp_x^*, δp_y^*, ... , δm_z^*, δm_ω^*, each term within braces and parentheses in Eq. (3.57) must vanish independently. Therefore, the following system of relations is obtained:

at the boundaries $\theta = 0$ and $\theta = \Theta$,

$$\lambda_1 - z_s\lambda_5 + y_s\lambda_6 - u^* + z_s\phi_y^* - y_s\phi_z^* = 0$$

$$\lambda_2 - v^* = 0 \qquad \lambda_3 - w^* = 0$$

$$\lambda_4 - \phi_x^* = 0 \qquad \lambda_5 - \phi_y^* = 0$$

$$\lambda_6 - \phi_z^* = 0 \qquad \lambda_7 + \chi^* = 0$$

..... (3.58)

along the girder axis,

$$R_s \frac{N_x}{E_s F_o} - \frac{d\lambda_1}{d\theta} + z_s \frac{d\lambda_5}{d\theta} - y_s \frac{d\lambda_6}{d\theta} - \lambda_2 - z_s\lambda_4 = 0$$

$$- \frac{d\lambda_2}{d\theta} + \lambda_1 + R_s\lambda_6 = 0$$

$$\frac{d\lambda_3}{d\theta} + R_s\lambda_5 = 0$$

$$R_o \frac{J_z M_y + J_{yz} M_z}{E_s (J_y J_z - J_{yz}^2)} - \frac{d\lambda_5}{d\theta} + \lambda_4 = 0$$

$$R_o \frac{J_{yz} M_y + J_y M_z}{E_s (J_y J_z - J_{yz}^2)} - \frac{d\lambda_6}{d\theta} = 0$$

$$R_s \frac{T_s^*}{G_s J_T^*} - \frac{d\lambda_4}{d\theta} - \lambda_5 = 0$$

$$\frac{1}{\nu^*} R_s \frac{T_\omega^*}{G_s J_T^*} - \frac{d\lambda_4}{d\theta} - \lambda_5 - R_s\lambda_7 = 0$$

$$R_s \frac{M_\omega^*}{E_s C_\omega^*} - \frac{d\lambda_7}{d\theta} = 0$$

..... (3.59)

and

$$\lambda_1 - u^* = 0 \qquad \lambda_2 - v^* = 0$$

$$\lambda_3 - w^* = 0 \qquad \lambda_4 - \phi_x^* = 0$$

$$\lambda_5 - \phi_y^* = 0 \qquad \lambda_6 - \phi_z^* = 0$$

$$\lambda_7 + \chi^* = 0$$

..... (3.60)

Finally, the constitutive equation for T_ω^* is found by introducing the values of λ_4 and λ_5 from Eqs. (3.60) into the seventh one of Eqs. (3.59) and taking the first two of Eqs. (2.4) into account. The result is as follows:

$$T_\omega^* = \nu^* G_s J_T^* \left\{ \frac{1}{R_s} \left(\frac{d\lambda_4}{d\theta} + \lambda_5 \right) + \lambda_7 \right\}$$

$$= \nu^* G_s J_T^* \left\{ \frac{1}{R_s} \left(\frac{d\phi}{d\theta} - \frac{1}{R_s} \frac{dw^*}{d\theta} \right) - \chi^* \right\}$$

..... (3.61)

or, by virtue of the second one of Eqs. (2.5),

$$T_\omega^* = \nu^* G_s J_T^* (\psi_x^* - \chi^*) \qquad (3.62)$$

Similarly, the values of Lagrange multipliers thus determined are introduced into the remaining ones of Eqs. (3.59), we find, as a matter of course, that the second and third ones of Eqs. (3.59) are identically satisfied and the remaining ones are in agreement with the results obtained earlier.

3.3.6 Formulation of Practical Governing Equations

In this subsection, we will restrict our study to the analysis of a curved box girder bridge supported in the manner shown in Fig. 3.5, loaded normal to the plane of its initial curvature. From the point of view of the design of the bridges, the analytical model considered herein is important practically.

The supports are such that radial and transverse displacements, and twist, are prevented at both ends of the bridge. Displacement in the longitudinal direction is permitted at one end, as are the rotations about the horizontal y-axis and vertical z-axis at both ends. The loads can be decomposed into two components p_z and m_x, that is, the other components p_x, p_y, m_y, m_z, and m_ω vanish.

Then, the analysis may be simplified since no stress resultants N_x and Q_y and stress couple M_z are developed along the girder axis under these boundary and loading conditions. Furthermore, we will avoid the unnecessary complexity of obtaining an exact description of the governing equations by assuming that the discrepancy between the shear center and the centroid can be disregarded, as it is a small quantity in comparison with the radius of curvature of a girder axis. This assumption may be admissible in the case of the curved box girder bridges in actual use, however. Therefore, we may put the ratio of R_o to R_s as unity. For the sake of simplicity, we will use the notation R hereafter in place of the radii of curvature R_o and R_s.

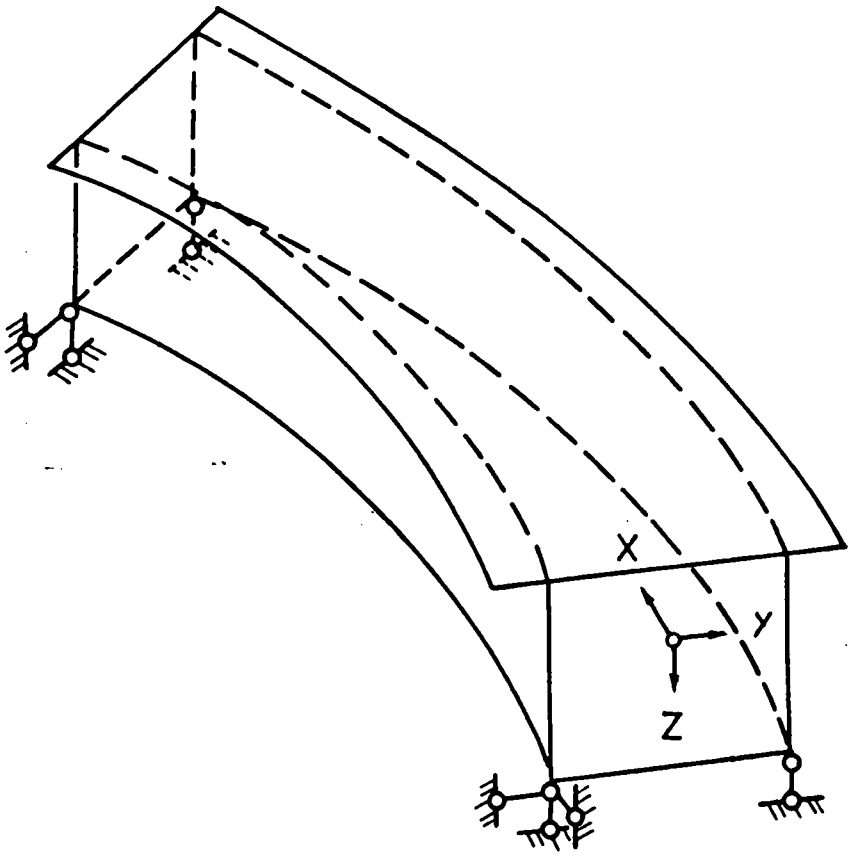

Fig. 3.5 Horizontally Curved Box Girder Bridge with Simply Supported Ends

With these assumptions, we will now derive the differential equations for determining the statical and kinematical quantities in the following way.

By eliminating Q_z^* and T_x^* from the last one of Eqs. (3.50) and the first two of Eqs. (3.51) and making use of the relationship $M_y^* = M_y - z_s N_x$ ($N_x = 0$), we get the differential equation governing M_y as follows:

$$\frac{d^2 M_y}{d\theta^2} + M_y = - R(Rp_z + m_x^*) \tag{3.63}$$

The second of Eqs. (3.56) and Eqs. (2.17) and (3.62) are combined to obtain the expression for ψ_x^* in the form:

$$\psi_x^* = \kappa^{*2}\chi^* + (1 - \kappa^{*2})\frac{T_x^*}{G_s J_T^*} \tag{q}$$

where

$$\kappa^{*2} = \frac{\nu^*}{1 + \nu^*} \tag{3.64}$$

In a special case where the cross-sectional property κ^* is permitted to approach unity (which is the same as the factor ν^* is permitted to approach infinity), we find from Eq. (q) that the intensity of warping, χ^*, coincides with the rate of twist of the shear center axis, ψ_x^*. Consequently, the conventional torsional bending theories may be regarded as a special case of the theory developed by the author.

Then, substituting Eq. (q) back into Eq. (3.62) gives:

$$T_\omega^* = \kappa^{*2}(T_x^* - G_s J_T^* \chi^*) \qquad (r)$$

The last one of Eqs. (3.8) and Eq. (3.39) are combined to obtain an alternative expression for T_ω^* in the form:

$$T_\omega^* = - E_s C_\omega^* \frac{1}{R^2} \frac{d^2\chi^*}{d\theta^2} \qquad (s)$$

Eliminating T_ω^* from Eqs. (r) and (s) yields

$$E_s C_\omega^* \frac{1}{R^2} \frac{d^2\chi^*}{d\theta^2} - \kappa^{*2} G_s J_T^* \chi^* = - \kappa^{*2} T_x^* \qquad (t)$$

We can eliminate χ^* and T_x^* from the first derivative of Eq. (t) with respect to θ by the use of the last one of Eqs. (3.8), the first of Eqs. (3.51), and the fourth of Eqs. (3.56) to obtain the governing differential equation for M_ω^*. The result is as follows:

$$\frac{d^2 M_\omega^*}{d\theta^2} - \kappa^{*2}\mu^{*2} M_\omega^* = - \kappa^{*2} R(M_y + R m_x^*) \qquad (3.65)$$

where the quantity μ^* is the dimensionless cross-sectional property defined by the equation

$$\mu^{*2} = R^2 \frac{G_s J_T^*}{E_s C_\omega^*} \qquad (3.66)$$

Eliminating w^* from the second and third of Eqs. (2.5)

leads to the relation

$$\frac{d\psi_x^*}{d\theta} - \psi_y^* = \frac{1}{R}\left(\frac{d^2\phi}{d\theta} + \phi\right) \qquad (u)$$

In a similar way, we can eliminate χ^* and T_x^* from the first derivative of Eq. (q) with respect to θ. This results in the relation:

$$\frac{d\psi_x^*}{d\theta} = (\kappa^{*2} - 1)\frac{1}{G_s J_T^*}(M_y + Rm_x^*) - \kappa^{*2}\frac{R}{E_s C_\omega^*} M_\omega^*$$

..... (v)

Then, substituting the second of Eqs. (3.8) and Eq. (v) into Eq. (u) yields the governing differential equation for ϕ as follows:

$$\frac{d^2\phi}{d\theta^2} + \phi$$

$$= \frac{1}{G_s J_T^*}\{(\kappa^{*2} - \beta - 1)RM_y - \kappa^{*2}\mu^{*2}M_\omega^* + (\kappa^{*2} - 1)R^2 m_x^*\}$$

..... (3.67)

where

$$\beta = \frac{G_s}{E_s}\frac{J_z J_T^*}{J_y J_z - J_{yz}^2} \qquad (3.68)$$

Combining the third of Eqs. (2.5) and the second of Eqs. (3.8) yields the differential equation for determining w^*:

$$\frac{d^2w^*}{d\theta^2} = - \frac{R^2 J_z}{E_s (J_y J_z - J_{yz}^2)} M_y - R\phi \qquad (3.69)$$

For the convenience of further studies, we will analyse the aforementioned curved box girder bridge under the loading conditions in which external concentrated torque $\tilde{T}$ and force $\tilde{P}$ act at some angle $\theta = \Phi$, and external bending and warping moments act at both ends of the bridge. Then, the statical and kinematical boundary conditions at both ends are given as follows:

$$\left.\begin{array}{ll} M_y = M_{y1}, & M_\omega^* = M_{\omega 1}^*, \\ \phi = 0, & w^* = 0 \end{array}\right\} \quad \text{at} \quad \theta = 0$$

$$\left.\begin{array}{ll} M_y = M_{y2}, & M_\omega^* = M_{\omega 2}^*, \\ \phi = 0, & w^* = 0 \end{array}\right\} \quad \text{at} \quad \theta = \Theta \qquad (3.70)$$

where Θ is the opening angle of the curved girder bridge.

We can determine M_y, M_ω^*, ϕ, and w^* without difficulty by solving Eqs. (3.63), (3.65), (3.67), and (3.69), since the right hand sides of these differential equations become known quantities when the equations are solved in this sequence. Since ψ_x^* is determined from the second of Eqs. (2.5) once ϕ and w^* are solved, we can find T_s^* from Eq. (2.17). Furthermore, T_ω^* can be determined by substituting M_ω^* into Eq. (3.39), and χ^* is determined from Eq. (3.62) by using ψ_x^* and T_ω^* thus obtained.

Part 2. Modified Torsional Bending Theory of Second Type

3.4 Formulation Performed by R. Dabrowski [19, 20]

In his works, the method of analysis was presented only in the case of a single-celled or separate twin-celled curved girder bridge with a vertical axis of symmetry[3]. In this section, however, the outline of the method of analysis for the former case will be presented.

In formulating the governing equations, he expressed none of the required quantities rigorously in terms of the cylindrical coordinates and especially substituted the geometrical quantities of the straight girder bridge for those of the curved girder bridge.

3.4.1 Secondary Normal Stress

After the analogy of S. U. Benscoter, R. Heilig represeneted the warping displacement U of a cross section in the form

$$U = - \hat{\omega}(s)\tilde{\chi}(\theta) \tag{3.71}$$

For a single-celled cross section, Saint-Venant's warping function $\hat{\omega}$ with respect to the shear center is given by the equation

---

3) As for the special case where the aforementioned cross sections are tilted, he proposed a way to modify the formulae for the cross-sectional constants [20].

$$\omega = \int_0^s r\,ds - \frac{\Omega}{\oint \frac{1}{t}\,ds} \int_0^s \frac{1}{t}\,ds \tag{3.72}$$

where r is the perpendicular distance from the shear center to the tangent drawn at any point on the contour of the cross section and Ω is the doubled area enclosed by the middle line of the cross section. It is convenient for the further analysis to note that Ω can be written as

$$\Omega = \oint r\,ds \tag{3.73}$$

Now, the secondary normal stress σ_ω due to restraint against warping is given by using Eq. (3.71) as follows:

$$\sigma_\omega = E\,\frac{1}{R}\,\frac{\partial U}{\partial \theta} = -\,E\,\frac{1}{R}\,\frac{d\tilde{\chi}}{d\theta}\,\omega \tag{3.74}$$

Using Eq. (3.74), the warping moment M_ω can be written as

$$M_\omega = \int_F \sigma_\omega \omega\,t\,ds = -\,EC_\omega\,\frac{1}{R}\,\frac{d\tilde{\chi}}{d\theta} \tag{3.75}$$

where

$$C_\omega = \int_F \omega^2\,t\,ds \tag{3.76}$$

Finally, combining Eqs. (3.74) and (3.75) gives

$$\sigma_{\omega} = \frac{M_{\hat{\omega}}}{C_{\hat{\omega}}} \hat{\omega} \tag{3.77}$$

3.4.2 Shear Flows Determined by Two Distinct Ways

The formula for the shear flow q_t due to restrained torsion can be obtained in two distinct ways, i.e., (a) by using an equilibrium condition, and (b) by using a strain-displacement relation. In the following, the superscripts (a) and (b) will be attached to the shear flows found by these means to distinguish one from another.

One method is as follows: By substituting Eq. (3.77) into the following equation of the equilibrium

$$\frac{1}{R} \frac{\partial \sigma_{\omega}}{\partial \theta} + \frac{\partial q_t}{\partial s} = 0 \tag{3.78}$$

and solving the above equation for q_t, we find

$$q_t^{(a)} = q_o - \frac{1}{R} \frac{dM_{\hat{\omega}}}{d\theta} \frac{S_{\hat{\omega}}}{C_{\hat{\omega}}} \tag{3.79}$$

where

$$S_{\hat{\omega}} = \int_0^s \hat{\omega}\, t\, ds \tag{3.80}$$

The integration constant q_o is to be determined by the requirement that the total torsional moment $T_{\tilde{x}}$ about the

shear center axis should be produced by the shear flows $q_t^{(a)}$, namely,

$$T_{\tilde{x}} = \int_F q_t^{(a)} r \, ds$$
$$= q_o \oint r ds - \frac{1}{C_{\hat{\omega}}} \frac{1}{R} \frac{dM_{\hat{\omega}}}{d\theta} \int_F S_{\hat{\omega}} r \, ds \tag{3.81}$$

from which, in view of Eq. (3.73), the constant q_o is found in the form:

$$q_o = \frac{T_{\tilde{x}}}{\Omega} - \frac{1}{C_{\hat{\omega}}\Omega} \frac{1}{R} \frac{dM_{\hat{\omega}}}{d\theta} \int_F S_{\hat{\omega}} r \, ds \tag{3.82}$$

Finally, substituting Eq. (3.82) into Eq. (3.79) gives

$$q_t^{(a)} = \frac{T_{\tilde{x}}}{\Omega} - \frac{1}{C_{\hat{\omega}}} \frac{1}{R} \frac{dM_{\hat{\omega}}}{d\theta} \left(S_{\hat{\omega}} - \frac{1}{\Omega} \int_F S_{\hat{\omega}} r \, ds \right) \tag{3.83}$$

Another method is as follows: According to the proper strain-displacement relation, the following equation holds

$$\frac{q_t}{Gt} = \frac{\partial U}{\partial s} + r\psi_{\tilde{x}} \tag{3.84}$$

where $\psi_{\tilde{x}}$ is the rate of change of twist of the shear center axis. By substituting Eq. (3.71) into Eq. (3.84) and making use of Eq. (3.72), we find another expression for q_t in the

form:

$$q_t^{(b)} = G\left[(\psi_{\tilde{x}} - \tilde{\chi})rt + \frac{\Omega}{\oint \frac{1}{t}\,ds}\,\tilde{\chi}\right] \tag{3.85}$$

3.4.3 Fundamental Equations in Torsional Bending

Solving Eq. (3.84) for U gives

$$U = U_o + \frac{1}{G}\int_0^s q_t \frac{1}{t}\,ds - \psi_{\tilde{x}}\int_0^s rds \tag{3.86}$$

where U_o represents the warping at $s = 0$. By performing the indicated integration around the entire closed contour of the cross section, we get the following condition of compatibility:

$$\frac{1}{G}\oint q_t \frac{1}{t}\,ds - \psi_{\tilde{x}}\Omega = 0 \tag{3.87}$$

The shear flow $q_t^{(b)}$ defined in Eq. (3.85) satisfies this condition identically. On the other hand, $q_t^{(a)}$ defined in Eq. (3.83) satisfies the following condition of equilibrium:

$$T_{\tilde{x}} = \int_F q_t r\,ds \tag{3.88}$$

Therefore, it seems reasonable to require that $q_t^{(a)}$ and $q_t^{(b)}$ should satisfy the other condition in each other, that is,

$$\frac{1}{G}\oint q_t^{(a)} \frac{1}{t} ds - \psi_{\tilde{x}}\Omega = 0 \tag{3.89}$$

and

$$T_{\tilde{x}} = \int_F q_t^{(b)} r \, ds \tag{3.90}$$

Substituting Eq. (3.83) into Eq. (3.89) results in the following equation after some algebraic maniplations, namely,

$$EC_{\hat{\Omega}} \frac{1}{R^2} \frac{d^2\tilde{\chi}}{d\theta^2} - GJ_{\hat{T}}\psi_{\tilde{x}} = - T_{\tilde{x}} \tag{3.91}$$

where

$$J_{\hat{T}} = \frac{\Omega^2}{\oint \frac{1}{t} ds} \tag{3.92}$$

Similarly, it follows from Eq. (3.90) that

$$\psi_{\tilde{x}} = \hat{\eta}^2\tilde{\chi} + (1 - \hat{\eta}^2)\frac{T_{\tilde{x}}}{GJ_{\hat{T}}} \tag{3.93}$$

where

$$\hat{\eta}^2 = 1 - \frac{J_{\hat{T}}}{J_{\hat{C}}} \tag{3.94}$$

and

$$J_{\hat{C}} = \int_F r^2 t \, ds \tag{3.95}$$

Then, we can eliminate $\psi_{\tilde{x}}$ from Eqs. (3.91) and (3.93) to obtain the differential equation governing $\tilde{\chi}$ in the form:

$$EC_{\hat{\omega}} \frac{1}{R^2} \frac{d^2\tilde{\chi}}{d\theta^2} - \hat{n}^2 GJ_{\hat{T}}\tilde{\chi} = - \hat{n}^2 T_{\tilde{x}} \tag{3.96}$$

Finally, by the same means as in the case of deriving Eq. (3.64), we can find the differential equation governing $M_{\hat{\omega}}$ from Eqs. (3.74) and (3.96). The result is as follows:

$$\frac{d^2 M_{\hat{\omega}}}{d\theta^2} - \hat{n}^2 \hat{\mu}^2 M_{\hat{\omega}} = \hat{n}^2 R \frac{dT_{\tilde{x}}}{d\theta} \tag{3.97}$$

where

$$\hat{\mu}^2 = R^2 \frac{GJ_{\hat{T}}}{EC_{\hat{\omega}}} \tag{3.98}$$

3.5 Generalization of the Theory [22]

3.5,1 Derivation of First Fundamental Equation

The shearing strain γ occuring in the middle surfaces of the plate elements can be expressed in terms of the displacement components as follows [3, 7]:

$$\gamma = \frac{\partial U}{\partial s} + \frac{R_s}{\rho} r_t^* \psi_x^* \qquad (3.99)$$

As before, it is assumed that the warping displacement U may be represented by Eq. (3.1). Then, by substituting Eq. (3.1) and making use of Eq. (3.38), we can rewrite Eq. (3.99) as

$$\gamma = \frac{R_s^2}{\rho^2} \tilde{q}_s \frac{n_g}{t} \chi^* + \frac{R_s}{\rho} r_t^* (\psi_x^* - \chi^*) \quad , \qquad (3.100)$$

The shear flow q developed in the cross section is related to the shearing strain γ by the formula

$$q = \frac{1}{n_g} G_s \gamma t \qquad (3.101)$$

The desired equation results from the substitution of Eq. (3.101), together with Eq. (3.100), into the formula for the total torsional moment T_x^* about the shear center axis. Using the notations defined in Eqs. (2.18) and (2.20), respectively, there results

$$T_x^* = \int_F q r_t^* \, ds = G_s J_T^* \chi^* + G_s J_c^* (\psi_x^* - \chi^*)$$

..... (3.102)

Here, let us introduce the notation η^* defined by the equation

$$\eta^{*2} = 1 - \frac{J_T^*}{J_C^*} \tag{3.103}$$

We find that the quantity η^* is a real number because of the inequality (2.22) and a dimensionless cross-sectional constant.

Then, with this notation, Eq. (3.102) can be again written to get the required first equation as follows:

$$\psi_x^* = \eta^{*2}\chi^* + (1 - \eta^{*2})\frac{T_x^*}{G_s J_T^*} \tag{3.104}$$

The equation (3.104) is equivalent to Eq. (3.93) and corresponds to Eq. (q). It should be noted that as the constant η^* approaches unity in the limit the quantity χ^* coincides with the rate of twist of ψ_x^* of the shear center axis.

3.5.2 Derivation of Second Fundamental Equation

To obtain the second fundamental equation relating the total torsional moment T_x^* to the quantities ψ_x^* and χ^*, Galerkin's method will be applied to the differential equation of equilibrium in the longitudinal direction for an infinitesimal plate element, expressed in terms of kinematical quantities.

The desired equilibrium equation is multiplied by ω^* and integrated over the entire cross-sectional area to obtain the following equation:

$$0 = \int_F \left[\frac{E_s}{n_e} \frac{\partial}{\partial\theta}(\varepsilon_\theta t) + \frac{G_s}{n_g} \frac{1}{\rho} \frac{\partial}{\partial s}(\rho^2 \gamma t) + \rho \tilde{p}_x \right] \omega^* \, ds$$

$$= \frac{E_s}{n_e} \int_F \frac{\partial}{\partial\theta}(\varepsilon_\theta t)\omega^* \, ds + \frac{G_s}{n_g} \int_F \frac{1}{\rho} \frac{\partial}{\partial s}(\rho^2 \gamma t)\omega^* \, ds + R_s m_\omega^* \qquad \ldots\ldots\ldots\ldots\ldots (3.105)$$

By substituting Eq. (3.5) into the first integral on the right side of Eq. (3.105), taking the orthogonality relations given by Eqs. (2.23) and (2.24), and using the notation C_ω^* defined in Eq. (3.9), we can evaluate the integral as follows:

$$\frac{E_s}{n_e} \int_F \frac{\partial}{\partial\theta}(\varepsilon_\theta t)\omega^* \, ds = - \frac{1}{R_s} E_s C_\omega^* \frac{d^2\chi^*}{d\theta^2} \qquad \ldots\ldots\ldots\ldots\ldots (w)$$

An evaluation of the second integral on the right side of Eq. (3.105), however, requires performing an integration by parts on the integral. With Eq. (3.101) in mind, this results in the relation

$$\frac{G_s}{n_g} \int_F \frac{1}{\rho} \frac{\partial}{\partial s}(\rho^2 \gamma t)\omega^* \, ds = \sum_j \int_{j,j+1} \frac{\omega^*}{\rho} \frac{\partial}{\partial s}(\rho^2 q) \, ds$$

$$= \sum_j \left[(\rho^2 q) \frac{\omega^*}{\rho} \right]_j^{j+1} - \sum_j \frac{G_s}{n_e} \int_{j,j+1} \rho^2 \gamma t \frac{\partial}{\partial s}\left(\frac{\omega^*}{\rho}\right) ds \qquad \ldots\ldots\ldots\ldots\ldots (x)$$

For the same reason as stated before, the first summation on the right side of the above equation vanishes [see Eq. (i)]. Therefore, substituting Eqs. (3.38) and (3.100) into the remaining integral and making use of the notations defined in Eqs. (2.18) through (2.20) gives

$$\frac{G_s}{n_g}\int_F \frac{1}{\rho}\frac{\partial}{\partial s}(\rho^2\gamma t)\omega^* \, ds$$

$$= R_s G_s J_T^*(\psi_x^* - \chi^*) + R_s G_s J_T^* \chi^* \qquad (y)$$

$$- R_s G_s J_C^*(\psi_x^* - \chi^*) - R_s G_s J_T^* \chi^*$$

By virtue of Eq. (3.102), the above equation can be written in the concise form:

$$\frac{G_s}{n_g}\int_F \frac{1}{\rho}\frac{\partial}{\partial s}(\rho^2\gamma t)\omega^* \, ds = R_s G_s J_T^* \psi_x^* - R_s T_x^*$$

..... (z)

Substituting Eqs. (w) and (z) into Eq. (3.105) and rearranging the resulting expression yields

$$E_s C_\omega^* \frac{1}{R_s^2}\frac{d^2\chi^*}{d\theta^2} - G_s J_T^* \psi_x^* = - T_x^* + m_\omega^* \qquad (3.106)$$

This equation is the required second equation and is very similar in form to Eq. (3.91), with the exception of the term m_ω^*.

3.5.3 Governing Equations and Solution Method

Let us consider the curved box girder bridge under the same loading and boundary conditions as those in the prceeding case. As before, the assumption $R_s \simeq R_o \equiv R$ will be made in deriving the governing equations.

We find, as a matter of course, that the governing differential equation for M_y is identical with Eq. (3.63).

Substituting Eq. (3.104) for ψ_x^* in Eq. (3.106) and making use of the notation defined in Eq. (3.103), we find

$$E_s C_\omega^* \frac{1}{R^2} \frac{d^2\chi^*}{d\theta^2} - \eta^{*2} G_s J_T^* \chi^* = - \eta^{*2} T_x^* \qquad (3.107)$$

If the same procedure as in the case of deriving Eq. (3.65) is followed, the governing differential equation for M_ω^* can be obtained from Eq. (3.107) as follows:

$$\frac{d^2 M_\omega^*}{d\theta^2} - \eta^{*2}\mu^{*2} M_\omega^* = - \eta^{*2} R(M_y + R m_x^*) \qquad (3.108)$$

If Eq. (3.104) is employed instead of Eq. (q), the same procedure as in the proceeding case can be followed to find the governing differential equations for ϕ and w^*. They are obtained by replacing κ^* by η^* in Eqs. (3.67) and (3.69), respectively. For the same reason as stated before, the quantites M_y, M_ω^*, ϕ, and w^* can be determined by solving these equations under the boundary conditions given by Eqs. (3.70).

Hence, it is clear that the solutions for these quantities considered in this section can be obtained by replacing κ^* by η^* in the corresponding expressions in Appendix II.

Once ϕ and w^* are solved, ψ_x^* are determined from the second of Eqs. (2.5).

The method for determining χ^* and T_x^* is as follows. Substituting Eq. (3.102) for T_x^* in Eq. (3.106) ($m_\omega^* = 0$), we obtain the governing differential equation for χ^* in the form:

$$\frac{d^2\chi^*}{d\theta^2} - \lambda^{*2}\mu^{*2}\chi^* = - \lambda^{*2}\mu^{*2}\psi_x^* \qquad (3.109)$$

where

$$\lambda^{*2} = \frac{\eta^{*2}}{1 - \eta^{*2}} \qquad (3.110)$$

Since ψ_x^* is already known, Eq. (3.109) can be solved under the boundary conditions

$$\frac{d\chi^*}{d\theta} = R\,\frac{M_{\omega 1}^*}{E_s C_\omega^*} \qquad \text{at} \quad \theta = 0$$

$$\frac{d\chi^*}{d\theta} = R\,\frac{M_{\omega 2}^*}{E_s C_\omega^*} \qquad \text{at} \quad \theta = \Theta \qquad (3.111)$$

which correspond to the fact that the warping moment M_ω^* can be evaluated from the last one of Eqs. (3.8).

The total torsional moment T_x^* are then evaluated from Eq. (3.104) using ψ_x^* and χ^*.

3.5.4 Some Remarks on Formula for Shear Flow

According to Eq. (3.100), it seems reasonable from a theoretical point of view to evaluate the shear flows q by the formula

$$q = G_s\left\{\frac{R_s^2}{\rho^2}\tilde{q}_s\chi^* + \frac{R_s}{\rho}\frac{t}{n_g}r_t^*(\psi_x^* - \chi^*)\right\} \qquad (3.112)$$

In fact, we can merely calculate the shear flows due to torsion by using this formula, as can be seen from the last one of Eqs. (3.8) and Eqs. (3.102) and (3.106). It appears inevitable that the shear flows q_b due to normal force and bending moments should be determined from the condition of equilibrium in the longitudinal direction, since the shearing deformations corresponding to these shear flows are not considered in the theory. Therefore, the shear flows q_b are to be evaluated from Eq. (3.18).

Hence, instead of employing Eq. (3.112), S. U. Benscoter [9] proposed the formula for the shear flows q_t due to torsion, which is in analogous agreement with Eq. (3.26). For the case of a curved girder bridge, the formula may be given by

$$q_t = \frac{R_s^2}{\rho^2}\tilde{q}_s G_s \psi_x^* - \frac{R_s^2}{\rho^2}(\tilde{q}_\omega - S_\omega^*)E_s\frac{1}{R_s^2}\frac{d^2\chi^*}{d\theta^2} \qquad (3.113)$$

This formula can be rewritten in various ways by making use of ψ_x^* or χ^* from the formulae given in the preceeding

subsections.

Equation (3.106) is solved for $G_s\psi_x^*$ and the result is substituted into Eq. (3.113) to obtain

$$q_t = \frac{T_x^*}{J_T^*}\frac{R_s^2}{\rho^2}\tilde{q}_s + \frac{C_\omega^*}{J_T^*}\frac{R_s^2}{\rho^2}\tilde{q}_s E_s \frac{1}{R_s^2}\frac{d^2\chi^*}{d\theta^2} - \frac{R_s^2}{\rho^2}(\tilde{q}_\omega - S_\omega^*)E_s \frac{1}{R_s^2}\frac{d^2\chi^*}{d\theta^2} \quad \ldots\ldots\ldots\ldots\ldots (3.114)$$

Substituting into Eq. (3.114) the first derivative of the last one of Eqs. (3.8) with respect to θ gives

$$q_t = \frac{T_x^*}{J_T^*}\frac{R_s^2}{\rho^2}\tilde{q}_s - \frac{1}{R_s}\frac{dM_\omega^*}{d\theta}\frac{R_s^2}{\rho^2}\tilde{q}_s + \frac{1}{R_s}\frac{d}{d\theta}\left(\frac{M_\omega^*}{C_\omega^*}\right)\frac{R_s^2}{\rho^2}(\tilde{q}_\omega - S_\omega^*) \quad \ldots\ldots\ldots\ldots\ldots (3.115)$$

In view of the last one of Eqs. (3.8), Eq. (3.39), and the second of Eqs. (3.56), it may be found that each of these formulae for q_t is equivalent to Eq. (3.26).

Part 3. Some Remarks on the Two Types of Modified Torsional Bending Theories

3.6 Inequality between Two Types of Warping Shear Correction Parameters [45]

It is interesting from a practical point of view to investigate which type of the modified torsional bending theories predicts much larger or smaller values for the stress couples related to restrained torsion.

Now, it can be shown that there exists an inequality between the two types of the warping shear correction parameters, κ^* and η^*. To this end, an alternative expression for C_ω^* is to be derived. We find from the parametric study performed in Chapter III that the inequality serves the aforementioned purpose.

3.6.1 An Alternative Expression for Warping Constant

After substitution of the expression for $\tilde{q}_s$ from Eq. (2.12) into the orthogonality relation (3.31) and rearrangement of the resulting expression, there results

$$\int_F \frac{R_s^2}{\rho^2}(\tilde{q}_\omega - S_\omega^*) r_t^* \, ds$$

$$= R_s \int_F (\tilde{q}_\omega - S_\omega^*) \frac{\partial}{\partial s}\left(\frac{\omega^*}{\rho}\right) ds = R_s \sum_j \int_{j,j+1} (\tilde{q}_\omega - S_\omega^*) \frac{\partial}{\partial s}\left(\frac{\omega^*}{\rho}\right) ds$$

..... (3.116)

Performing an integration by parts on the integral on the right

side of the above equation gives

$$R_s \sum_j \int_{j,j+1} (\tilde{q}_\omega - S_\omega^*) \frac{\partial}{\partial s} \frac{\omega^*}{\rho} \, ds$$

$$= R_s \sum_j \left[\frac{\omega^*}{\rho} (\tilde{q}_\omega - S_\omega^*) \right]_j^{j+1} - R_s \sum_j \int_{j,j+1} \frac{\omega^*}{\rho} \frac{\partial}{\partial s} (\tilde{q}_\omega - S_\omega^*) ds$$

..... (3.117)

By substituting the expression for $\tilde{q}_\omega - S_\omega^*$ from Eq. (3.19) into the first summation on the right side of Eq. (3.117) and rearranging the resulting expression, we find that

$$R_s \sum_j \left[\frac{\omega^*}{\rho} (\tilde{q}_\omega - S_\omega^*) \right]_j^{j+1} = \frac{1}{R_s} \frac{1}{K_\omega^*} \sum_j' \left\{ \frac{\omega^*}{\rho} \Delta_j (\rho^2 q_\omega) \right\} = 0$$

..... (3.118)

In view of Eq. (3.23) and noting that the quantities $\tilde{q}_\omega$ are constants, we can rewrite the remaining summation as follows:

$$R_s \sum_j \int_{j,j+1} \frac{\omega^*}{\rho} \frac{\partial}{\partial s} (\tilde{q}_\omega - S_\omega^*) ds$$

$$= - R_s \sum_j \int_{j,j+1} \frac{1}{\rho} \omega^{*2} \frac{t}{n_e} \, ds = - C_\omega^*$$

..... (3.119)

Finally, combining Eq. (3.116) through Eq. (3.119) gives

$$C_\omega^* = \int_F \frac{R_s^2}{\rho^2} (\tilde{q}_\omega - S_\omega^*) r_t^* \, ds \qquad (3.120)$$

3.6.2 Derivation of the Inequality

In this subsection, the inequality $\eta^* \geq \kappa^*$ will be proved with the help of the formulae derived in the preceding sections. To this end, the following equation is to be derived from Eqs. (2.21) and (3.103), i.e.,

$$\frac{J_c^*}{J_T^*} - 1 = \frac{1}{1 - \eta^{*2}} = \sum_j \int_{j,j+1} f(s)^2 ds \qquad (3.121)$$

where

$$f(s) = \frac{R_s}{\sqrt{J_T^*}} \sqrt{(\rho/R_s)^3 (t/n_g)} \; \frac{\partial}{\partial s}\left(\frac{\omega^*}{\rho}\right) \qquad (3.122)$$

Furthermore, Eq. (3.42) is to be rewritten in the form:

$$\frac{1}{\nu^*} = \sum_j \int_{j,j+1} g(s)^2 ds \qquad (3.123)$$

where

$$g(s) = \frac{\sqrt{J_T^*}}{C_\omega^*} \sqrt{(R_s/\rho)^3 (n_g/t)} \; (\tilde{q}_\omega - S_\omega^*) \qquad (3.124)$$

Then, it follows from Eqs. (3.122) and (3.124) that

$$\sum_j \int_{j,j+1} f(s)g(s)ds = \frac{R_s}{C_\omega^*} \sum_j \int_{j,j+1} (\tilde{q}_\omega - S_\omega^*) \frac{\partial}{\partial s}\left(\frac{\omega^*}{\rho}\right) ds \qquad (3.125)$$

Substituting the expression for $\frac{\partial}{\partial s}\left(\frac{\omega^*}{\rho}\right)$ from Eq. (2.12) into

the integral on the right side of the above equation and noting the expression for C_ω^* given in Eq. (3.120) and orthogonality relation (3.31) along with Eq. (3.19), we find that

$$\sum_j \int_{j,j+1} f(s)g(s)ds = 1 \qquad (3.126)$$

In applying Schwartz's inequality to both the functions $f(s)$ and $g(s)$, one should note the fact that they are single-valued function within the interval of the individual plate element; however, they are in general multiple-valued function when being observed throughout the range of s. This is because the properly selected points on the walls of the adjoining plate elements are likely to have the same values with regard to the coordinate s.

According to Schwartz's inequality, the following inequality holds

$$\sqrt{\int_{j,j+1} f(s)^2 ds \int_{j,j+1} g(s)^2 ds}$$

$$\geq \sqrt{\left\{\int_{j,j+1} f(s)g(s)ds\right\}^2} \geq \int_{j,j+1} f(s)g(s)ds$$

..... (3.127)

Hence, it follows from Eqs. (3.126) and (3.127) that

$$\sum_j \sqrt{\int_{j,j+1} f(s)^2 ds \int_{j,j+1} g(s)^2 ds} \geq \sum_j \int_{j,j+1} f(s)g(s)ds = 1 > 0$$

..... (3.128)

We can regard the individual definite integrals in Eqs. (3.121) and (3.123) as the squares of certain numbers, since the integrals are greater than, or equal to, zero. With this in mind, we use Schwartz's inequality once again, along with the inequality (3.128), to obtain the relation

$$\begin{aligned} &\sum_j \int_{j,j+1} f(s)^2 ds \sum_j \int_{j,j+1} g(s)^2 ds \\ &\geq \left\{ \sum_j \sqrt{\int_{j,j+1} f(s)^2 ds} \sqrt{\int_{j,j+1} g(s)^2 ds} \right\}^2 \\ &= \left\{ \sum_j \sqrt{\int_{j,j+1} f(s)^2 ds \int_{j,j+1} g(s)^2 ds} \right\}^2 \\ &\geq \left\{ \sum_j \int_{j,j+1} f(s)g(s)ds \right\}^2 = 1 \end{aligned} \qquad (3.129)$$

Therefore, it follows that

$$\sum_j \int_{j,j+1} f(s)^2 ds \sum_j \int_{j,j+1} g(s)^2 ds \geq 1 \qquad (3.130)$$

In view of Eqs. (3.121) and (3.123), the above inequality is identical with

$$\frac{1}{\nu^*}\left(\frac{1}{1-\eta^{*2}}-1\right) \geq 1 \tag{3.131}$$

Noting that $\nu^* \geq 0$ and $1-\eta^{*2} \geq 0$ because of Eq. (3.42) and Eq. (3.103) and inequality (2.22), respectively, we can transform the inequality (3.131) to obtain

$$\eta^{*2} \geq 1 - \frac{1}{1+\nu^*} = \frac{\nu^*}{1+\nu^*} = \kappa^{*2} \tag{3.132}$$

Finally, we find from the above inequality that the following desired inequality holds

$$1 \geq \eta^* \geq \kappa^* \geq 0 \tag{3.133}$$

3.7 Concluding Remarks

In the modified torsional bending theories [9, 10, 21, 22], one more unknown quantity χ^*, the intensity of warping, in addition to those used in the conventional ones [1, 2, 3, 4, 5, 6, 7] is introduced to deal with the secondary shear deformation due to nonuniform torsion, called the warping-shear deformation. One supplementary condition is, therefore, needed for the determination of the quantity χ^*, and it can be provided by means of Galerkin's averaging technique.

When applying Galerkin method, the modified torsional bending theory of first type requires that the equation of equilibrium in the longitudinal direction for a differential plate element should be expressed in terms of stresses, while the theory of second type requires that the equation should be expressed in terms of the kinematical quantities of the reference axis of a girder.

In the modified torsional bending theory of first type, the warping-shear correction factor ν^* appears in the constitutive equation for warping torque [see Eq. (3.62)], which is derived from the requirement that the principle of complementary virtual work should be employed as a basis for establishing compatible state of deformation. Then, the warping-shear correction parameter κ^* defined in Eq. (3.65) appears in Eq. (q), which is obtained by eliminating the primary and warping torque from the constitutive equations for these quantitites. In the modified torsional bending theory of second type, on the other hand, the warping-shear correction

parameter η^* defined in Eq. (3.103) appears in the first fundamental equation relating the total torsional moment T_x^* to the quantities ψ_x^* and χ^*, which results from the requirement that the shear flows expressed in terms of the kinematical quantities of the reference axis of girder bridge should satisfy the equation of allover equilibrium [see Eqs. (3.90) and (3.102)].

Between κ^* and η^*, the warping-shear correction parameters, there exists an inequality such that $1 \geq \eta^* \geq \kappa^* \geq 0$.

The avenue of the formulation of these modified torsional bending theories is shown in Table 3.1 diagramatically. In the final analysis, the foregoing considerations may be briefly summed up as follows: The fundamental equations in the modified torsional bending theory of first type are derived on the basis of the idea of force method, while those in the theory of second type are derived on the basis of the idea of displacement method.

Furthermore, in the limit as the parameters κ^* and η^* approach unity, respectively, the modified torsional bending theories agree with the conventional ones. Therefore, we see that the conventional torsional bending theories may be regarded as special cases of the modified ones.

Table 3.1 The Avenue of the Formulation of the Modified Torsional Bending Theories

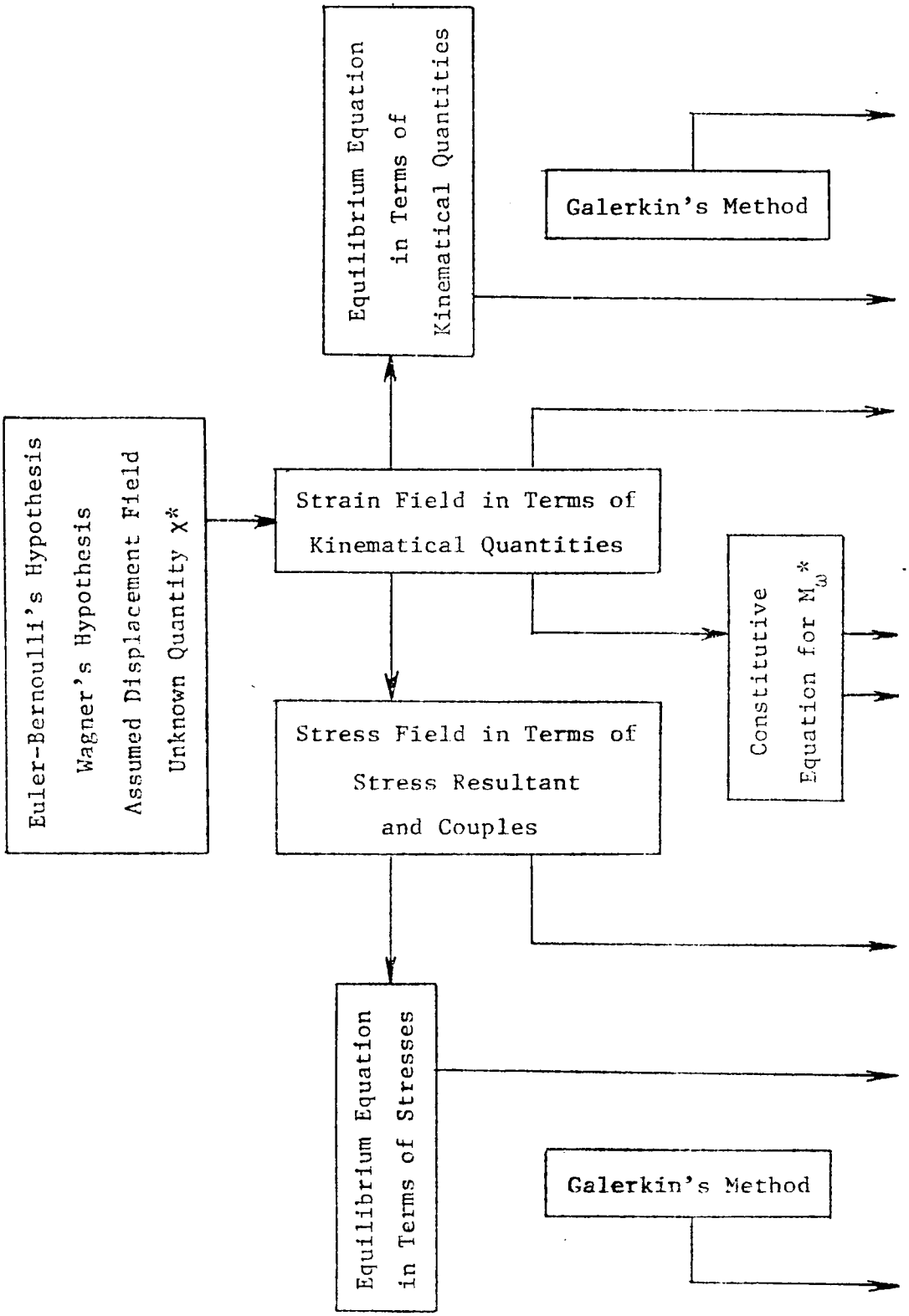

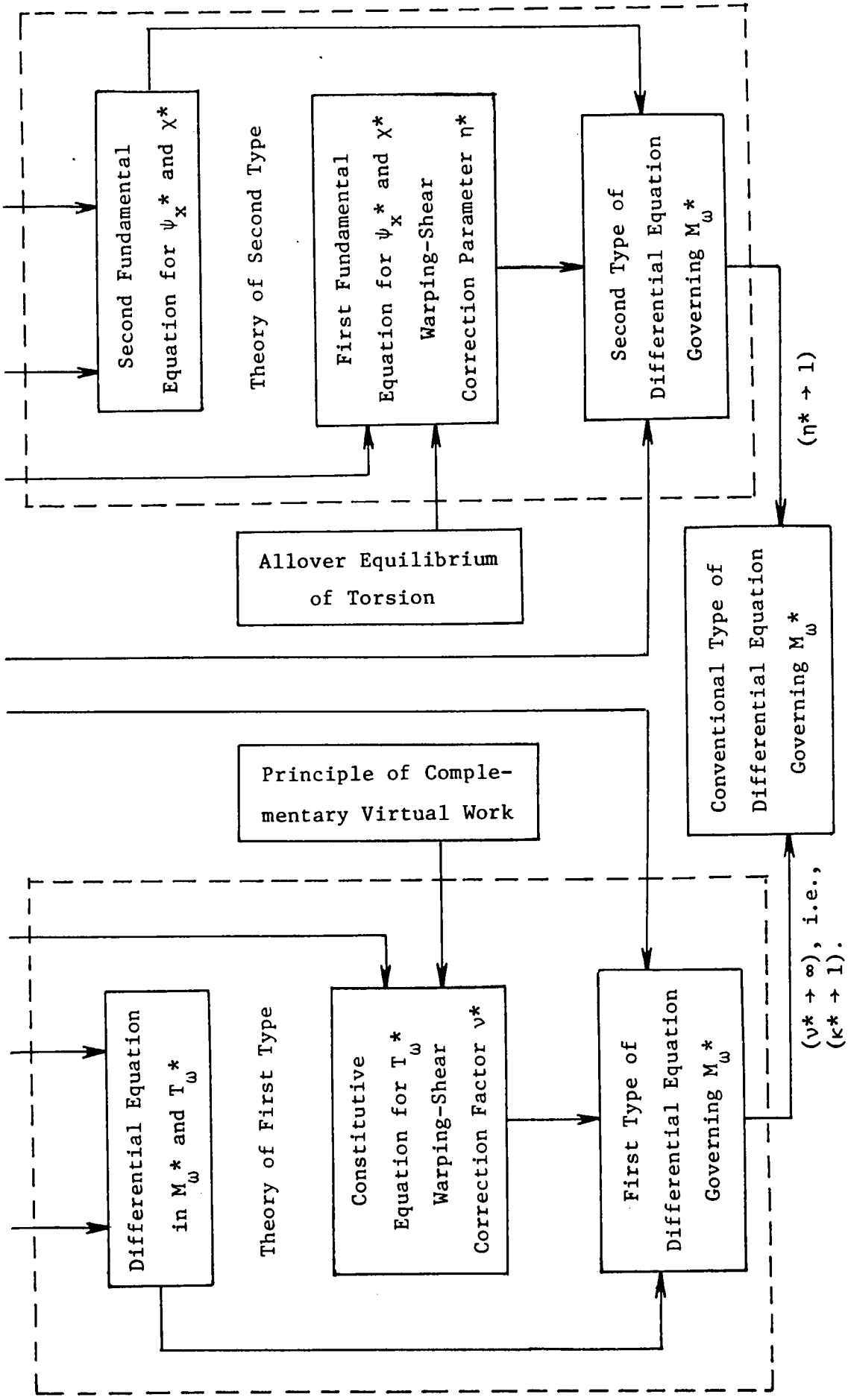
Second Fundamental Equation for ψ_x^* and χ^*
Theory of Second Type
First Fundamental Equation for ψ_x^* and χ^* Warping-Shear Correction Parameter η^*
Second Type of Differential Equation Governing M_ω^*
$(\eta^* \to 1)$
Allover Equilibrium of Torsion
Conventional Type of Differential Equation Governing M_ω^*
Principle of Complementary Virtual Work
Differential Equation in M_ω^* and T_ω^*
Theory of First Type
Constitutive Equation for T_ω^* Warping-Shear Correction Factor ν^*
First Type of Differential Equation Governing M_ω^*
$(\nu^* \to \infty)$, i.e., $(\kappa^* \to 1)$.

IV. NUMERICAL EXAMPLES [46]

4.1 Geometrical Characteristics of Curved Box Girder Bridges

It is interesting to evaluate the dimensionless cross-sectional characteristics $\mu^*\theta$, ν^*, κ^*, η^*, and β for several types of cross sections, since they are the important parameters which characterize the statical behaviour of curved box girder bridges.

The cross-sectional dimensions used for computation were quoted from the specifications of the bridges constructed by Hanshin Express Highway Corporation and were modified a little for the sake of convenience of computation.

Fig. 4.1(a), (b), and (c) show the cross sections of curved box girder bridges which are made composite with a reinforced concrete deck slab. In cases (a) and (c), it was assumed that the steel box sections would resist alone when carrying their own weight and those of the concrete slabs, and that the composite sections would resist the moments due to live loads and those due to dead loads added after the concrete decks had hardened. In case (b), however, it was assumed that the cross sections resist the moments due to all kinds of the loads after the composite action of the sections was ensured. Furthermore, the values of the ratios n_e and n_g were assumed to be 7.0 and 6.3, respectively. Fig. 4.1(d) and (e) show the cross sections of curved box girder bridges with an orthotropic steel deck plate.

The results obtained are tabulated in Table 4.1. In cases

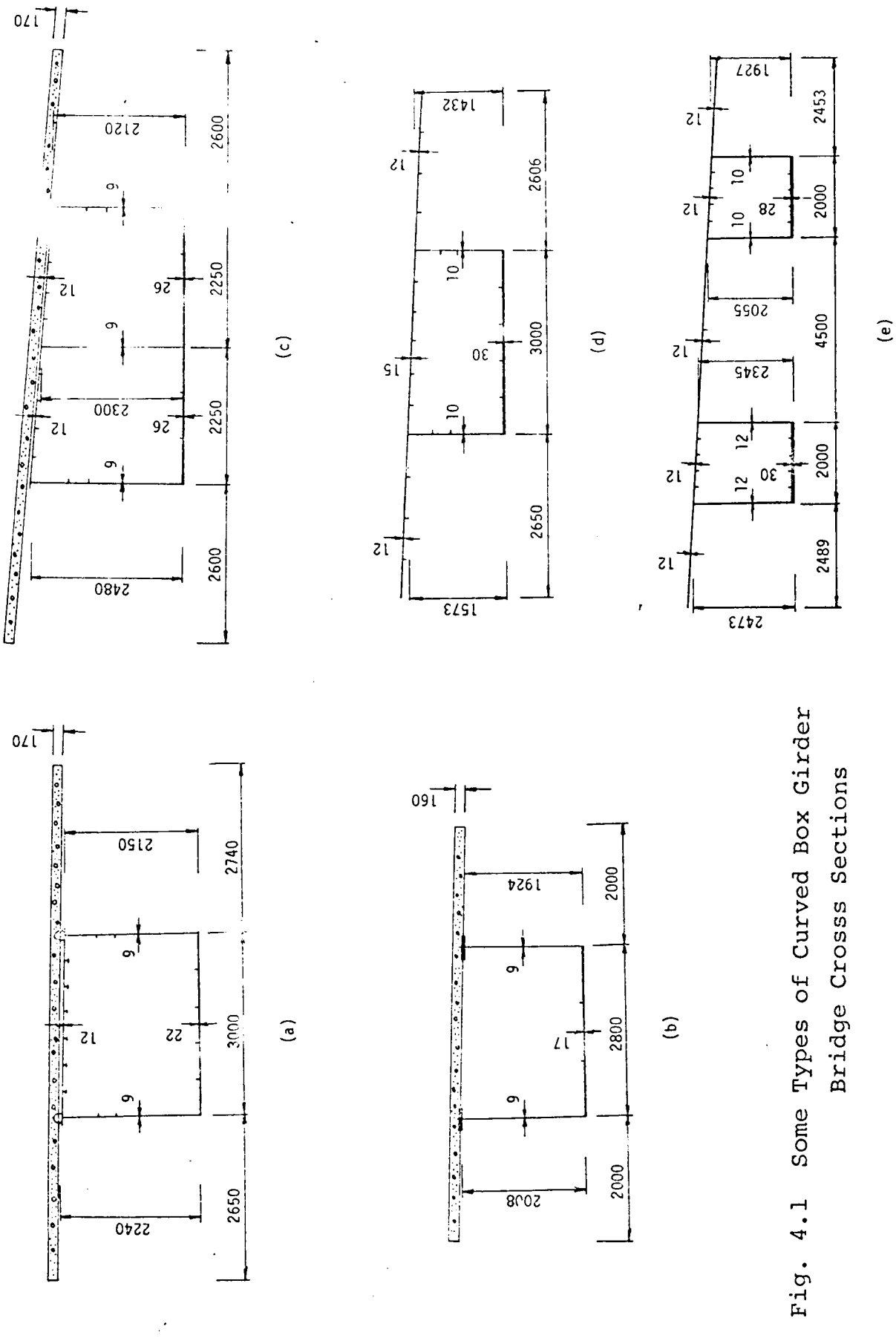

Fig. 4.1 Some Types of Curved Box Girder Bridge Crosss Sections

Table 4.1 Geometrical Characteristics of Curved Box Girder Bridges.

Types of Box Cross Sections	Dimensionless Cross-Sectional Characteristics				
	$\mu^*\theta$	ν^*	κ^*	η^*	β
(a)	35 (191)	0.491 (0.0143)	0.574 (0.119)	0.587 (0.132)	0.317 (0.573)
(b)	43	0.281	0.468	0.475	0.386
(c)	49 (786)	0.251 (0.00109)	0.448 (0.0330)	0.463 (0.0358)	0.415 (0.672)
(d)	55	0.259	0.454	0.661	0.447
(e)	66	3.24	0.874	0.934	0.255

(a) and (c), the numbers in parentheses indicate the corresponding values of the cross-sectional constants for the steel box sections alone.

Additionally, the values of κ^* and η^* for a rectangular box cross section are plotted against the various values of the ratio of height to width, b/a, while the wall thickness and the area enclosed by the median line of the cross section are kept constant. We should be reminded that the torsional rigidities $G_S J_T^*$ of the cross sections are kept constant under these conditions, except for curvature effect. The results are represented in Fig. 4.2.

What is evident from Table 4.1 and Fig. 4.2 is that the values of η^* are always slightly larger than those of κ^* as is predicted theoretically in Subsection 3.6.2.

4.2 Influence-Lines for Stress Couples Related to Restrained Torsion, Intensity of Warping, and Angle of Rotation

In this section, we will investigate to what extent the warping-shear correction factor ν^* affects the influence-line ordinates for the stress couples related to restrained torsion, M_ω^*, T_S^*, and T_ω^*, the intensity of warping, χ^*, and the angle of rotation of cross section, ϕ. For this purpose, let us consider a curved box girder bridge continuous over two spans, supported in the manner shown in Fig. 4.3, as a simple example. The bridge has two equal developed span lengths and constant curvature throughout its axis.

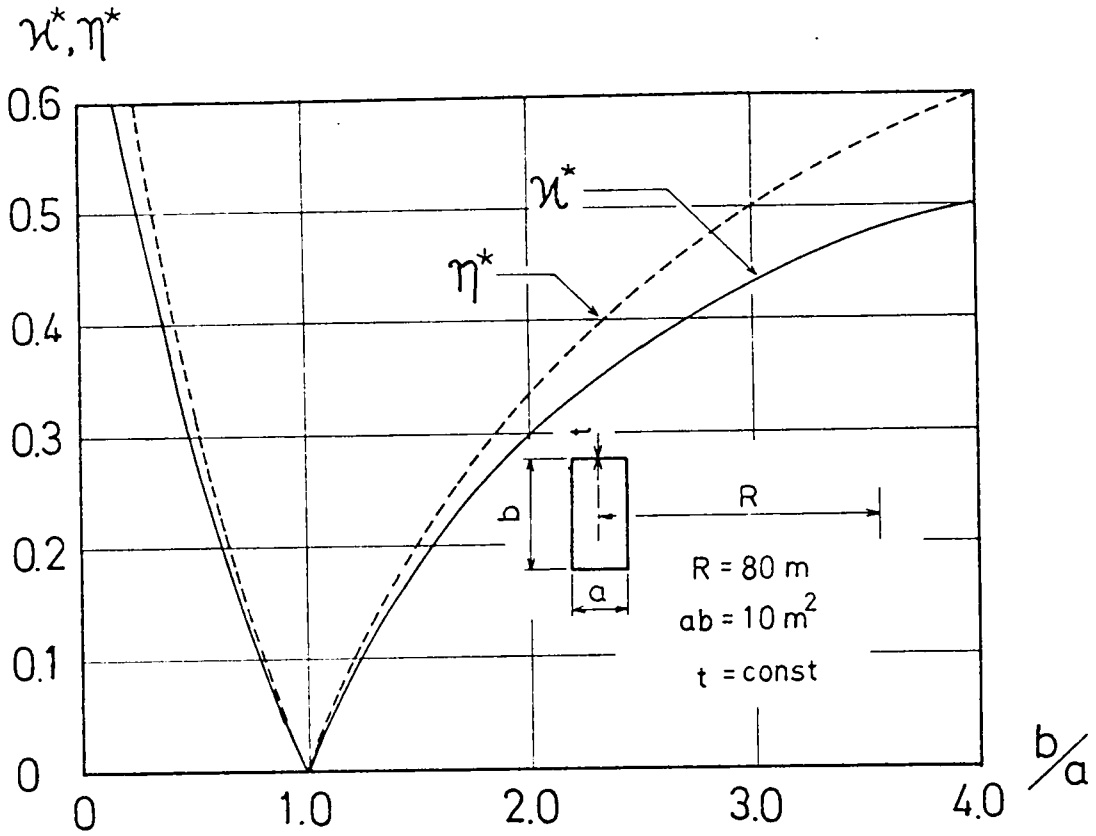

Fig. 4.2 Warping-Shear Correction Parameters for Rectangular Cross Sections

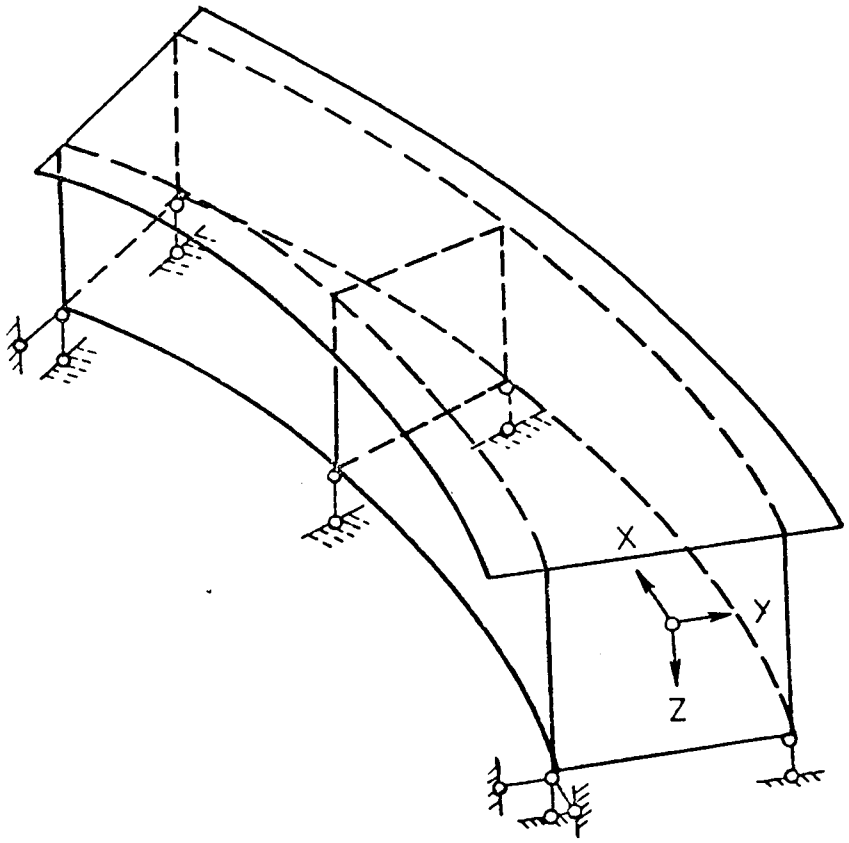

Fig. 4.3 Curved Box Girder Bridge Continuous over Two Spans

The bridge is statically indeterminate to the second degree. For the analysis of this indeterminate system, it is convenient to treat the bending moment M_y and warping moment M_ω^* developed on the cross section on the intermediate support as the redundants. Let us denote these stress couples by X_1 and X_2, respectively. The equations of consistent deformations are given in the form:

$$\begin{aligned} \delta_{11}X_1 + \delta_{12}X_2 + \delta_{10} &= 0 \\ \delta_{21}X_1 + \delta_{22}X_2 + \delta_{20} &= 0 \end{aligned} \qquad (4.1)$$

The first (second) equation indicates the compatibility condition physically stating that the deflection angle $\frac{1}{R}\frac{dw^*}{d\theta}$ (warping U — which amounts to the same as the intensity of warping, χ^*, as is evident from Eq. (3.1) —) of the left side relative to the right side at the cross section on the intermediate support must be zero. The flexibility coefficients δ_{ij} (i = 1, 2 and j = 1, 2) and δ_{i0} (i = 1, 2) in Eqs. (4.1) can be obtained from the expressions for w^* and χ^* given in Appendix III.

Using Eqs. (4.1), the computation to find the influence-lines for the aforementioned quantities at some points on the reference girder axis was carried out for the loading cases of unit concentrated torque $\tilde{T}$ and force $\tilde{P}$ moving across the bridge, separately. The results obtained for the former loading case are represented in Fig. 4.4 through Fig. 4.12.

The influence-line diagrams for the latter loading case, however, are omitted because it has been found from the computation that the influence-line ordinates are scarcely affected by the factor ν^*, in other words, they are in close agreement with the corresponding ones obtained from the conventional theory.

For the sake of generality, the influence-line diagrams are represented in a non-dimensional form by making use of the dimensionless quantities by

$$\hat{M}_\omega^* = \frac{M_\omega^*}{G_S J_T^*} , \quad \hat{T}_S^* = \frac{RT_S^*}{G_S J_T^*} , \quad \hat{T}_\omega^* = \frac{RT_\omega^*}{G_S J_T^*} \qquad \text{..... (4.2)}$$

and

$$\hat{\chi}^* = R\chi^* , \qquad \hat{\phi} = \phi \qquad \text{..... (4.3)}$$

In the diagrams, the dimensionless quantities mentioned above versus θ/Θ are plotted for the three values of the factor ν^* as parameter, namely, 0.3(dot-dash line), 1.0(broken line), and infinity(solid line), while $\mu^*\Theta$ is kept to 20 or 50, β to 0.4, and Θ to 0.4.

4.3 Shear Flows- and Normal Stresses- Distributions in a Cross Section

By inspecting the influence-lines for the stress couples related to restrained torsion, we can suppose that the influence of the factor ν^* on the distributions of stresses in a

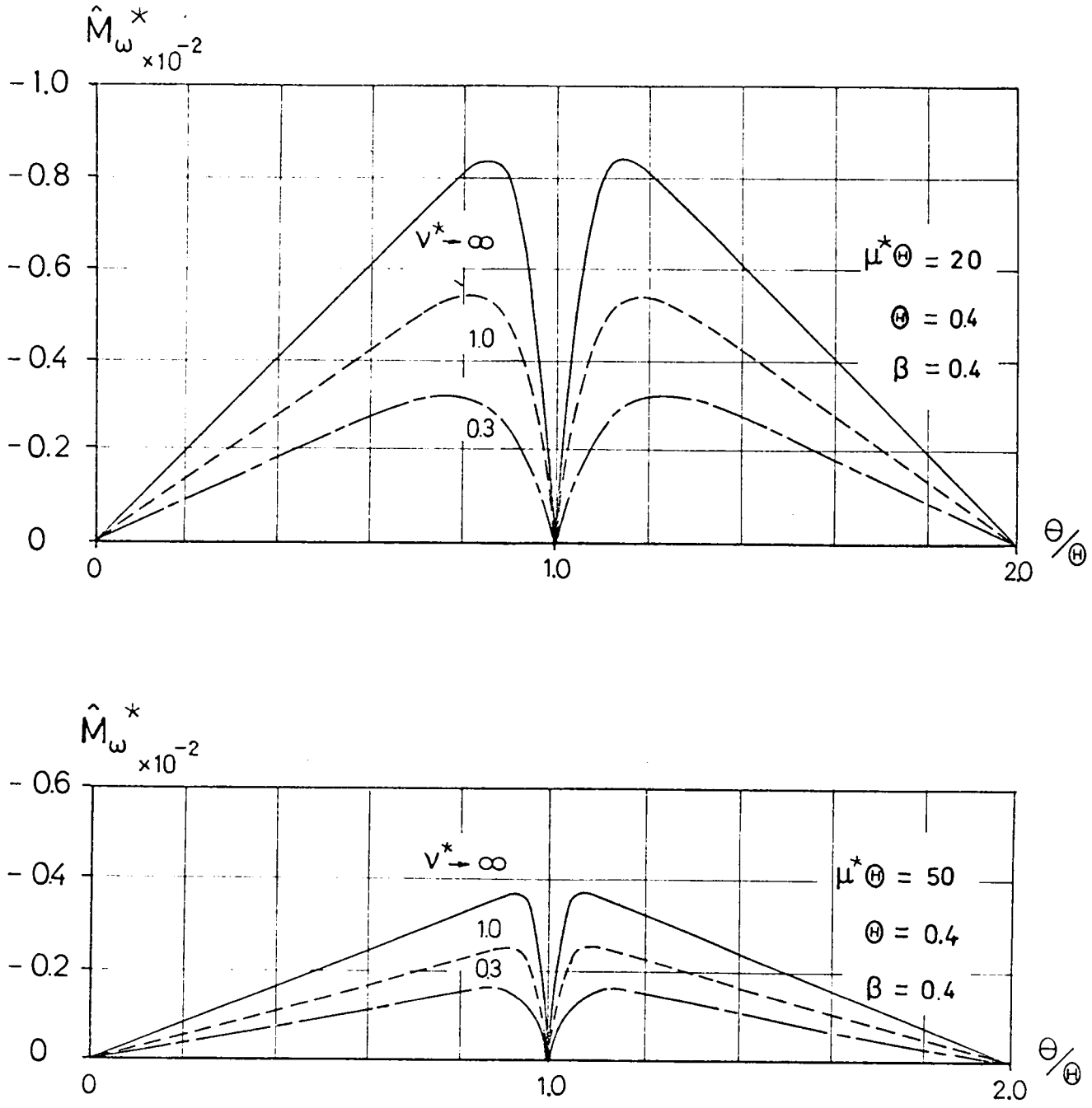

Fig. 4.4 Influence-Lines for the Warping Moment $\hat{M}_\omega^*$ on the Cross Section on the Intermediate Support.

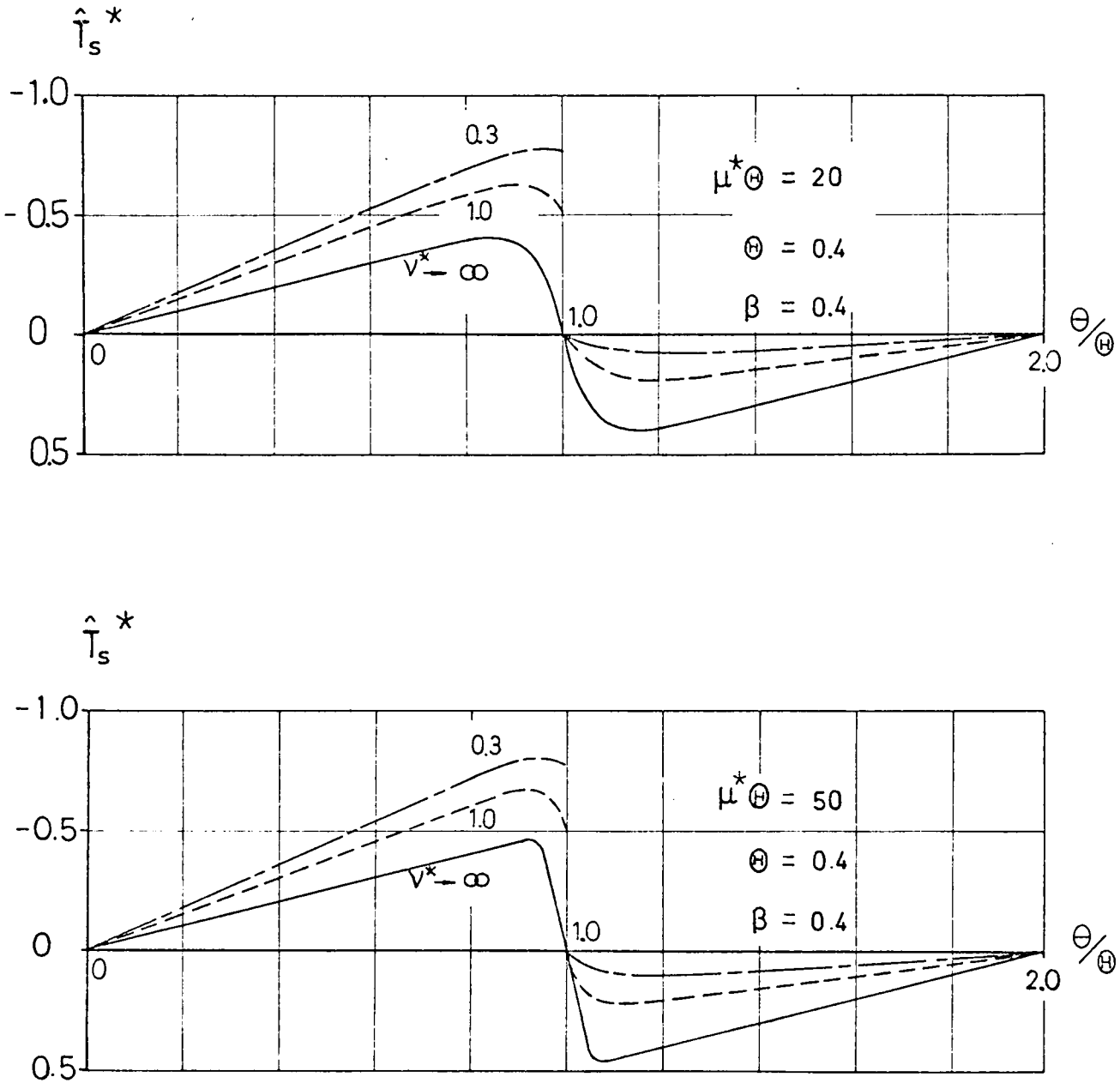

Fig. 4.5 Influence-Lines for the Primary Torsional Moment $\hat{T}_s^*$ on the Cross Section Just to the Right of the Intermediate Support.

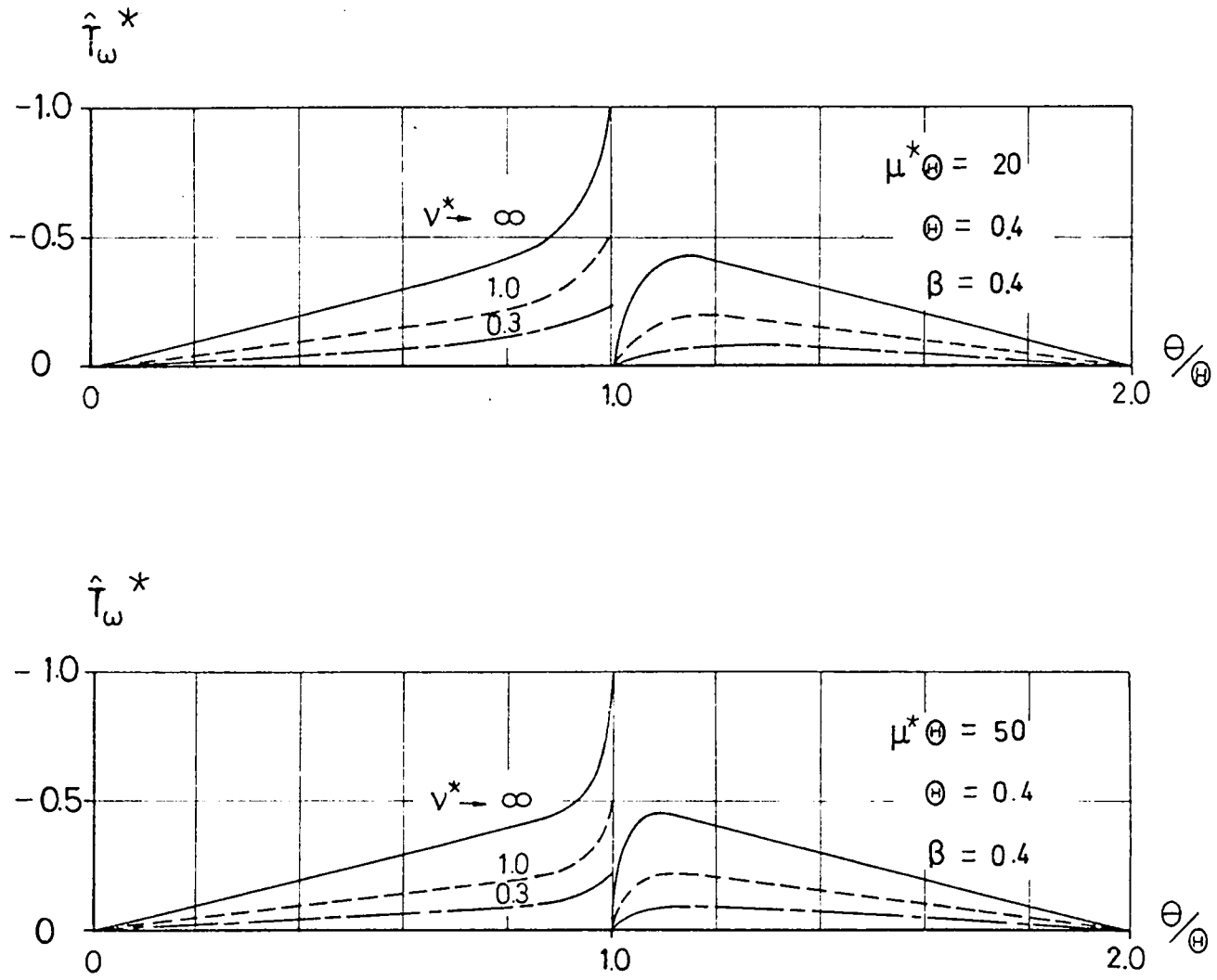

Fig. 4.6 Influence-Lines for the Secondary Torsional Moment $\hat{T}_\omega^*$ on the Cross Section Just to the Right of the Intermediate Support.

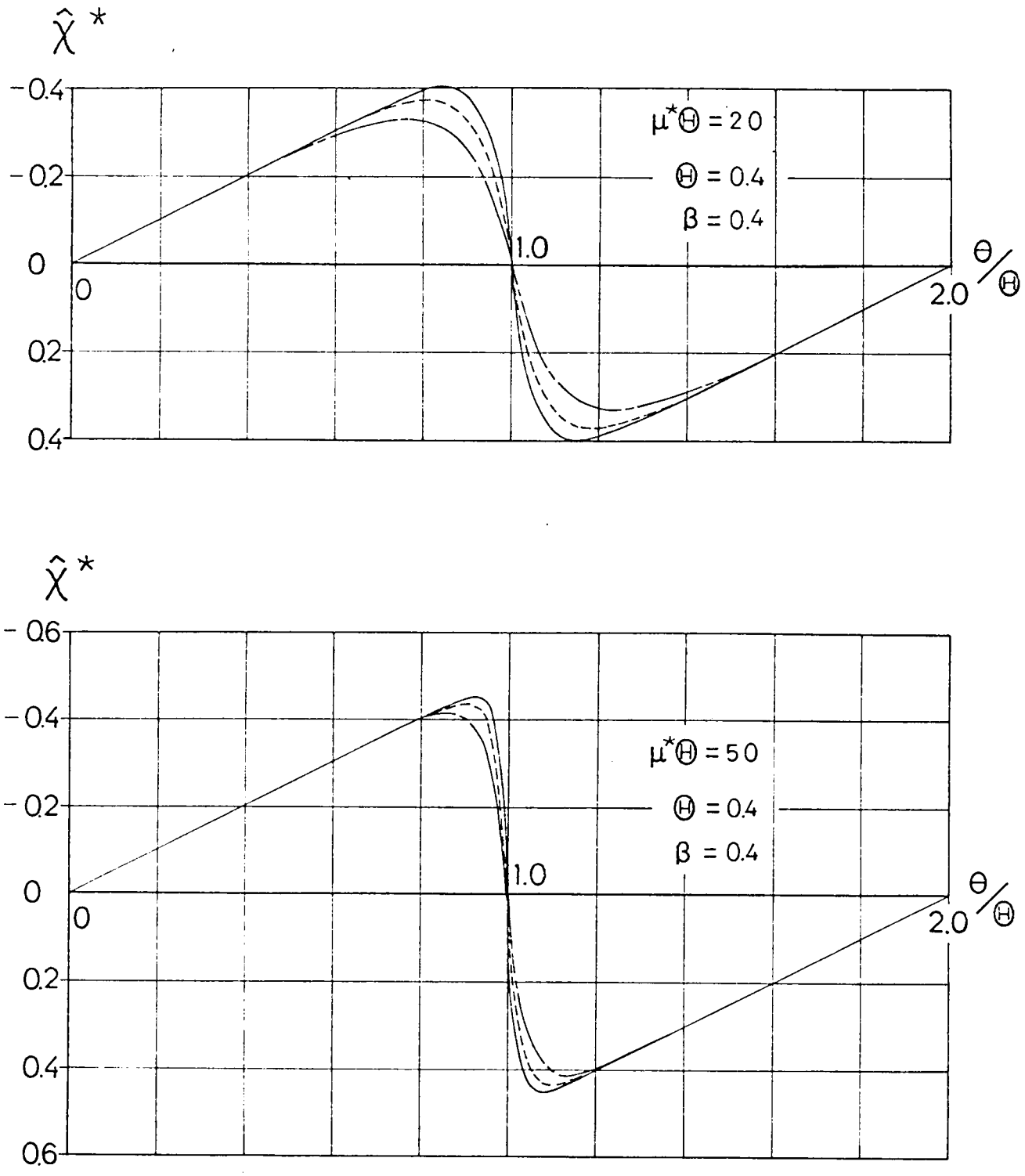

Fig. 4.7 Influence-Lines for the Intensity of Warping, $\hat{\chi}^*$, with Respect to the Shear Center Axis at the Middle and Four-Fifth Points of the First Span.

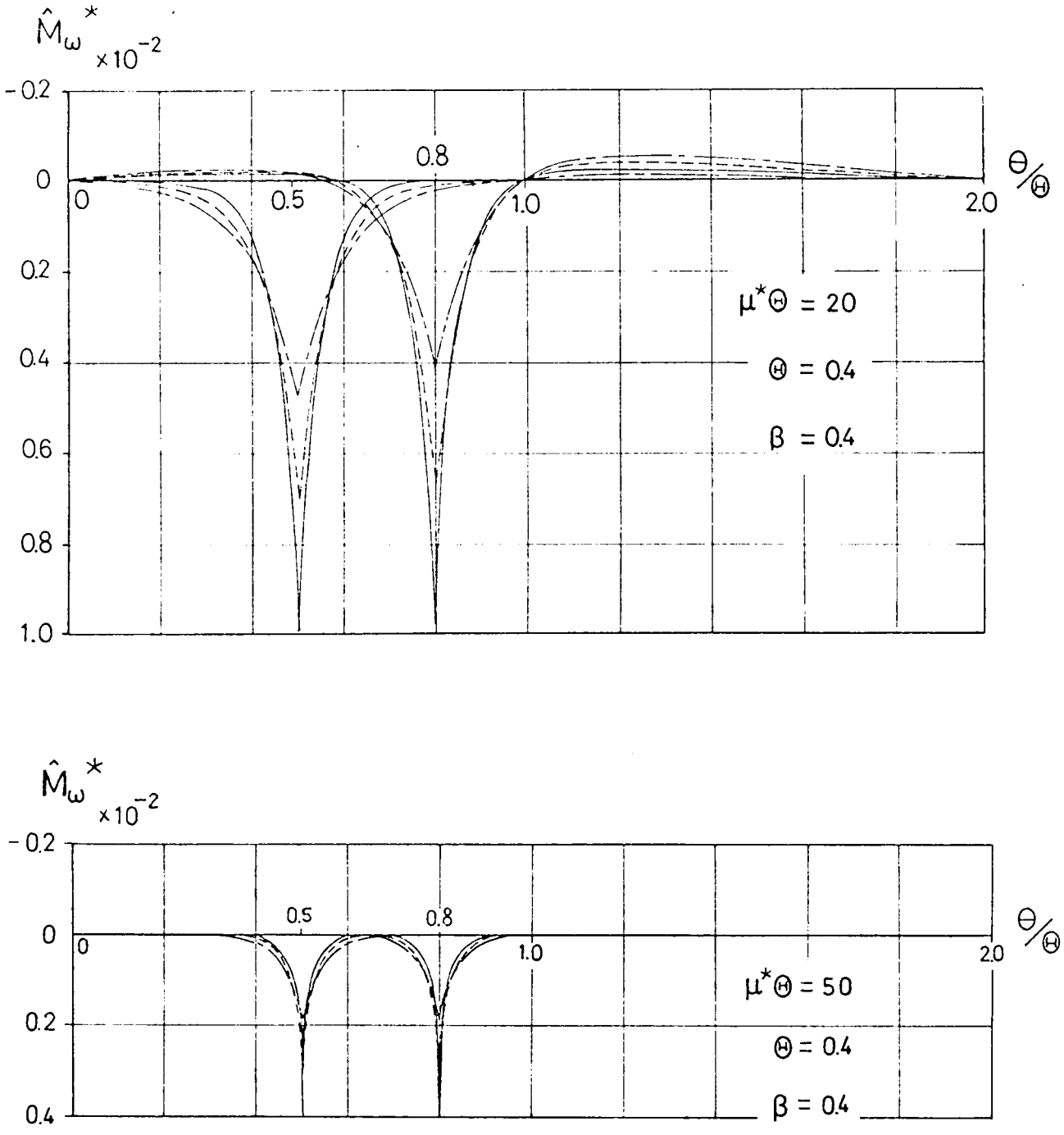

Fig. 4.8 Influence-Lines for the Warping Moment $\hat{M}_\omega^*$ on the Cross Section Located at the Middle and Four-Fifth Points of the First Span.

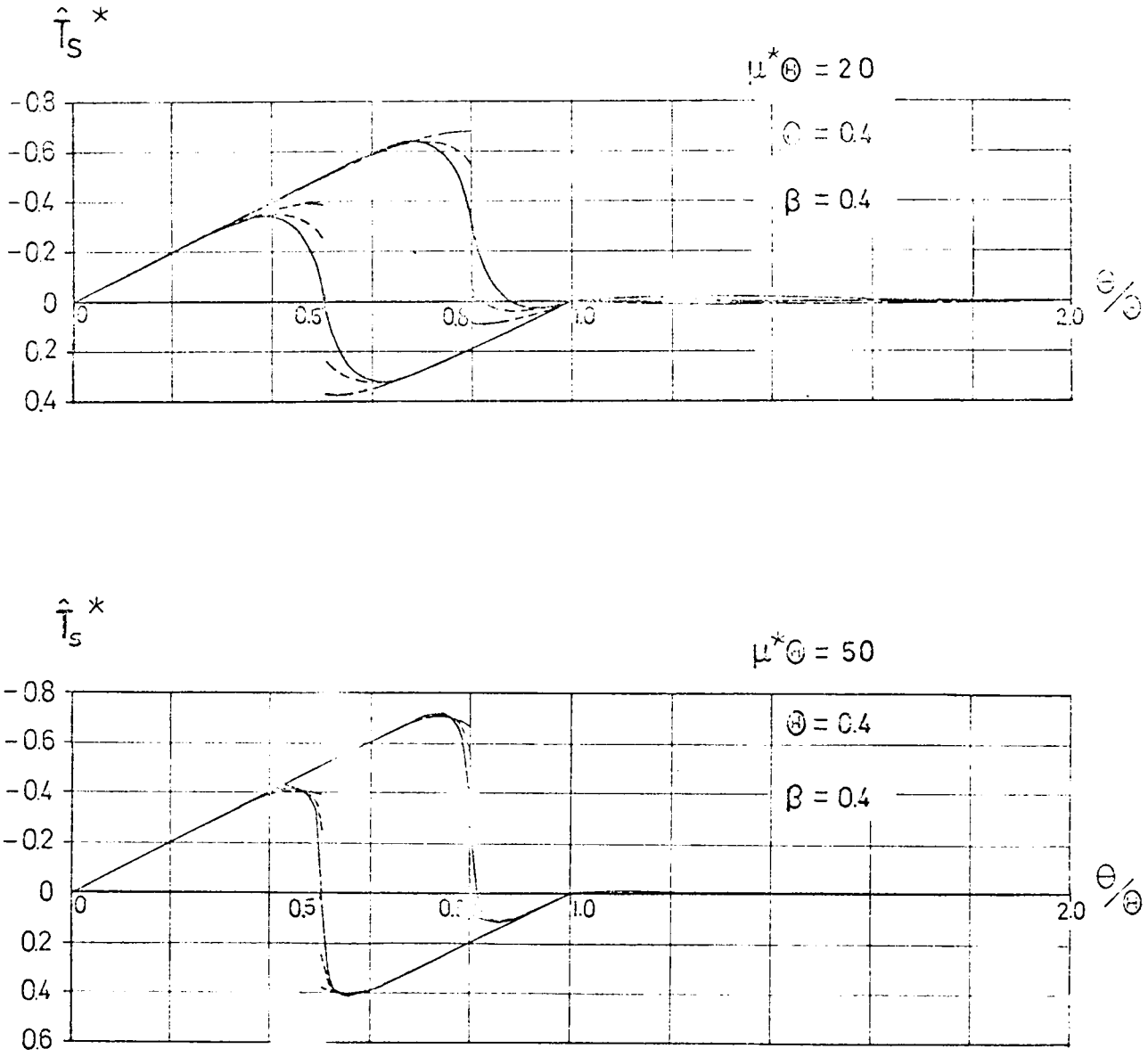

Fig. 4.9 Influence-Lines for the Primary Torsional Moment $\hat{T}_s^*$ on the Cross Sections Located at the Middle and Four-Fifth Points of the First Span.

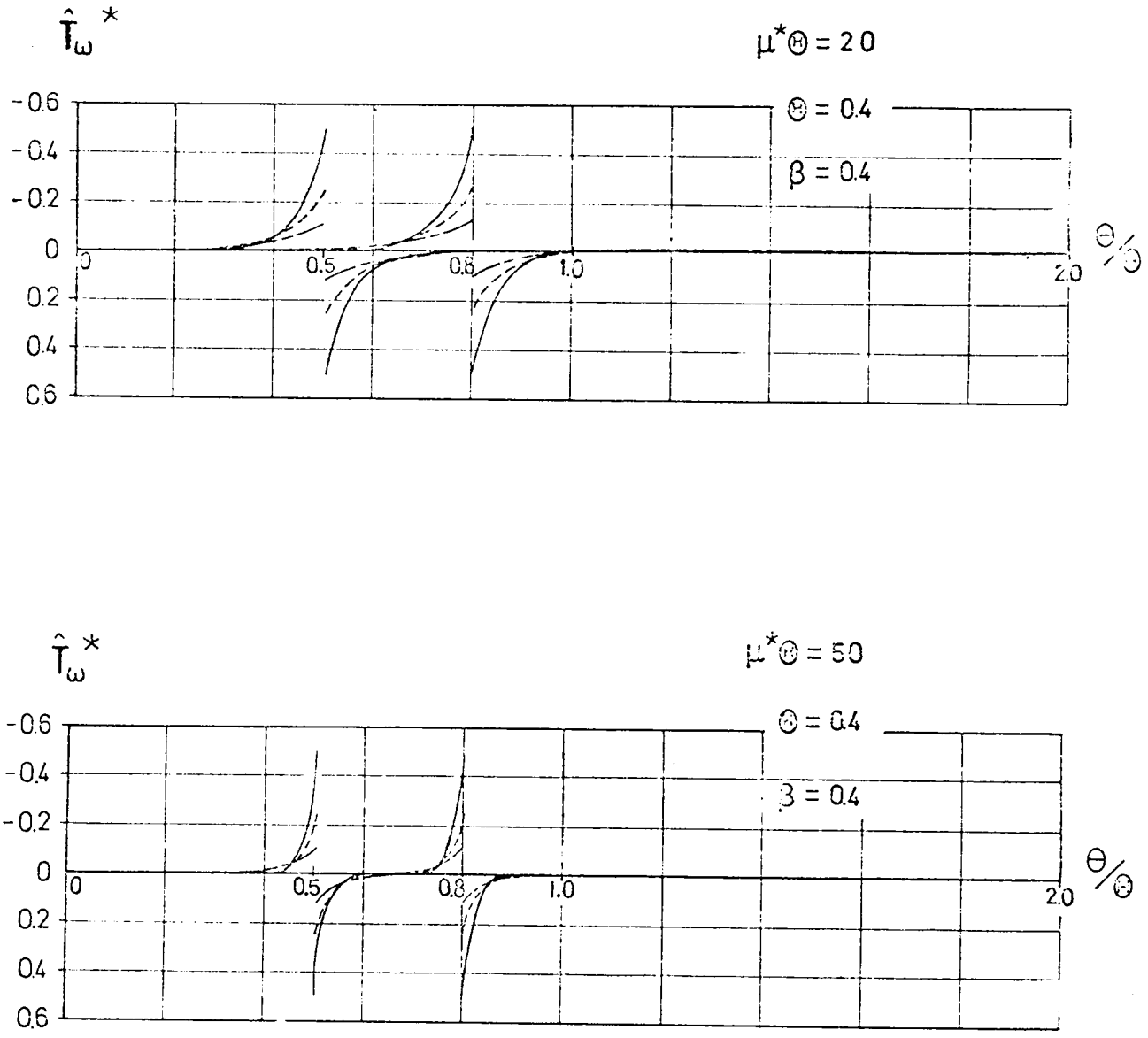

Fig. 4.10 Influence-Lines for the Secondary Torsional Moment $\hat{T}_\omega^*$ on the Cross Sections Located at the Middle and Four-Fifth Points of the First Span

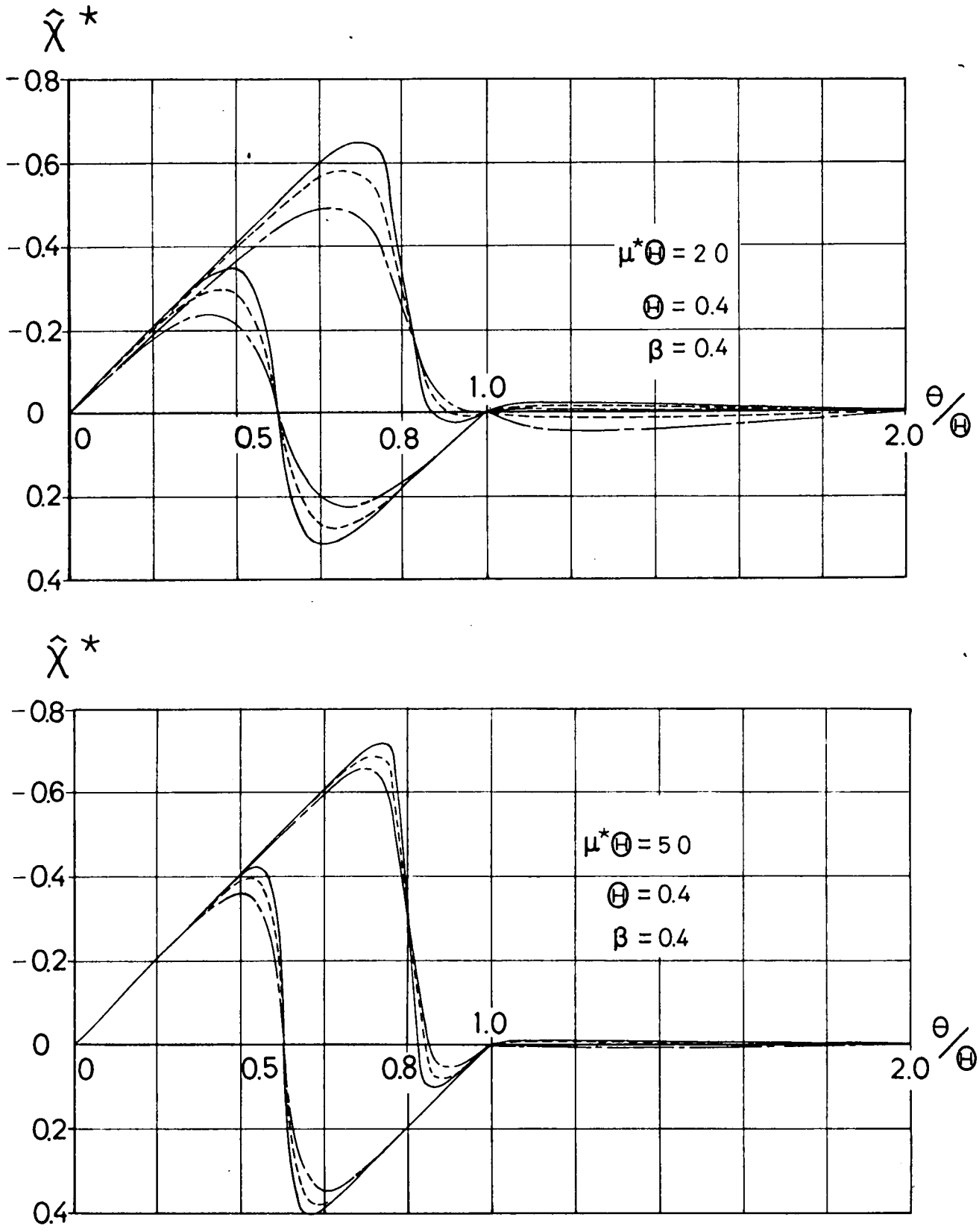

Fig. 4.11 Influence-Lines for the Intensity of Warping, $\hat{\chi}^*$, with Respect to the Shear Center Axis at the Middle and Four-Fifth Points of the First Span.

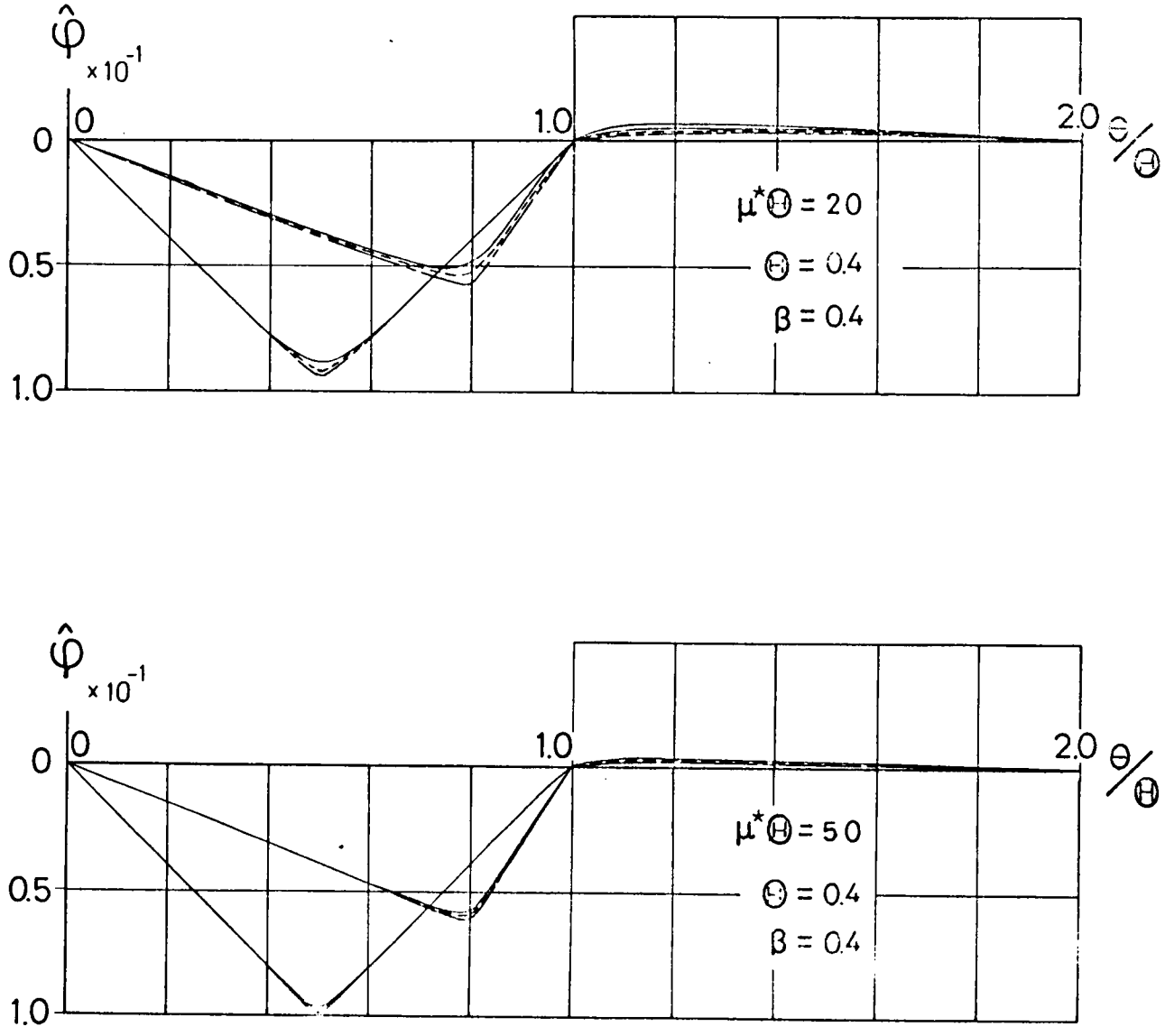

Fig. 4.12 Influence-Lines for the Angle of Rotation, $\hat{\phi}$, of the Cross Sections Located at the Middle and Four-Fifth Points of the First Span.

cross section may appear to some extent at the cross sections where torsion is highly restrained. In the case of composite box girder bridges used frequently as ramp structures, as shown in Fig. 4.1(a) and (b), larger amounts of influence may arise in the cross sections mentioned above. This is because it seems that the cross-sectional characteristics $\mu^*\Theta$ and ν^* of the composite box girder bridges are relatively small (see Table 4.1). It is well known that, in this case, stress analysis with the help of the torsional bending theory is available [47, 48].

In consideration of the conjecture mentioned above, the calculations were carried out to find the distributions of shear flows and normal stresses in the cross section, respectively, just to the right of and on the intermediate support of the curved composite box girder bridge continuous over two spans. The brdige used for the numerical calculation purposes has the same geometrical characteristics as those considered in Section 4.2 and the cross section shown in Fig. 4.1(a). The geometrical characteristics of the bridge considered herein are given below.

(1) Opening angle, $\Theta_1 = \Theta_2 \equiv \Theta = 0.3200$ radian.

(2) Radius of curvature, $R_1 = R_2 \equiv R = 0.8000 \times 10^8$ cm.

(3) Cross-sectional constants

for the steel box section alone,

$J_y = 0.1354 \times 10^8$ cm^4, $J_T^* = 0.2012 \times 10^8$ cm^4,
$J_z = 0.1699 \times 10^8$ cm^4, $C_\omega^* = 0.2254 \times 10^{10}$ cm^6,
$J_{yz} = -0.2268 \times 10^6$ cm^4.

for the composite section,

$J_y = 0.3325 \times 10^8$ cm^4, $J_T^* = 0.2732 \times 10^8$ cm^4,
$J_z = 0.1378 \times 10^9$ cm^4, $C_\omega^* = 0.1353 \times 10^{12}$ cm^6,
$J_{yz} = -0.2643 \times 10^7$ cm^4.

Calculations were carried out by using the standard design load L-20 specified in the Bridge Specifications of the Japan Load Association. Various critical combinations of loading which produce unfavourable stresses in the aforementioned cross sections were determined by inspecting the characteristics of the influence-lines as follows. To calculate the shear flows (normal stresses), the standard line load P was placed at the point where the absolute value of the ordinate to the influence-line for the quantity $dM_y/d\theta$ (bending moment M_y) is at a maximum. It was considered necessary to check the magnitudes of the shear flows developed on the cross section under the two loading conditions with reference to the standard distributed load p. Hereafter, let us denote these loading conditions by Loading A and Loading B, respectively (Fig. 4.13). In Loading A, the standard load was placed in the first span as close to the

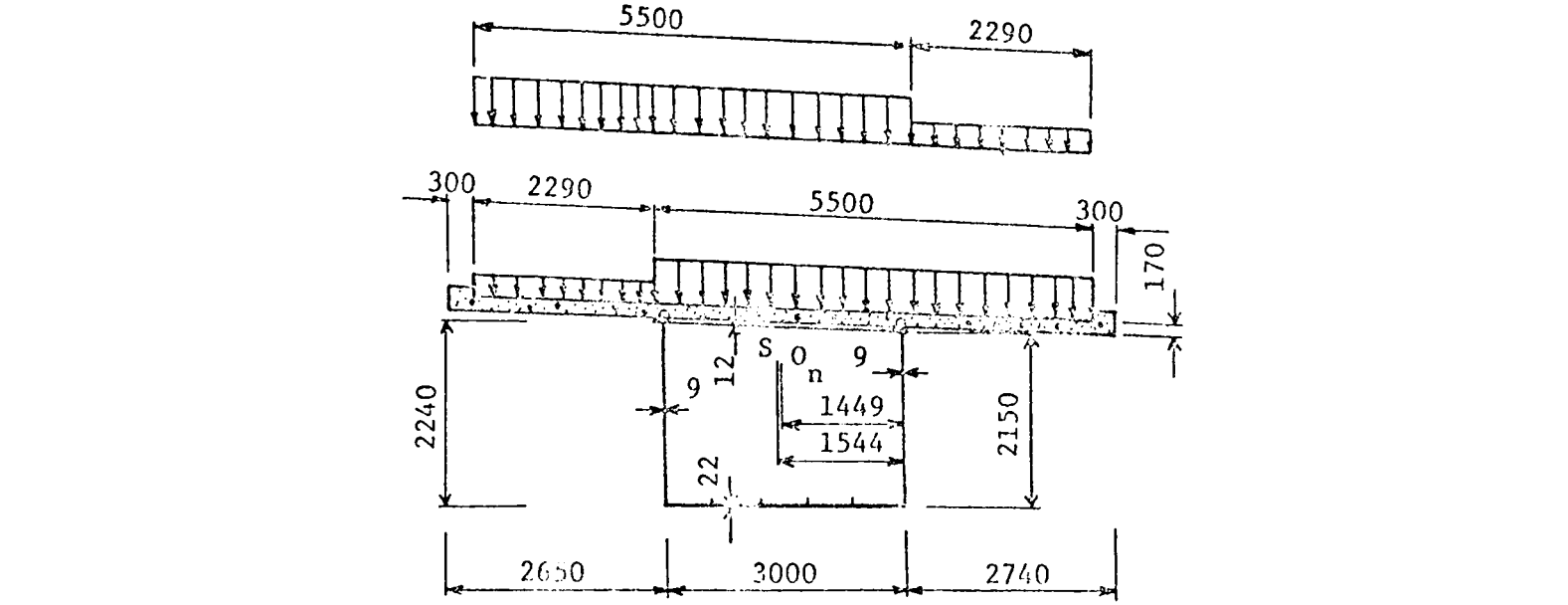

Loading A

Loading B

Loading C

Fig. 4.13 Loadings Based on the Bridge Specifications of the Japan Load Association

inner curb and in the second span as close to outer curb, respectively, as was required by the specifications. In Loading B, the load was placed in both the spans as close to the inner curb as was required by the specifications. To evaluate the normal stresses, however, the load was placed on the opposite side of the lane to that occupied by Loading B so as to produce the torque loads in the reverse direction. Let us denote this loading condition by Loading C (Fig. 4.13).

The shear flows and normal stresses distributions in the cross sections of the bridge are shown in Fig. 4.14 through Fig. 4.21. The dashed line in the figures indicates the distributions of these quantities in the case where the influence of the warping-shear correction factor ν^* is taken into consideration. The numbers in the parentheses in the figures indicate the corresponding values.

The values of the shear flows and normal stresses shown in the figures have units of kg/cm and kg/cm^2, respectively.

Shear flows and normal stresses evaluated from the two types of the modified torsional bending thoeries are tabulated in Table 4.2 through Table 4.4 for the sake of comparison. The directions of the shear flows agree with those indicated with arrows in Fig. 4.15 through Fig. 4.18. Fig. 4.22 shows the numbers of the nodal points of the cross section.

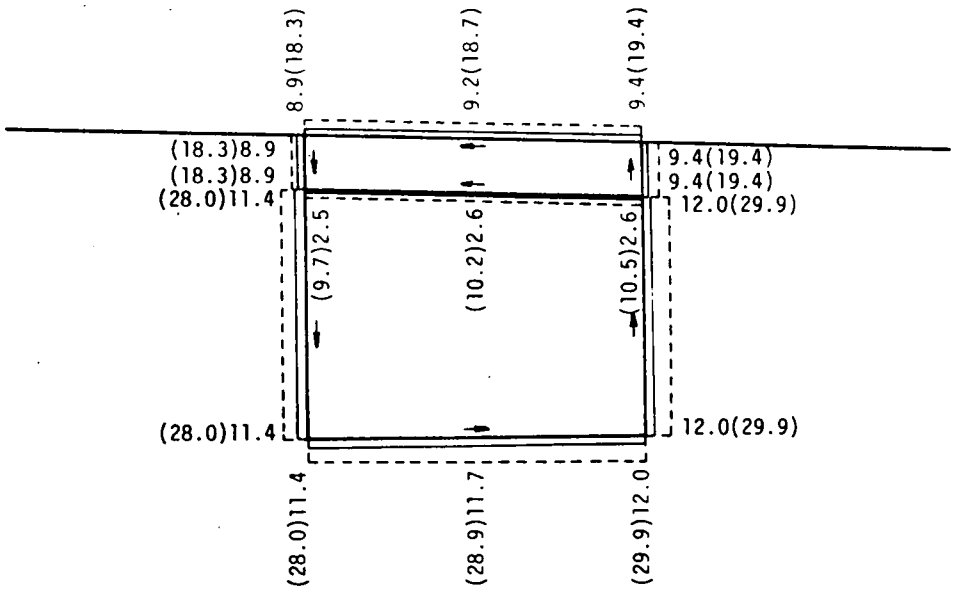

(a) Loading A

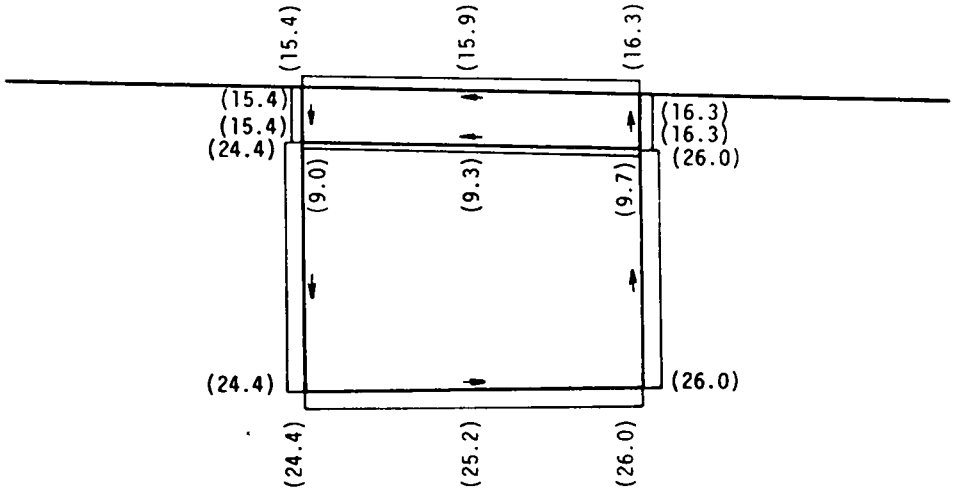

(b) Loading B

Fig. 4.14 Shear Flows Due to Primary Torsional Moment T_s^*

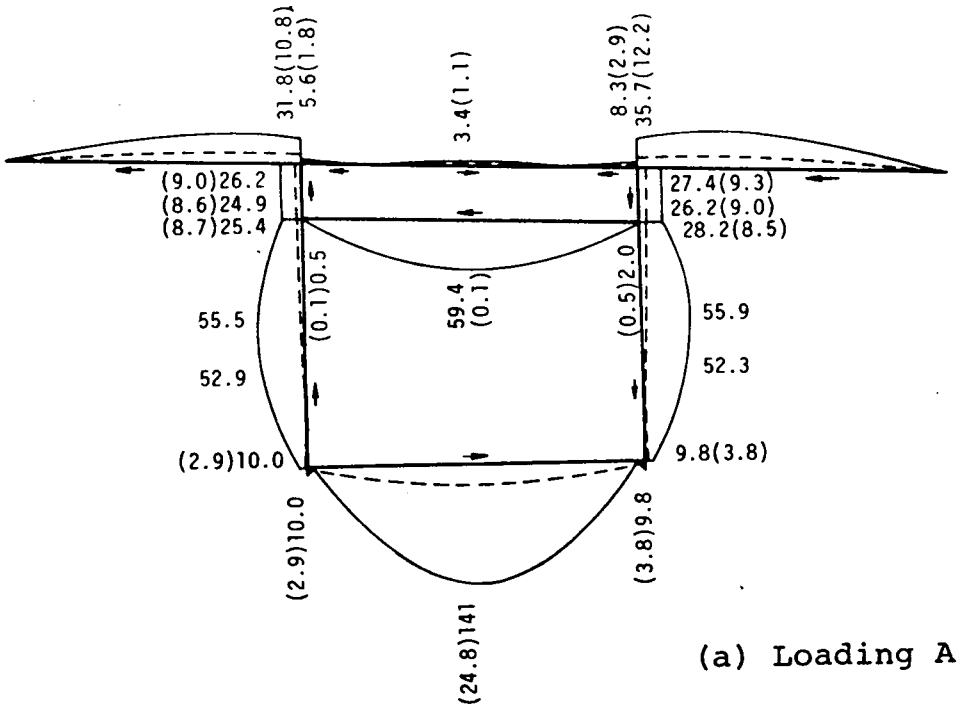

(a) Loading A

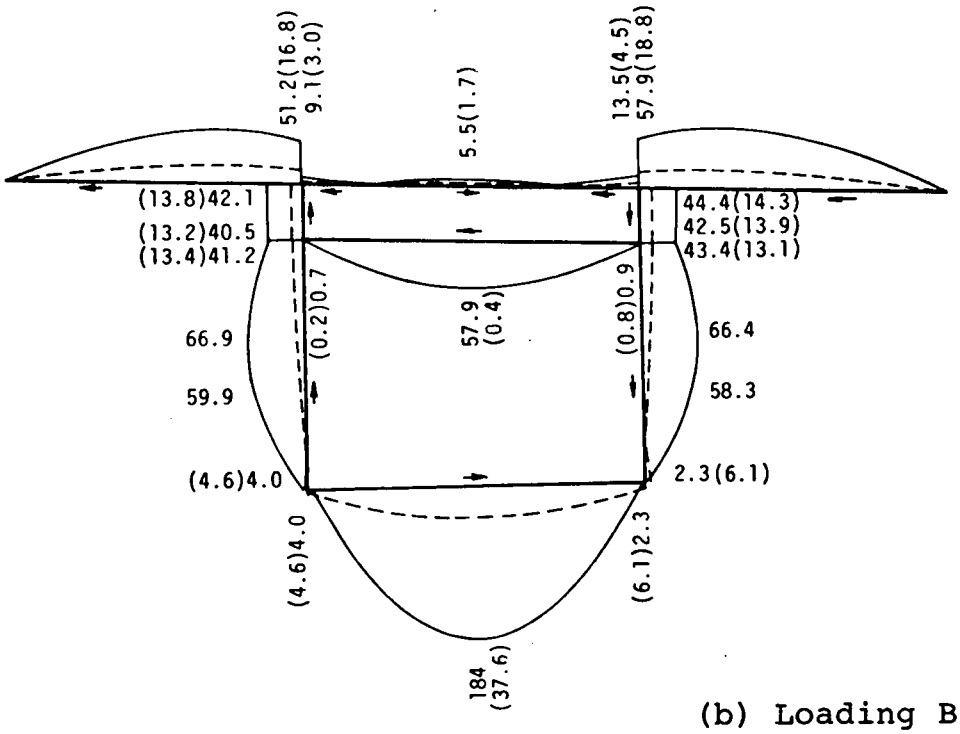

(b) Loading B

Fig. 4.15 Shear Flows Due to Secondary Torsional Moment T_ω^*

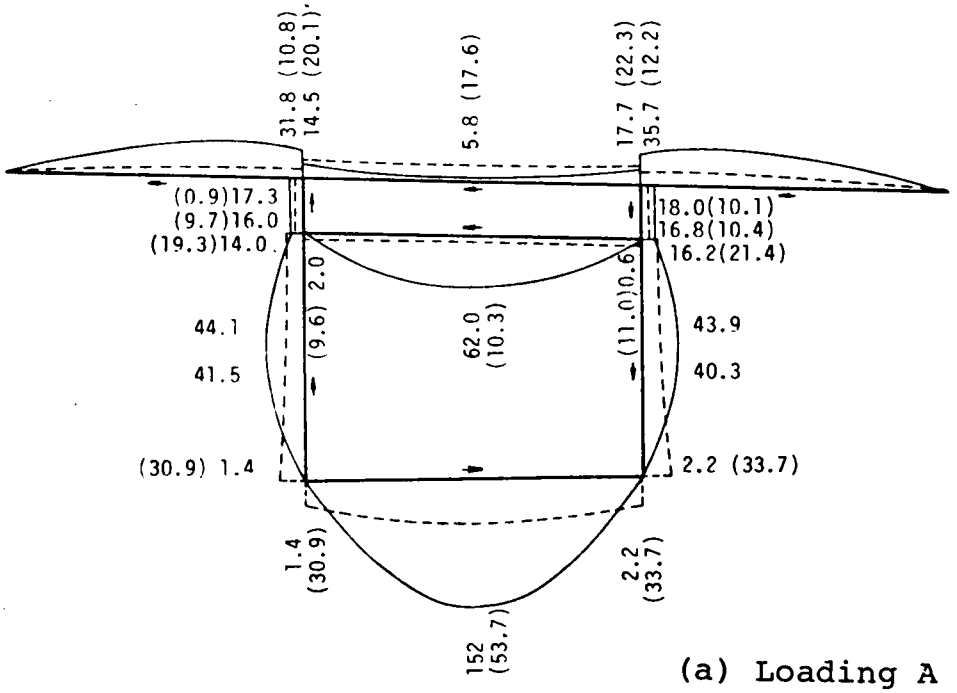

(a) Loading A

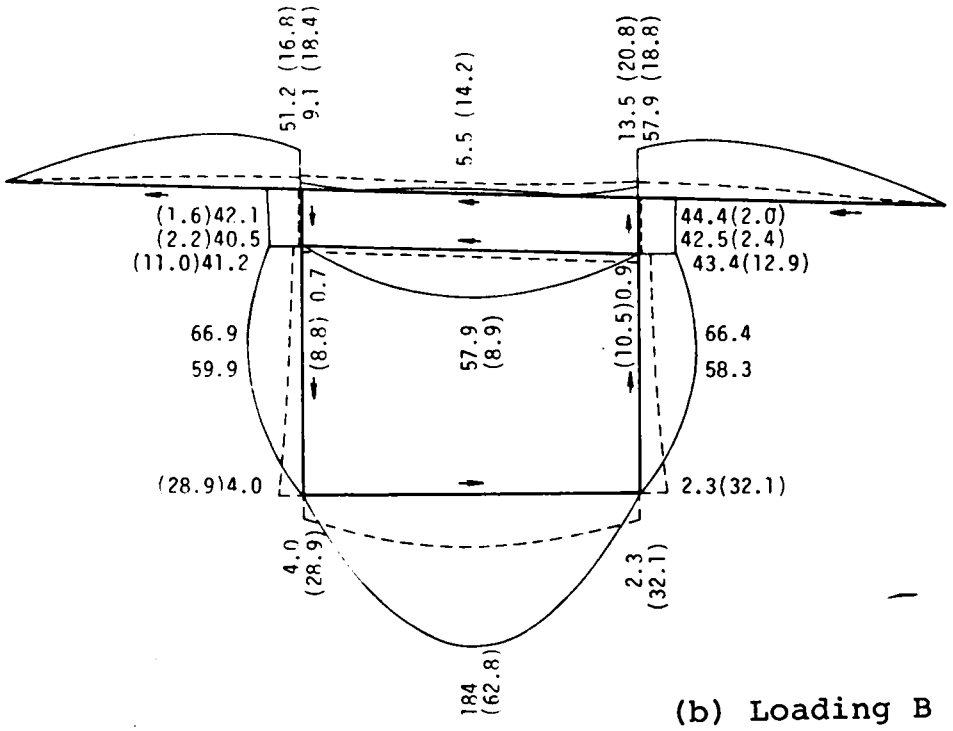

(b) Loading B

Fig. 4.16 Shear Flows Due to Total Torsional Moment T_x^*

$T_x^* (= T_s^* + T_\omega^*)$

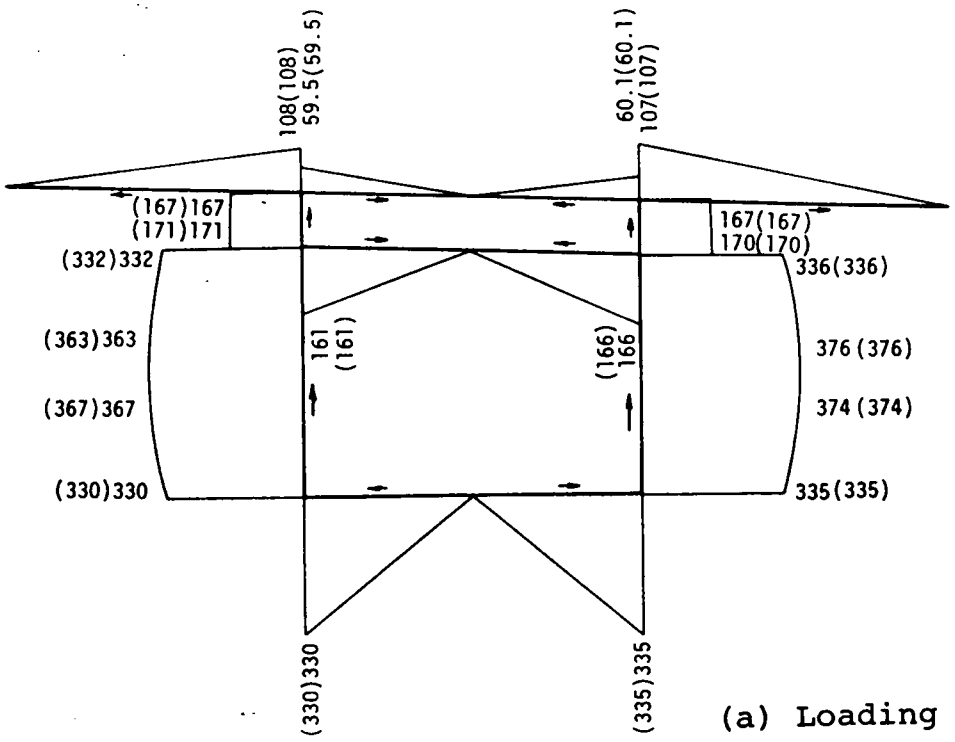

(a) Loading A

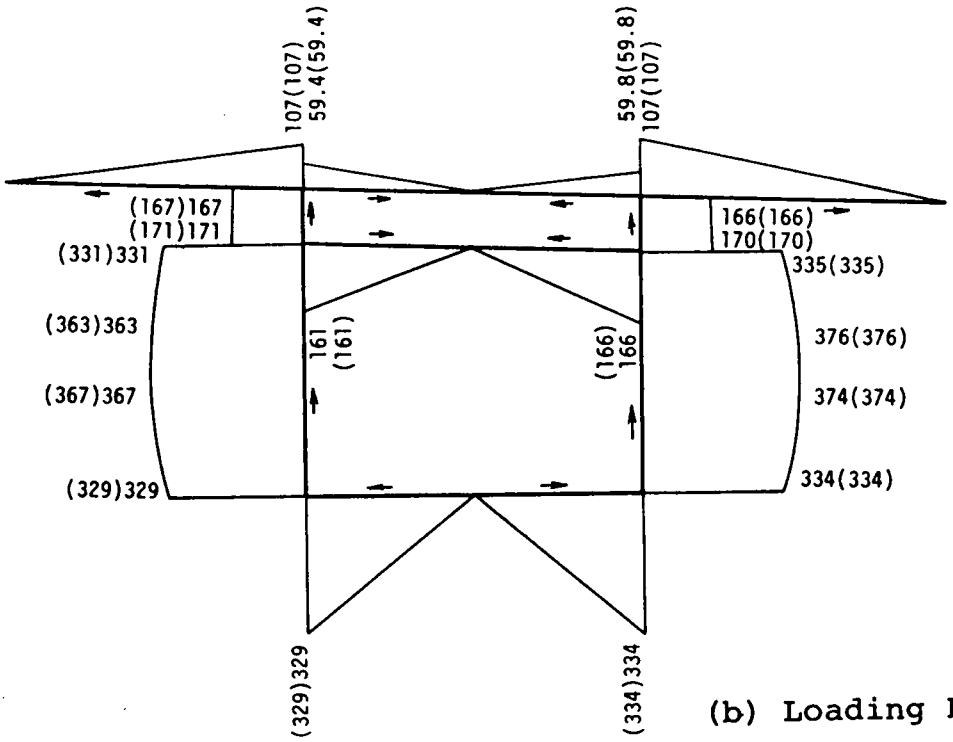

(b) Loading B

Fig. 4.17 Shear Flows Due to Bending Moment M_y

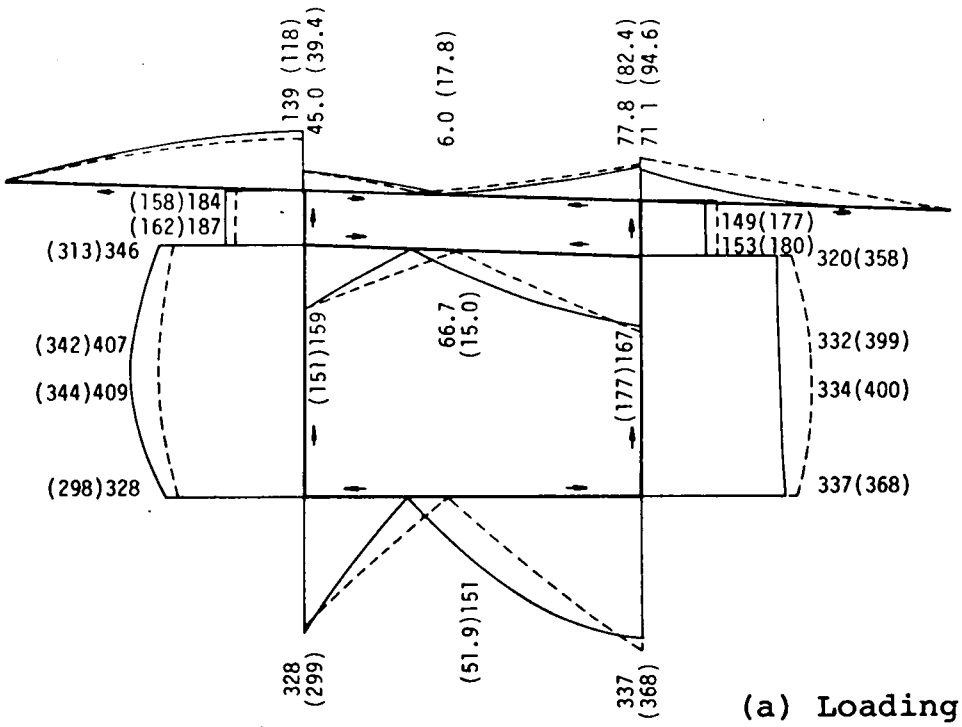

Fig. 4.18 Final Shear Flows Distribution on the Indicated Section

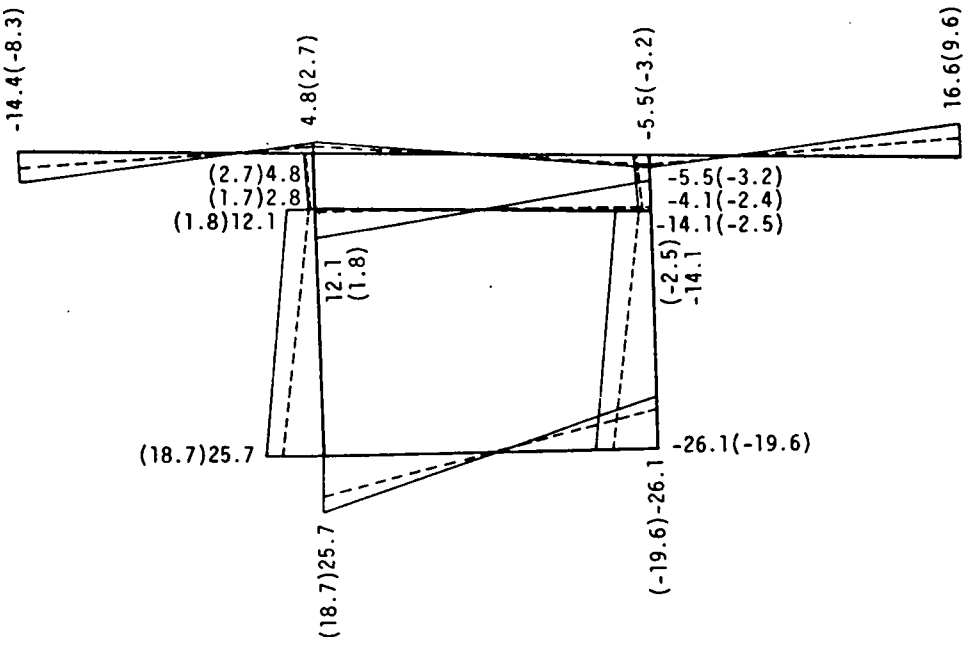

Fig. 4.19 Normal Stresses Due to Warping Moment M_ω*

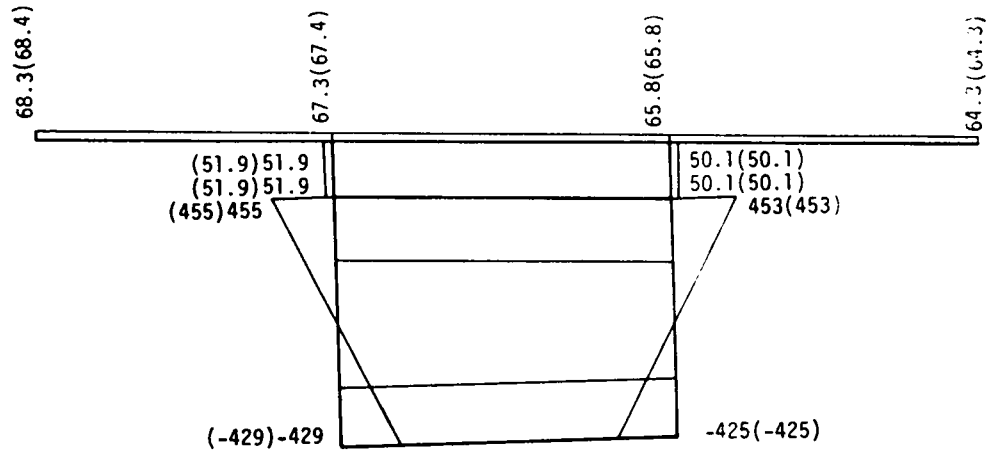

Fig. 4.20 Normal Stresses Due to Bending Moment M_y

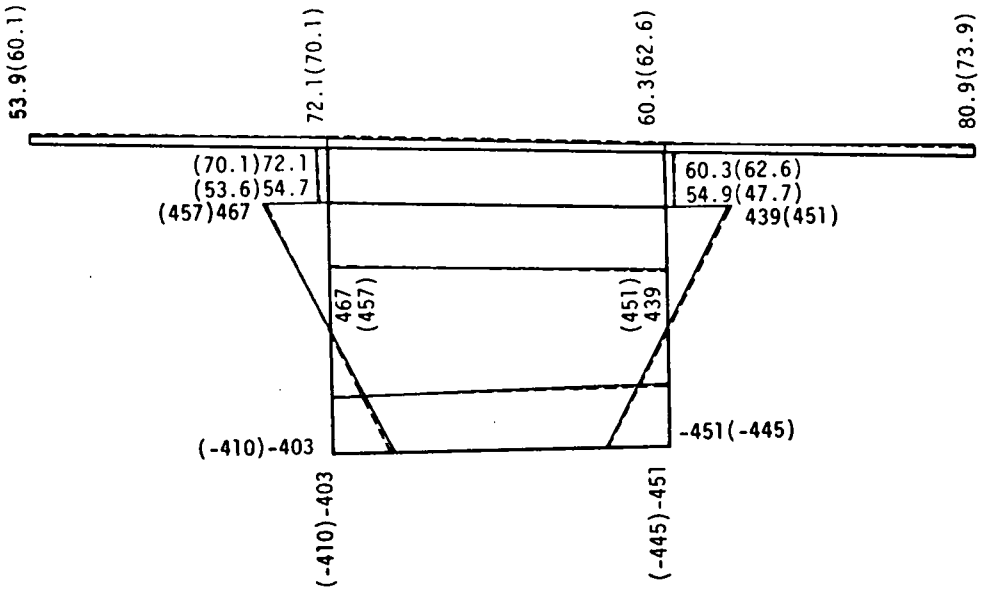

Fig. 4.21 Final Normal Stresses Distribution on the Indicated Section

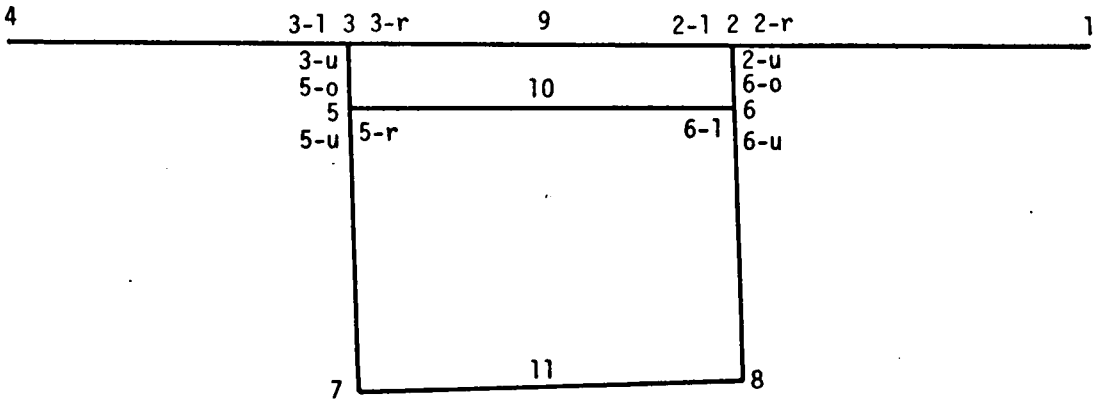

Fig. 4.22 Number of the Nodal Points of the Cross Section

Table 4.2 Comparison of Shear Flows Evaluated Using Two Types of the Theories under Loading A

(a) Theory of First Type
(b) Theory of Second Type

Nodal Point	Shear Flow q_s		Shear Flow q_ω		Shear Flow q_b		Shear Flow q	
	(a)	(b)	(a)	(b)	(a)	(b)	(a)	(b)
1	0	0	0	0	0	0	0	0
2-r	0	0	12.2	12.7	107	107	94.6	94.3
2-l	19.4	16.1	2.9	3.0	60.1	60.1	82.4	79.1
2-u	19.4	16.1	9.3	9.7	167	167	177	173
3-r	18.3	15.2	1.8	1.9	59.5	59.5	39.4	42.4
3-l	0	0	10.8	11.4	108	108	118	119
3-u	18.3	15.2	9.0	9.5	167	167	158	161
4	0	0	0	0	0	0	0	0
5-r	9.7	8.9	0.1	0.1	161	161	151	152
5-o	18.3	15.2	8.6	8.9	171	171	162	165
5-u	28.0	24.1	8.7	9.0	332	332	312	317
6-l	10.5	9.5	0.5	0.5	166	166	177	176
6-o	19.4	16.1	9.0	9.4	170	170	180	177
6-u	29.9	25.6	8.5	8.9	336	336	358	353
7	28.0	24.1	2.9	3.2	330	330	299	303
8	29.9	25.6	3.8	3.9	335	335	368	364
9	18.7	15.8	1.1	1.1	0.2	0.2	17.8	14.9
10	10.2	9.1	0.1	0.3	4.7	4.7	15.0	14.1
11	28.9	24.8	24.8	26.0	1.8	1.8	51.9	49.0

Table 4.3 Comparison of Shear Flows Evaluated Using Two Types of the Theories under Loading B

(a) Theory of First Type
(b) Theory of Second Type

Nodal Point	Shear Flow q_s		Shear Flow q_ω		Shear Flow q_b		Shear Flow q	
	(a)	(b)	(a)	(b)	(a)	(b)	(a)	(b)
1	0	0	0	0	0	0	0	0
2-r	0	0	18.8	19.7	107	107	87.8	86.9
2-1	16.3	19.2	4.5	4.6	59.8	59.8	80.6	83.6
2-u	16.3	19.2	14.3	15.3	166	166	168	171
3-r	15.4	18.1	3.0	3.1	59.4	59.3	41.0	38.1
3-1	0	0	16.8	17.5	107	107	124	125
3-u	15.4	18.1	13.8	14.4	167	167	165	163
4	0	0	0	0	0	0	0	0
5-r	9.0	9.5	0.2	0.2	161	161	152	151
5-o	15.4	18.1	13.2	13.8	171	171	169	166
5-u	24.4	27.6	13.4	14.0	331	331	320	318
6-1	9.7	10.3	0.8	0.8	166	166	176	177
6-o	16.3	19.2	13.9	14.6	170	170	172	174
6-u	26.0	29.5	13.1	13.8	335	336	348	351
7	24.4	27.6	4.6	5.1	329	329	300	297
8	26.0	29.5	6.1	6.3	334	334	366	370
9	15.9	18.8	1.7	1.9	0.2	0.2	14.4	17.1
10	9.3	10.0	0.4	0.2	4.7	4.7	7.2	14.5
11	25.2	28.5	37.6	19.4	1.8	1.8	61.0	66.1

Table 4.4 Comparison of Normal Stresses Evaluated Using Two Types of the Theories under Loading C

Nodal Point	Normal Stress σ_ω		Normal Stress σ_b		Normal Stress σ	
	(a)	(b)	(a)	(b)	(a)	(b)
1	9.6	9.8	64.3	64.3	73.9	74.1
2	-3.2	-3.2	65.8	65.8	62.6	62.6
3	2.7	2.8	67.4	67.4	70.1	70.2
4	-8.3	-8.5	68.4	68.4	60.1	59.9
5	1.8	1.9	455	455	457	457
6	-2.5	-2.6	453	453	451	450
7	18.7	18.9	-429	-429	-410	-410
8	-19.6	-19.3	-425	-425	-445	-444

(a) Theory of First Type

(b) Theory of Second Type

V. SUMMARY AND CONCLUSIONS

It seems that, in the conventional torsional bending theories, the influence of the secondary shear deformation due to restrained torsion is not taken into consideration in deriving the fundamental equations. In the case of a girder bridge with closed cross sections, however, disregard of the secondary shear deformation will lead to an unsatisfactory result, especially at the sections highly restrained against torsion. This is because the secondary shear deformations appear, in general, to be about the same amount as, or, according to circumstances, to be considerably greater than the primary ones evaluated from the Saint-Venant solution as the first order approximation of the shear deformation.

It should be noted that torsional moments play a still more important role in the design of the curved girder bridges, since much higher torsional moments develope throughout their length owing to the curvature effects of their longitudinal axes even though they are subjected to the transverse loadings. Therefore, it is desirable to analyse more precisely the stresses produced by torsional moments.

From this viewpoint, the author has developed the two kinds of the modified torsional bending theories, in which the influence of the secondary shear deformations due to restrained torsion is taken into account, so as to cover the circularly curved box girder bridges. In the theories, the dimensionless cross-sectional properties, κ^* and η^*, are newly introduced.

They may serve as a measure for evaluating the influence of the secondary shear deformation on the distribution of the stresses in the cross sections. Therefore, they are called the "warping-shear correction parameters". As these parameters approach unity in the limit, respectively, the modified torsional bending theories agree with the conventional ones. Therefore, we see that the conventional torsional bending theories may be regarded as special cases of the modified ones.

The fact that between these parameters there exists an inequality such that $1 \geqq \eta^* \geqq \kappa^* \geqq 0$ was derived from a theoretical study by the author. This will provide us with information as to which one of the theories gives a moderate or higher estimate of the statical and kinematical quantities related to restrained torsion, as can be seen from the conclusions stated below.

The summary of the results obtained by using the modified torsional bending theory of first-type is shown below. However, it should be noted that the same may be said of the theory of second-type because in both the theories the fundamental equations governing torsional bending phenomenon are of the same form. If it is possible to generalize from the numerical examples invetigated in Chapter IV, it would appear that:

(1) As the value of the warping-shear correction factor ν^* gets larger (which is the same as the warping-shear parameter κ^* or η^* getting larger), the absolute values of the ordinates to the influence-line for $\hat{T}_S^*$ on the cross section just

to the right of the intermediate support become smaller in the first span. However, the relation is reversed in the second span. Under the same condition, the absolute values for $\hat{M}_\omega^*$ on the cross section of the intermediate support and $\hat{T}_\omega^*$ on the cross section just to the right of the intermediate support become larger in both the spans (see Fig. 4.4 through Fig. 4.6).

(2) The ordinates to the influence-lines for $\hat{M}_\omega^*$, $\hat{T}_s^*$, and $\hat{T}_\omega^*$ on the intermediate sections located at the middle and four-fifths points of the first span decrease rapidly from the sections under consideration toward both end sections (see Fig. 4.8 through Fig. 4.10).

(3) When the parameter $\mu^*\theta$ changes from 20 to 50, the absolute values of the ordinates to the influence-line for $\hat{M}_\omega^*$ become smaller as a whole; however, those for $\hat{T}_s^*$ and $\hat{T}_\omega^*$ show no appreciable changes except in the neighbourhood of the sections under consideration (see Fig. 4.4 through Fig. 4.6 and Fig. 4.8 through Fig. 4.10).

(4) As the value of the parameter ν^* gets larger, the absolute values of the ordinates to the influence-line for $\hat{\chi}^*$ on the section just to the right of the intermediate support and on the intermediate sections become larger. In the former case, however, there appears no appreciable changes except in the neighbourhood of the sections under consideration (see Figs. 4.7 and 4.10).

(5) When the parameter $\mu^*\theta$ changes from 20 to 50, the influence of the factor ν^* on the ordinates to the influence-lines for $\hat{\chi}^*$ is reduced as a matter of course (see Figs. 4.7

and 4.11).

(6) The ordinates to the influence-lines for $\hat{\phi}$ on the intermediate sections are scarcely affected by the factor ν^* except in the neighbourhood of the sections under consideration (see Fig. 4.12).

(7) In the section just to the right of the intermediate support where torsion is highly restrained, the distributions of shear flows has the following tendency. As the parameter ν^* approaches infinity in the limit, the value of the final shear flows increases in the web plate and the shear connector of the outer side and decreases in those of the inner side, at the most, by about 20 percent (see Fig. 4.18).

(8) In the case of curved composite box girder bridges used frequently as the ramp structures, the values of the cross-sectional characteristics $\mu^*\Theta$ and ν^* seem to be relatively small (see Table 4.1). Since this is the case, the influence of the factor ν^* on the distributions of the shear flows in a cross section of such structures appears to some extent at the cross section where torsion is highly restrained.

(9) The value of the normal stresses is scarcely affected by the factor ν^* even on the section where torsion is highly restrained (see Fig. 4.12).

(10) As can be seen from Table 4.1, there seems to exist no appreciable deffernces between the values of the two types of the warping-shear correction parameters, κ^* and η^*. Therefore, it can be supposed that the computation using the two types of the modified torsional bending theories will lead

to nearly the same results for the stress couples, $\hat{M}_{\omega}^{*}$, $\hat{T}_{s}^{*}$, and $\hat{T}_{\omega}^{*}$, and hence, for the stresses distributions (see Table 4.2 through Table 4.4).

The results mentioned above will be useful in the determination of the strength of web plates required to prevent buckling and in the design of shear connectors of the curved composite box girder bridges.

It should be noted that these results are derived from theoretical investigations. Therefore, we must wait for the detailed experimental studies to confirm the correctness of these conclusions.

APPENDIX I.

Demonstration of Orthogonality Relation with an Example

To demonstrate the procedure for proof, let us consider a two-celled structure shown in Fig. 3.3(a). In the figure, the positive directions of paths along which integrations are to be performed are indicated by the arrows. The flow type of quantities $\tilde{q}_s$, $\tilde{q}_\omega$, and S_ω^* are taken as positive when they act in the directions indicated by the arrows, as shown in Fig. 3.3(b), (c), and (d), respectively.

In order to reduce the structure to a thin-walled open section, imaginary cuts will be made at the right ends of the cover plates. Then, according to Eq. (3.32), the equations of consistent deformation for the secondary shear flows q_ω can be written in an expanded form as follows:

$$\tilde{q}^0_{\omega,1}\left\{\int_{0,1}\frac{1}{\rho^3}\frac{n_g}{t}\,ds+\int_{1,4}\frac{1}{\rho^3}\frac{n_g}{t}\,ds+\int_{4,5}\frac{1}{\rho^3}\frac{n_g}{t}\,ds+\int_{5,0}\frac{1}{\rho^3}\frac{n_g}{t}\,ds\right\}-\tilde{q}^0_{\omega,2}\int_{1,4}\frac{1}{\rho^3}\frac{n_g}{t}\,ds$$

$$=\oint_1\frac{1}{\rho^3}S_\omega^*\frac{n_g}{t}\,ds \qquad \text{..... (A.1)}$$

$$\tilde{q}^0_{\omega,2}\left\{\int_{1,2}\frac{1}{\rho^3}\frac{n_g}{t}\,ds + \int_{2,3}\frac{1}{\rho^3}\frac{n_g}{t}\,ds + \int_{3,4}\frac{1}{\rho^3}\frac{n_g}{t}\,ds + \int_{4,1}\frac{1}{\rho^3}\frac{n_g}{t}\,ds\right\} - \tilde{q}^0_{\omega,1}\int_{4,1}\frac{1}{\rho^3}\frac{n_g}{t}\,ds$$

$$= \oint_2 \frac{1}{\rho^3} S_\omega^* \frac{n_g}{t}\,ds \qquad \text{..... (A.2)}$$

The expression obtained from the addition of two expressions, Eq. (A.1) multiplied by $\tilde{q}^0_{s,1}$ and Eq. (A.2) multiplied by $\tilde{q}^0_{s,2}$, can be rearranged as follows:

$$\tilde{q}^0_{s,1}\oint_1 \frac{1}{\rho^3} S_\omega^* \frac{n_g}{t}\,ds + \tilde{q}^0_{s,2}\oint_2 \frac{1}{\rho^3} S_\omega^* \frac{n_g}{t}\,ds$$

$$= \tilde{q}^0_{s,1}\tilde{q}^0_{\omega,1}\left\{\int_{0,1}\frac{1}{\rho^3}\frac{n_g}{t}\,ds + \int_{4,5}\frac{1}{\rho^3}\frac{n_g}{t}\,ds + \int_{5,0}\frac{1}{\rho^3}\frac{n_g}{t}\,ds\right\}$$

$$+ \tilde{q}^0_{s,2}\tilde{q}^0_{\omega,2}\left\{\int_{1,2}\frac{1}{\rho^3}\frac{n_g}{t}\,ds + \int_{2,3}\frac{1}{\rho^3}\frac{n_g}{t}\,ds + \int_{3,4}\frac{1}{\rho^3}\frac{n_g}{t}\,ds\right\}$$

$$+ \tilde{q}^0_{s,1}(\tilde{q}^0_{\omega,1} - \tilde{q}^0_{\omega,2})\int_{1,4}\frac{1}{\rho^3}\frac{n_g}{t}\,ds$$

$$- \tilde{q}^0_{s,2}(\tilde{q}^0_{\omega,1} - \tilde{q}^0_{\omega,2})\int_{4,1}\frac{1}{\rho^3}\frac{n_g}{t}\,ds$$

$$= \tilde{q}^0_{s,1}\tilde{q}^0_{\omega,1}\left\{\int_{0,1} \frac{1}{\rho^3}\frac{n_g}{t}\,ds + \int_{4,5} \frac{1}{\rho^3}\frac{n_g}{t}\,ds + \int_{5,0} \frac{1}{\rho^3}\frac{n_g}{t}\,ds\right\}$$

$$+ \tilde{q}^0_{s,2}\tilde{q}^0_{\omega,2}\left\{\int_{1,2} \frac{1}{\rho^3}\frac{n_g}{t}\,ds + \int_{2,3} \frac{1}{\rho^3}\frac{n_g}{t}\,ds + \int_{3,4} \frac{1}{\rho^3}\frac{n_g}{t}\,ds\right\}$$

$$+ (\tilde{q}^0_{s,1} - \tilde{q}^0_{s,2})(\tilde{q}^0_{\omega,1} - \tilde{q}^0_{\omega,2})\int_{1,4} \frac{1}{\rho^3}\frac{n_g}{t}\,ds$$

$$= \int_F \tilde{q}_s\tilde{q}_\omega \frac{1}{\rho^3}\frac{n_g}{t}\,ds$$

..... (A.3)

By noting the positive directions of the flow type of quantities S_ω^*, we can transform the left side of Eq. (A.3) into the following alternative form:

$$\tilde{q}^0_{s,1}\oint_1 \frac{1}{\rho^3} S_\omega^* \frac{n_g}{t}\,ds + \tilde{q}^0_{s,2}\oint_2 \frac{1}{\rho^3} S_\omega^* \frac{n_g}{t}\,ds$$

$$= \tilde{q}^0_{s,1}\left\{\int_{0,1} \frac{1}{\rho^3} S_\omega^* \frac{n_g}{t}\,ds + \int_{1,4} \frac{1}{\rho^3} S_\omega^* \frac{n_g}{t}\,ds\right.$$

$$\left. + \int_{4,5} \frac{1}{\rho^3} S_\omega^* \frac{n_g}{t}\,ds + \int_{5,0} \frac{1}{\rho^3} S_\omega^* \frac{n_g}{t}\,ds\right\}$$

$$+ \tilde{q}^0_{s,2}\left\{\int_{1,2} \frac{1}{\rho^3} S_\omega^* \frac{n_g}{t}\,ds + \int_{2,3} \frac{1}{\rho^3} S_\omega^* \frac{n_g}{t}\,ds\right.$$

$$+ \int_{3,4} \frac{1}{\rho^3} S_\omega^* \frac{n_g}{t} ds + \int_{4,1} \frac{1}{\rho^3} S_\omega^* \frac{n_g}{t} ds \Big\}$$

$$= \tilde{q}^0_{s,1} \Big\{ \int_{0,1} \frac{1}{\rho^3} S_\omega^* \frac{n_g}{t} ds + \int_{4,5} \frac{1}{\rho^3} S_\omega^* \frac{n_g}{t} ds$$

$$+ \int_{5,0} \frac{1}{\rho^3} S_\omega^* \frac{n_g}{t} ds \Big\}$$

$$+ \tilde{q}^0_{s,2} \Big\{ \int_{1,2} \frac{1}{\rho^3} S_\omega^* \frac{n_g}{t} ds + \int_{2,3} \frac{1}{\rho^3} S_\omega^* \frac{n_g}{t} ds$$

$$+ \int_{3,4} \frac{1}{\rho^3} S_\omega^* \frac{n_g}{t} ds \Big\}$$

$$+ (\tilde{q}^0_{s,1} - \tilde{q}^0_{s,2}) \int_{1,4} \frac{1}{\rho^3} S_\omega^* \frac{n_g}{t} ds$$

$$= \int_F \tilde{q}_s S_\omega^* \frac{1}{\rho^3} \frac{n_g}{t} ds$$

..... (A.4)

Thus, we find from Eqs. (A.3) and (A.4) that the orthogonality relation (3.30) holds for the two-celled structure.

APPENDIX II.

List of Solutions for Statical and Kinematical Quantities

For simplicity, we introduce the following notations

$$\tilde{\theta} = \Theta - \theta \qquad \beta = \frac{G_s}{E_s} \frac{J_z J_T^*}{J_y J_z - J_{yz}^2}$$

$$\tilde{\Phi} = \Theta - \Phi$$

$$\alpha = \frac{1}{2}\left(1 - \frac{\kappa^{*2}}{1 + \kappa^{*2}\mu^{*2}} + \beta\right) \qquad \text{..... (A.5)}$$

Then, the solutions are given by

$$M_y(\theta)$$

$$= M_{y1} \frac{\sin\tilde{\theta}}{\sin\Theta} + M_{y2} \frac{\sin\theta}{\sin\Theta} + \begin{cases} (\tilde{T} + R\tilde{P}) \dfrac{\sin\tilde{\Phi}}{\sin\Theta} \sin\theta & \text{for } 0 \leq \theta \leq \Phi \\ (\tilde{T} + R\tilde{P}) \dfrac{\sin\tilde{\theta}}{\sin\Theta} \sin\Phi & \text{for } \Phi \leq \theta \leq \Theta \end{cases}$$

..... (A.6)

$$M_\omega^*(\theta)$$

$$= RM_{y1} \frac{\kappa^{*2}}{1 + \kappa^{*2}\mu^{*2}} \left(\frac{\sin\tilde{\theta}}{\sin\Theta} - \frac{\sinh\kappa^*\mu^*\tilde{\theta}}{\sinh\kappa^*\mu^*\Theta}\right)$$

$$+ RM_{y2} \frac{\kappa^{*2}}{1 + \kappa^{*2}\mu^{*2}} \left(\frac{\sin\theta}{\sin\Theta} - \frac{\sinh\kappa^*\mu^*\theta}{\sinh\kappa^*\mu^*\Theta}\right)$$

$$+ M_{\omega 1}{}^{*} \frac{\sinh\kappa^{*}\mu^{*}\tilde{\theta}}{\sinh\kappa^{*}\mu^{*}\Theta} + M_{\omega 2}{}^{*} \frac{\sinh\kappa^{*}\mu^{*}\theta}{\sinh\kappa^{*}\mu^{*}\Theta}$$

$$\left\{ \begin{array}{l} + \dfrac{\kappa^{*2}}{1 + \kappa^{*2}\mu^{*2}} (R\tilde{T} + R^{2}\tilde{P}) \dfrac{\sin\tilde{\Phi}}{\sin\Theta} \sin\theta \\ \qquad + \left(\kappa^{*}\mu^{*}R\tilde{T} - \dfrac{1}{\kappa^{*}\mu^{*}} R^{2}\tilde{P} \right) \dfrac{\sinh\kappa^{*}\mu^{*}\tilde{\Phi}}{\sinh\kappa^{*}\mu^{*}\Theta} \sinh\kappa^{*}\mu^{*}\theta \\ \qquad\qquad \text{for} \quad 0 \leq \theta \leq \Phi \\ + \dfrac{\kappa^{*2}}{1 + \kappa^{*2}\mu^{*2}} (R\tilde{T} + R^{2}\tilde{P}) \dfrac{\sin\Phi}{\sin\Theta} \sin\tilde{\theta} \\ \qquad + \left(\kappa^{*}\mu^{*}R\tilde{T} - \dfrac{1}{\kappa^{*}\mu^{*}} R^{2}\tilde{P} \right) \dfrac{\sinh\kappa^{*}\mu^{*}\Phi}{\sinh\kappa^{*}\mu^{*}\Theta} \sinh\kappa^{*}\mu^{*}\tilde{\theta} \\ \qquad\qquad \text{for} \quad \Phi \leq \theta \leq \Theta \end{array} \right.$$

.....(A.7)

$$T_{s}{}^{*}(\theta)$$

$$= - M_{y1} \left\{ \left(1 - \frac{\kappa^{*2}}{1 + \kappa^{*2}\mu^{*2}} \right) \frac{\cos\tilde{\theta}}{\sin\Theta} + \frac{\kappa^{*3}\mu^{*}}{1 + \kappa^{*2}\mu^{*2}} \frac{\cosh\kappa^{*}\mu^{*}\tilde{\theta}}{\sinh\kappa^{*}\mu^{*}\Theta} - \frac{1}{\Theta} \right\}$$

$$+ M_{y2} \left\{ \left(1 - \frac{\kappa^{*2}}{1 + \kappa^{*2}\mu^{*2}} \right) \frac{\cos\theta}{\sin\Theta} + \frac{\kappa^{*3}\mu^{*}}{1 + \kappa^{*2}\mu^{*2}} \frac{\cosh\kappa^{*}\mu^{*}\theta}{\sinh\kappa^{*}\mu^{*}\Theta} - \frac{1}{\Theta} \right\}$$

$$+ \frac{1}{R} M_{\omega 1}{}^{*} \left(\kappa^{*}\mu^{*} \frac{\cosh\kappa^{*}\mu^{*}\tilde{\theta}}{\sinh\kappa^{*}\mu^{*}\Theta} - \frac{1}{\Theta} \right) - \frac{1}{R} M_{\omega 2}{}^{*} \left(\kappa^{*}\mu^{*} \frac{\cosh\kappa^{*}\mu^{*}\theta}{\sinh\kappa^{*}\mu^{*}\Theta} - \frac{1}{\Theta} \right)$$

$$
\begin{cases}
+ (\tilde{T} + R\tilde{P})\left(1 - \dfrac{\kappa^{*2}}{1 + \kappa^{*2}\mu^{*2}}\right)\dfrac{\sin\tilde{\Phi}}{\sin\Theta}\cos\theta - R\tilde{P}\,\dfrac{\tilde{\Phi}}{\Theta} \\
\qquad - (\tilde{T} - R\tilde{P})\dfrac{\kappa^{*4}\mu^{*2}}{1 + \kappa^{*2}\mu^{*2}}\,\dfrac{\sinh\kappa^{*}\mu^{*}\tilde{\Phi}}{\sinh\kappa^{*}\mu^{*}\Theta}\cosh\kappa^{*}\mu^{*}\theta \\
\qquad\qquad\qquad\qquad \text{for} \quad 0 \leq \theta \leq \Phi \\
- (\tilde{T} + R\tilde{P})\left(1 - \dfrac{\kappa^{*2}}{1 + \kappa^{*2}\mu^{*2}}\right)\dfrac{\sin\Phi}{\sin\Theta}\cos\tilde{\theta} + R\tilde{P}\,\dfrac{\Phi}{\Theta} \\
\qquad + (\tilde{T} - R\tilde{P})\dfrac{\kappa^{*4}\mu^{*2}}{1 + \kappa^{*2}\mu^{*2}}\,\dfrac{\sinh\kappa^{*}\mu^{*}\Phi}{\sinh\kappa^{*}\mu^{*}\Theta}\cosh\kappa^{*}\mu^{*}\tilde{\theta} \\
\qquad\qquad\qquad\qquad \text{for} \quad \Phi \leq \theta \leq \Theta
\end{cases}
$$

..... (A.8)

$$
\begin{aligned}
& T_{\omega}^{*}(\theta) \\
= & - M_{y1}\,\frac{\kappa^{*2}}{1 + \kappa^{*2}\mu^{*2}}\left(\frac{\cos\tilde{\theta}}{\sin\Theta} - \kappa^{*}\mu^{*}\,\frac{\cosh\kappa^{*}\mu^{*}\tilde{\theta}}{\sinh\kappa^{*}\mu^{*}\Theta}\right) \\
& + M_{y2}\,\frac{\kappa^{*2}}{1 + \kappa^{*2}\mu^{*2}}\left(\frac{\cos\theta}{\sin\Theta} - \kappa^{*}\mu^{*}\,\frac{\cosh\kappa^{*}\mu^{*}\theta}{\sinh\kappa^{*}\mu^{*}\Theta}\right) \\
& - \frac{1}{R}\,M_{\omega 1}^{*}\,\kappa^{*}\mu^{*}\,\frac{\cosh\kappa^{*}\mu^{*}\tilde{\theta}}{\sinh\kappa^{*}\mu^{*}\Theta} + \frac{1}{R}\,M_{\omega 2}^{*}\,\kappa^{*}\mu^{*}\,\frac{\cosh\kappa^{*}\mu^{*}\theta}{\sinh\kappa^{*}\mu^{*}\Theta} \\
& \begin{cases}
+ \dfrac{\kappa^{*2}}{1 + \kappa^{*2}\mu^{*2}}\left\{(\tilde{T} + R\tilde{P})\dfrac{\sin\tilde{\Phi}}{\sin\Theta}\cos\theta + \right.
\end{cases}
\end{aligned}
$$

$$
\left\{
\begin{array}{l}
\qquad\qquad + (\kappa^{*2}\mu^{*2}\tilde{T} - R\tilde{P})\dfrac{\sinh\kappa^*\mu^*\tilde{\Phi}}{\sinh\kappa^*\mu^*\Theta}\cosh\kappa^*\mu^*\theta\Big\} \\
\qquad\qquad\qquad\qquad\qquad\qquad\qquad\qquad \text{for} \quad 0 \leq \theta \leq \Phi \\
-\dfrac{\kappa^{*2}}{1+\kappa^{*2}\mu^{*2}}\Big\{(\tilde{T} + R\tilde{P})\dfrac{\sin\Phi}{\sin\Theta}\cos\tilde{\theta} + \\
\qquad\qquad + (\kappa^{*2}\mu^{*2}\tilde{T} - R\tilde{P})\dfrac{\sinh\kappa^*\mu^*\Phi}{\sinh\kappa^*\mu^*\Theta}\cosh\kappa^*\mu^*\tilde{\theta}\Big\} \\
\qquad\qquad\qquad\qquad\qquad\qquad\qquad\qquad \text{for} \quad \Phi \leq \theta \leq \Theta
\end{array}
\right.
$$

.....(A.9)

$$
T_x^*(\theta)
$$

$$
= -M_{y1}\frac{\cos\tilde{\theta}}{\sin\Theta} + M_{y2}\frac{\cos\theta}{\sin\Theta} - \frac{1}{R}M_{\omega 1}^*\frac{1}{\Theta} + \frac{1}{R}M_{\omega 2}^*\frac{1}{\Theta}
$$

$$
\left\{
\begin{array}{l}
+ (\tilde{T} + R\tilde{P})\dfrac{\sin\tilde{\Phi}}{\sin\Theta}\cos\theta - R\tilde{P}\dfrac{\tilde{\Phi}}{\Theta} \\
\qquad\qquad - R\tilde{P}\kappa^{*2}\dfrac{1-\kappa^{*2}\mu^{*2}}{1+\kappa^{*2}\mu^{*2}}\dfrac{\sinh\kappa^*\mu^*\tilde{\Phi}}{\sinh\kappa^*\mu^*\Theta}\cosh\kappa^*\mu^*\theta \\
\qquad\qquad\qquad\qquad\qquad\qquad\qquad\qquad \text{for} \quad 0 \leq \theta \leq \Phi \\
- (\tilde{T} + R\tilde{P})\dfrac{\sin\Phi}{\sin\Theta}\cos\tilde{\theta} + R\tilde{P}\dfrac{\Phi}{\Theta} \\
\qquad\qquad + R\tilde{P}\kappa^{*2}\dfrac{1-\kappa^{*2}\mu^{*2}}{1+\kappa^{*2}\mu^{*2}}\dfrac{\sinh\kappa^*\mu^*\Phi}{\sinh\kappa^*\mu^*\Theta}\cosh\kappa^*\mu^*\tilde{\theta} \\
\qquad\qquad\qquad\qquad\qquad\qquad\qquad\qquad \text{for} \quad \Phi \leq \theta \leq \Theta
\end{array}
\right.
$$

.....(A.10)

$$G_s J_T \chi^*(\theta)$$

$$= - M_{y1} \frac{\kappa^{*2}\mu^{*2}}{1 + \kappa^{*2}\mu^{*2}} \left(\frac{\cos\tilde{\theta}}{\sin\theta} + \frac{\kappa^*\mu^*}{1 + \kappa^{*2}\mu^{*2}} \frac{\cosh\kappa^*\mu^*\tilde{\theta}}{\sinh\kappa^*\mu^*\theta} - \frac{1}{\theta} \right)$$

$$+ M_{y2} \frac{\kappa^{*2}\mu^{*2}}{1 + \kappa^{*2}\mu^{*2}} \left(\frac{\cos\theta}{\sin\theta} + \frac{\kappa^*\mu^*}{1 + \kappa^{*2}\mu^{*2}} \frac{\cosh\kappa^*\mu^*\theta}{\sinh\kappa^*\mu^*\theta} - \frac{1}{\theta} \right)$$

$$+ \frac{1}{R} M_{\omega 1}{}^* \left(\frac{\mu^*}{\kappa^*} \frac{\cosh\kappa^*\mu^*\tilde{\theta}}{\sinh\kappa^*\mu^*\theta} - \frac{1}{\theta} \right) - \frac{1}{R} M_{\omega 2}{}^* \left(\frac{\mu^*}{\kappa^*} \frac{\cosh\kappa^*\mu^*\theta}{\sinh\kappa^*\mu^*\theta} - \frac{1}{\theta} \right)$$

$$\begin{cases} + \dfrac{\kappa^{*2}\mu^{*2}}{1 + \kappa^{*2}\mu^{*2}} \left\{ (\tilde{T} + R\tilde{P}) \dfrac{\sin\tilde{\Phi}}{\sin\theta} \cos\theta \right. \\ \qquad \left. - \left(\tilde{T} - \dfrac{1}{\kappa^{*2}\mu^{*2}} R\tilde{P} \right) \dfrac{\sinh\kappa^*\mu^*\tilde{\Phi}}{\sinh\kappa^*\mu^*\theta} \cosh\kappa^*\mu^*\theta \right\} - R\tilde{P} \dfrac{\tilde{\Phi}}{\theta} \\ \qquad\qquad \text{for} \quad 0 \leq \theta \leq \Phi \\ - \dfrac{\kappa^{*2}\mu^{*2}}{1 + \kappa^{*2}\mu^{*2}} \left\{ (\tilde{T} + R\tilde{P}) \dfrac{\sin\Phi}{\sin\theta} \cos\tilde{\theta} \right. \\ \qquad \left. - \left(\tilde{T} - \dfrac{1}{\kappa^{*2}\mu^{*2}} R\tilde{P} \right) \dfrac{\sinh\kappa^*\mu^*\Phi}{\sinh\kappa^*\mu^*\theta} \cosh\kappa^*\mu^*\tilde{\theta} \right\} + R\tilde{P} \dfrac{\Phi}{\theta} \\ \qquad\qquad \text{for} \quad \Phi \leq \theta \leq \Theta \end{cases}$$

..... (A.11)

$$G_s J_T^* \phi(\theta)$$

$$= - RM_{y1}\left\{\frac{\kappa^{*4}\mu^{*2}}{(1+\kappa^{*2}\mu^{*2})^2}\left(\frac{\sin\tilde{\theta}}{\sin\theta} - \frac{\sinh\kappa^*\mu^*\tilde{\theta}}{\sinh\kappa^*\mu^*\theta}\right) - \right.$$

$$\left. - \alpha\left(\tilde{\theta}\,\frac{\cos\tilde{\theta}}{\sin\theta} - \frac{\theta\cos\theta}{\sin^2\theta}\sin\tilde{\theta}\right)\right\}$$

$$- RM_{y2}\left\{\frac{\kappa^{*4}\mu^{*2}}{(1+\kappa^{*2}\mu^{*2})^2}\left(\frac{\sin\theta}{\sin\theta} - \frac{\sinh\kappa^*\mu^*\theta}{\sinh\kappa^*\mu^*\theta}\right) - \right.$$

$$\left. - \alpha\left(\theta\,\frac{\cos\theta}{\sin\theta} - \frac{\theta\cos\theta}{\sin^2\theta}\sin\theta\right)\right\}$$

$$+ M_{\omega 1}^*\,\frac{\kappa^{*2}\mu^{*2}}{1+\kappa^{*2}\mu^{*2}}\left(\frac{\sin\tilde{\theta}}{\sin\theta} - \frac{\sinh\kappa^*\mu^*\tilde{\theta}}{\sinh\kappa^*\mu^*\theta}\right)$$

$$+ M_{\omega 2}^*\,\frac{\kappa^{*2}\mu^{*2}}{1+\kappa^{*2}\mu^{*2}}\left(\frac{\sin\theta}{\sin\theta} - \frac{\sinh\kappa^*\mu^*\theta}{\sinh\kappa^*\mu^*\theta}\right)$$

$$\left\{ + (\kappa^{*2}\mu^{*2}R\tilde{T} - R^2\tilde{P})\frac{\kappa^{*4}\mu^{*2}}{(1+\kappa^{*2}\mu^{*2})^2}\left(\frac{\sin\tilde{\Phi}}{\sin\theta}\sin\theta - \right.\right.$$

$$\left. - \frac{1}{\kappa^*\mu^*}\,\frac{\sinh\kappa^*\mu^*\tilde{\Phi}}{\sinh\kappa^*\mu^*\theta}\sinh\kappa^*\mu^*\theta\right)$$

$$\left. - (R\tilde{T} + R^2\tilde{P})\alpha\left\{\frac{\sin\tilde{\Phi}}{\sin\theta}\left(\theta\cos\theta\,\frac{\sin\theta}{\sin\theta} - \theta\cos\theta\right) + \right.\right.$$

$$
\left.
\begin{aligned}
&\qquad\qquad + (\sin\tilde{\Phi} - \tilde{\Phi}\cos\tilde{\Phi})\frac{\sin\theta}{\sin\Theta}\Big\} \\
&+ R\tilde{T}(1 - \kappa^{*2})\frac{\sin\tilde{\Phi}}{\sin\Theta}\sin\theta \\
&\qquad\qquad\qquad\qquad\qquad\qquad \text{for} \quad 0 \leq \theta \leq \Phi \\
&+ (\kappa^{*2}\mu^{*2}R\tilde{T} - R^2\tilde{P})\frac{\kappa^{*4}\mu^{*2}}{(1 + \kappa^{*2}\mu^{*2})^2}\Big\{\frac{\sin\tilde{\Phi}}{\sin\Theta}\sin\theta - \\
&\qquad\qquad - \frac{1}{\kappa^{*}\mu^{*}}\frac{\sinh\kappa^{*}\mu^{*}\tilde{\Phi}}{\sinh\kappa^{*}\mu^{*}\Theta}\sinh\kappa^{*}\mu^{*}\theta\Big)
\end{aligned}
\right.
$$

$$
\begin{aligned}
&- (R\tilde{T} + R^2\tilde{P})\alpha\Big\{\frac{\sin\Phi}{\sin\theta}\Big(\Theta\cos\Theta\,\frac{\sin\tilde{\theta}}{\sin\Theta} - \tilde{\theta}\cos\tilde{\theta}\Big) + \\
&\qquad\qquad + (\sin\Phi - \Phi\cos\Phi)\frac{\sin\tilde{\theta}}{\sin\Theta}\Big\} \\
&+ R\tilde{T}(1 - \kappa^{*2})\frac{\sin\Phi}{\sin\Theta}\sin\tilde{\theta} \\
&\qquad\qquad\qquad\qquad\qquad\qquad \text{for} \quad \Phi \leq \theta \leq \Theta
\end{aligned}
$$

$$\qquad\qquad\qquad\qquad\qquad\qquad\qquad\qquad\qquad\qquad \ldots\ldots\ldots\ldots\ldots (A.12)$$

$$
\begin{aligned}
&G_s J_T^{*} w^{*}(\theta) \\
&= R^2 M_{y1}\Big\{\frac{\kappa^{*2}}{(1 + \kappa^{*2}\mu^{*2})^2}\Big(\frac{\sin\tilde{\theta}}{\sin\theta} - \frac{\sinh\kappa^{*}\mu^{*}\tilde{\theta}}{\sinh\kappa^{*}\mu^{*}\Theta}\Big) - \frac{\sin\tilde{\theta}}{\sin\Theta} + \frac{\tilde{\theta}}{\Theta} + \\
&\qquad\qquad + \alpha\Big(\tilde{\theta}\,\frac{\cos\tilde{\theta}}{\sin\Theta} - \frac{\Theta\cos\Theta}{\sin^2\Theta}\sin\tilde{\theta}\Big)\Big\}
\end{aligned}
$$

$$+ R^2 M_{y2}\left\{\frac{\kappa^{*2}}{(1+\kappa^{*2}\mu^{*2})^2}\left(\frac{\sin\theta}{\sin\Theta} - \frac{\sinh\kappa^*\mu^*\theta}{\sinh\kappa^*\mu^*\Theta}\right) - \frac{\sin\theta}{\sin\Theta} + \frac{\theta}{\Theta} + \right.$$

$$\left. + \alpha\left(\theta\,\frac{\cos\theta}{\sin\Theta} - \frac{\Theta\cos\Theta}{\sin^2\Theta}\sin\theta\right)\right\}$$

$$+ RM_{\omega 1}{}^*\left(\frac{\kappa^{*2}\mu^{*2}}{1+\kappa^{*2}\mu^{*2}}\,\frac{\sin\tilde{\theta}}{\sin\Theta} + \frac{1}{1+\kappa^{*2}\mu^{*2}}\,\frac{\sinh\kappa^*\mu^*\tilde{\theta}}{\sinh\kappa^*\mu^*\Theta} - \frac{\tilde{\theta}}{\Theta}\right)$$

$$+ RM_{\omega 2}{}^*\left(\frac{\kappa^{*2}\mu^{*2}}{1+\kappa^{*2}\mu^{*2}}\,\frac{\sin\theta}{\sin\Theta} + \frac{1}{1+\kappa^{*2}\mu^{*2}}\,\frac{\sinh\kappa^*\mu^*\theta}{\sinh\kappa^*\mu^*\Theta} - \frac{\theta}{\Theta}\right)$$

$$\left\{\begin{array}{l}
- (\kappa^{*2}\mu^{*2}R^2\tilde{T} - R^3\tilde{P})\dfrac{\kappa^{*2}}{(1+\kappa^{*2}\mu^{*2})^2}\left(\dfrac{\sin\tilde{\Phi}}{\sin\Theta}\sin\theta - \right. \\
\qquad\qquad \left. - \dfrac{1}{\kappa^*\mu^*}\,\dfrac{\sinh\kappa^*\mu^*\tilde{\Phi}}{\sinh\kappa^*\mu^*\Theta}\sinh\kappa^*\mu^*\theta\right) \\
- (R^2\tilde{T} + R^3\tilde{P})\alpha\left\{\dfrac{\sin\tilde{\Phi}}{\sin\Theta}\left(\Theta\cos\Theta\,\dfrac{\sin\theta}{\sin\Theta} - \theta\cos\theta\right) + (\sin\tilde{\Phi} - \tilde{\Phi}\cos\tilde{\Phi})\dfrac{\sin\theta}{\sin\Theta}\right\} \\
- R^3\tilde{P}\left(\dfrac{\sin\tilde{\Phi}}{\sin\Theta}\sin\theta - \dfrac{\tilde{\Phi}}{\Theta}\theta\right) \\
\qquad\qquad\qquad\qquad\qquad\qquad \text{for} \quad 0 \leq \theta \leq \Phi \\
- (\kappa^{*2}\mu^{*2}R^2\tilde{T} - R^3\tilde{P})\dfrac{\kappa^{*2}}{(1+\kappa^{*2}\mu^{*2})^2}\left(\dfrac{\sin\Phi}{\sin\Theta}\sin\tilde{\theta} - \right.
\end{array}\right.$$

$$- \frac{1}{\kappa^*\mu^*} \frac{\sinh\kappa^*\mu^*\Phi}{\sinh\kappa^*\mu^*\Theta} \sinh\kappa^*\mu^*\tilde{\theta}\Big)$$

$$- (R^2\tilde{T} + R^3\tilde{P})\alpha\left\{\frac{\sin\Phi}{\sin\Theta}\left(\Theta\cos\Theta \frac{\sin\tilde{\theta}}{\sin\Theta} - \tilde{\theta}\cos\tilde{\theta}\right) + (\sin\Phi - \Phi\cos\Phi)\frac{\sin\tilde{\theta}}{\sin\Theta}\right\}$$

$$- R^3\tilde{P}\left(\frac{\sin\Phi}{\sin\Theta} \sin\tilde{\theta} - \frac{\Phi}{\Theta} \tilde{\theta}\right)$$

for $\Phi \leq \theta \leq \Theta$

.....(A.13)

APPENDIX III.

Flexibility Coefficients in Equations of Consistent Deformation

$$\delta_{11} = - \frac{2R}{G_s J_T^*}\left\{\frac{\kappa^{*2}}{(1 + \kappa^{*2}\mu^{*2})^2}\left(\frac{\cos\Theta}{\sin\Theta} - \kappa^*\mu^* \frac{\cosh\kappa^*\mu^*\Theta}{\sinh\kappa^*\mu^*\Theta}\right) -\right.$$

$$\left. - \alpha\left(\Theta - \frac{\cos\Theta}{\sin\Theta} + \frac{\cos^2\Theta}{\sin^2\Theta}\right) - \frac{\cos\Theta}{\sin\Theta} + \frac{1}{\Theta}\right\}$$

$$\delta_{22} = \frac{2}{G_s J_T^*}\left(\frac{\mu^*}{\kappa^*} \frac{\cosh\kappa^*\mu^*\Theta}{\sinh\kappa^*\mu^*\Theta} - \frac{1}{\Theta}\right)$$

$$\delta_{12} = \delta_{21} = - \frac{2}{G_s J_T^*}\left(\frac{\kappa^{*2}\mu^{*2}}{1 + \kappa^{*2}\mu^{*2}} \frac{\cos\Theta}{\sin\Theta} +\right.$$

$$+ \frac{\kappa^*\mu^*}{1 + \kappa^{*2}\mu^{*2}} \frac{\cosh\kappa^*\mu^*\theta}{\sinh\kappa^*\mu^*\theta} - \frac{1}{\theta}\Big)$$

.....(A.14)

In the case where the unit concentrated torque $\tilde{T}$ or load $\tilde{P}$ moves across the first span, the flexibility coefficients δ_{10} and δ_{20} are given by

$$\delta_{10} = - \frac{R\tilde{T}}{G_s J_T^*}\Big\{\frac{\kappa^{*4}\mu^{*2}}{(1 + \kappa^{*2}\mu^{*2})^2}\Big(\frac{\sin\Phi}{\sin\theta} - \frac{\sinh\kappa^*\mu^*\Phi}{\sinh\kappa^*\mu^*\theta}\Big) +$$

$$+ \alpha\Big(\theta \frac{\cos\theta}{\sin\theta}\frac{\sin\Phi}{\sin\theta} - \Phi \frac{\cos\Phi}{\sin\theta}\Big)\Big\}$$

or

$$\delta_{10} = \frac{R^2\tilde{P}}{G_s J_T^*}\Big\{\frac{\kappa^{*2}}{(1 + \kappa^{*2}\mu^{*2})^2}\Big(\frac{\sin\Phi}{\sin\theta} - \frac{\sinh\kappa^*\mu^*\Phi}{\sinh\kappa^*\mu^*\theta}\Big) -$$

$$- \alpha\Big(\theta \frac{\cos\theta}{\sin\theta}\frac{\sin\Phi}{\sin\theta} - \Phi \frac{\cos\Phi}{\sin\theta}\Big) - \frac{\sin\Phi}{\sin\theta} + \frac{\Phi}{\theta}\Big\}$$

and

$$\delta_{20} = \frac{\tilde{T}}{G_s J_T^*} \frac{\kappa^{*2}\mu^{*2}}{1 + \kappa^{*2}\mu^{*2}}\Big(\frac{\sin\Phi}{\sin\theta} - \frac{\sinh\kappa^*\mu^*\Phi}{\sinh\kappa^*\mu^*\theta}\Big)$$

or

$$\delta_{20} = \frac{R\tilde{P}}{G_s J_T^*} \frac{\kappa^{*2}\mu^{*2}}{1 + \kappa^{*2}\mu^{*2}}\Big(\frac{\sin\Phi}{\sin\theta} + \frac{1}{1 + \kappa^{*2}\mu^{*2}} \frac{\sinh\kappa^*\mu^*\Phi}{\sinh\kappa^*\mu^*\theta} - \frac{\Phi}{\theta}\Big)$$

..... (A.15)

In the case where the unit concentrated torque $\tilde{T}$ or load $\tilde{P}$ moves across the second span, the corresponding expressions for δ_{10} and δ_{20} can be obtained by replacing in the above expressions by $\theta - \Phi$.

REFERENCES

[1] Th. von Kármán and N. B. Christensen: Methods of Analysis for Torsion with Variable Twist, Journal of the Aeronautical Sciences, Vol. 11, No. 2, April, 1944, pp. 110-124.

[2] F. W. Bornscheuer: Systematische Darstellung des Biege- und Verdrehvorgangs unter besonderer Berücksichtigung der Wölbkrafttorsion, Der Stahlbau 21, Heft 1, 1952, S. 1-9.

[3] I. Konishi and S. Komatsu: On the Fundamental Theory of Thin-Walled Curved Girder, Japan Society of Civil Engineers-Transactions, No. 87, Nov., 1962, pp. 35-48, (in Japanese).

[4] ————————————: Three Dimensional Analysis of Simply Supported Curved Girder Bridges, ibid., No. 90, Feb., 1963, pp. 11-28, (in Japanese).

[5] ————————————: Three Dimensional Analysis for Continuous Curved Girder Bridges, ibid., No. 91, March, 1963, pp. 13-24, (in Japanese).

[6] S. Kuranishi: Analysis of Thin-Walled Curved Beams, ibid., No. 108, Aug., 1964, pp. 7-12, (in Japanese).

[7] Y. Fukazawa: Fundamental Theory of Thin-Walled Curved Bars in Static Analysis, ibid., No. 110, Oct., 1964, pp. 30-51, (in Japanese).

[8] E. Reissner: On Non-Uniform Torsion of Cylindrical Rods, Journal of Mathematics and Physics, Vol. 31, 1952, pp. 214-221.

[9] S. U. Benscoter: A Theory of Torsion Bending for Multicell Beams, Journal of Applied Mechanics, Vol. 21, No. 1, 1954, pp. 25-34.

[10] R. Heilig: Beitrag zur Theorie der Kastenträger beliebiger Querschnittsform, Der Stahlbau 30, Heft 11, 1961, S. 333-349.

[11] W. Graße: Wölbkrafttorsion dünnwandiger prismatischer Stäbe beliebigen Querschnitts, Ingenieur-Archiv 34, Heft 5, 1965, S. 330-338.

[12] E. Schlechte: Die Torsion dünnwandiger Stabe mit Schubverformung aus behinderter Querschnittsverwölbung, Bauplanung-Bautechnik, Jg. 18, Heft 11, Nov., 1964, S. 556-560.

[13] K. Roik und G. Sedlacek: Theorie der Wölbkrafttorsion unter Berücksichtigung der sekundären Schubverformungen– Analogie-Betrachtung zur Berechnung des Querbelasteten Zugstabes, Der Stahlbau 35, Heft 2, 1966, S. 43-52.

[14] D. Schade: Zur Wölbkrafttorsion von Stäben mit dünnwandigem Querschnitt, Ingenieur-Archiv 38, Heft 1, 1969, S. 25-34.

[15] K. Washizu: Some Consideration on the Center of Shear, Trans. Japan Soc. Aero. Space Sci., Vol. 9, No. 15, 1966, pp. 77-83.

[16] P. Müller: Torsion von Kastenträgern mit elastisch verformbarem symmetrischem Querschnitt, Schweizerische Bauzeitung, Jg. 71, Nr. 46, Nov., 1953, S. 673-676.

[17] R. Dabrowski: Der Schubverformungseinfluss auf die Wölbkrafttorsion der Kastenträger mit verformbarem biegesteifem Profil, Der Bauingenieur, Jg. 40, Heft 11, 1965, S. 444-449.

[18] A. Steinle: Torsion und Profilverformung beim einzelligen Kastenträger, Beton- und Stahlbetonbau 65, Heft 9, 1970, S. 215-222.

[19] R. Dabrowski: Näherungsberechnung der gekrümmten Kastenträger mit verformbarem Querschnitt, IABSE, Seventh Congress, Rio de Janeiro, Prelim. Publ. VI, 1964, pp. 299-306.

[20] ————————: Gekrümmte dünnwandige Trager, Springer-Verlag, Berlin-Göttingen-Heidelberg-New York, 1968.

[21] I. Konishi, N. Shiraishi, and S. Kambe: A Study on the Torsional Bending Theory of the Curved Girder Bridge with Thin-Walled Closed Cross Sections Taking the Secodary Shear Deformation into Account, 14th National Simposium on Bridge and Structural Engineering, Japan Soc. of Civ. Eng., Dec., 1967, pp. 153-167.

[22] S. Kambe and H. Tanaka: On the Torsional Bending Theories of S. U. Benscoter and R. Heilig's Type for the Curved Box Girder Bridges, The Abstract of 24th Annual Conference of the Japan Soc. of Civ. Eng., Oct., 1973.

[23] V. Z. Vlasov: Thin-Walled Elastic Beams, 2nd Ed., Moscow, 1959, Israel Program for Scientific Translations, Jerusalem, 1961.

[24] G. Lacher: Zur Berechnung des Einflusses der Querschnittsverformung auf die Spannungsverteilung bei durch elastische order starre Querschotte versteiften Tragwerken mit prismatischem, offenem oder geschlossenem biegesteifem Querschnitt unter Querlast, Der Stahlbau 10, Heft 6, 1962, S. 299-308.

[25] S. R. Abdel-Samad, R. N. Wright, and A. R. Robinson: Analysis of Box Girders with Diaphragms, Journal of the Structural Division, ASCE, Vol. 94, No. ST10, Proc. Paper 6153, Oct., 1968, pp. 2231-2256.

[26] T. Okumura and F. Sakai: Distorsional Behaviours and Influence of Diaphragms in Ribbed Trapezoidal Box Girders, Proceedings of the Japan Society of Civil Engineers, No. 209, Jan., 1973, pp. 1-14.

[27] S. Ochiai: Analysis of Box Girder Taking the Influence of diaphragms into Consideration, Civil Engineering, Vol. 23, No. 2, 1968, pp. 49-57, (in Japanese).

[28] S. Ochiai and S. Kitahara: Characteristic Behaviour of Diaphragms on Box Girder, The Bridge and Foundation Engineering, Vol. 5, No. 4, 1970, pp. 1-7, (in Japanese).

[29] Z. P. Bazant: Piece longue a voiles epais et calcul des poutres a section deformable, Annales des Pont et Chaussees, No. III, Mai-Juin, 1968, pp. 155-169.

[30] J. E. Goldenberg and H. L. Leve: Theory of Prismatic Folded Plate Structures, Publs. of IABSE, Zürich, Vol. 17, 1957, pp. 69-86.

[31] A. C. Scordelis: A Matrix Formulation of the Folded Plate Equations, Journal of the Structural Division, ASCE, Vol. 86, ST10, Oct., 1960, pp. 1-22.

[32] Y. K. Cheung: Folded Plate Structures by Finite Strip Method, ibid., Vol. 95, ST12, Dec., 1969, pp. 2963-2979.

[33] K. H. Chu and S. G. Pinjarkar: Multiple Folded Plate Structures, ibid., Vol. 92, ST2, Apr., 1966, pp. 297-321.

[34] K. S. Lo and A. C. Scordelis: Finite Segment Analysis of Folded Plates, ibid., Vol. 95, ST5, May, 1969, pp. 831-852.

[35] A. DeFrie-Skene and A. C. Scordelis: Direct Stiffness Solution for Folded Plates, ibid., Vol. 90, ST4, Aug., 1964, pp. 15-47.

[36] C. Meyer and A. C. Scordelis: Analysis of Curved Folded Plate Structures, ibid., Vol. 97, ST10, Oct., 1971, pp. 2459-2480.

[37] K. H. Chu and S. G. Pinjarkar: Analysis of Horizontally Curved Box Girder Bridges, ibid., Vol. 97, ST10, Oct., 1971, pp. 2481-2501.

[38] K. C. Lockey, J. L. Bannister, and H. R. Evans: Developments in Bridge Design and Construction, Crosby Lockwood & Son Ltd., 1971, p. 204.

[39] S. P. Timoshenko: History of Strength of Material, Mcgraw-Hill Book Co., Inc., 1953, pp. 152-155.

[40] S. Kambe and N. Takaoka: Contemporary Trend of the Analysis of Box Girder Bridges, Reports of the Faculty of Engineering, Tottori University, Vol. 3, No. 2, March, 1973, pp. 57-62, (in Japanese).

[41] P. F. McManus, G. A. Nasir, and C. G. Culver: Horizontally Curved Girders — State of the Art, Journal of the Structural Division, ASCE, Vol. 95, ST5, May, 1969, pp. 853-870.

[42] Th. von Karman and W. Z. Chien: Torsion with Variable Twist, Journal of the Aeronautical Sciences, Vol. 13, No. 10, Oct., 1946, pp. 503-510.

[43] N. Saeki: Warping Torsion Theory in Consideration of the Deformation Due to Secondary Shearing Stress and Its Numerical Examples, Proceedings of the Japan Society of Civil Engineers, No. 209, Jan., 1973, pp. 27-36 (in Japanese).

[44] S. Timoshenko and J. N. Goodier: Theory of Elasticity, 2nd ed., McGraw-Hill Book Company, Inc., 1951 (Asian Students' Edition, Kogakusha Company, Ltd., Tokyo).

[45] S. Kambe: The Relation between Two Types of the Torsional Bending Theories after S. U. Benscoter and R. Heilig, Reports of the Faculty of Engineering, Tottori University, Vol. 4, No. 1, Sept., 1973, pp. 92-104.

[46] S. Kambe and H. Tanaka: A Study on the Continuous Curved Girder Bridge with Closed Cross Section, ibid., Vol. 2, No. 2, March, 1972, pp. 100-111.

[47] S. Komatsu, H. Nakai, and Y. Taido: A Proposition for Designing the Horizontally Curved Girder Bridges in Connection with Ratio between Torsional and Flexural Rigidities, Proceedings of the Japan Sciety of Civil Engineers, No. 224, April, 1974, pp. 55-66 (in Japanese).

[48] N. Watanabe: Theory and Calculation of Curved Girder, Gihodo Book Co., 1967.